



**COUNTERION AND MICROCRYSTALLINE CELLULOSE EFFECTS ON  
THE STRUCTURAL PROPERTIES OF STARCH  
AT LOW MOISTURE CONTENTS**

A thesis submitted in fulfillment of the requirements for

The degree of Doctor of Philosophy

**Lillian Chuang**

BSc Food Science & Technology 2003

RMIT University

School of Science

College of Science Engineering and Health

RMIT University

JUNE 2016

# **DECLARATION**

I certify that except where due acknowledgement has been made, the work described in this thesis is that of the author alone; the work has not been submitted previously, in whole or in part, to qualify for any other academic award; the content of the thesis is the result of work which has been carried out since the official commencement date of the approved research program; and, any editorial work, paid or unpaid, carried out by a third party is acknowledged; and, ethics procedures and guidelines have been followed.

Lillian Chuang

17/06/2016

## **ACKNOWLEDGEMENTS**

It was the greatest honor in my life to have this opportunity to undertake this PhD at RMIT University with my Senior Supervisor, Professor Stefan Kasapis without those knowledge, guidance and support, this work would not have be completed, thank you so much!!! Also to my Co-Supervisor, Emeritus Professor Robert Shanks, thanks for being very helpful with my PhD journey with your knowledge and support.

To my close research colleagues, especially Ms Lita Katopo, Dr Naksit Panyoyai, who have been encouraged me with my thesis writing, the time they have spent with me was enormous and I just cannot really put into words the support they have provided.

I am also grateful to, Ms Christine Chow, who was the School Manager when I enrolled in this PhD program and who encouraged me to enhance my professional development as a PhD candidate at RMIT University.

To the School of Applied Sciences Technical Teams within the College of Science, Engineering and Health, Applied Chemistry – Mr Karl Lang, the Lab Manager; Mrs. Dianne Mileo, the Chemistry Store Manager; Ms. Zahra Homan, the Lab Coordinator; Mrs. Nadia Zakhartchouk, the Technical Coordinator; Mr. Frank Antolasic, the Senior Technical Officer; Mrs. Ruth Cepriano-Hall, Mr. Howard Anderson, the Technical Officers; RMIT Microscopy and Microanalysis Facility (RMMF) - Mr. Phil Francis, Mr. Peter Rimmel and all the duty officers from the same facility; Physics Lab Manager - Dr Arwen Pagon; Environmental Science, Professional Officer - Ms. Susan Holden; and lastly, from Chemical Engineering - Mr. Cameron Crombie and Mr. Mike Allen.

To my colleagues and friends, Dr Naksit Panyoyai, Lita Katopo, Vilia Paramita, Carine Semazaka, Nashi Khalid N Alqahtani, Jasmeet Kaur, Yakindra Prasad Timilsena, Bo Wang, Billy Lo, Geethu Gopinatha Kurup who were always supportive and encouraging towards my work, and brightened up my day.

A very special thanks to my ex Direct Manager Mr. Karl Lang, who has been very helpful and supportive when I required time off to pursue my studies.

To my wonderful work colleagues Ms. Yan Chen, Ms. Fiona De-Mendonca, Ms. Mary Karagiozakis and my current Manager Ms. Julianne Aloe, thanks for all your understanding and support.

To my ex-research colleagues and friends, Vinita Chaudhary, Paul George, Natasha Yang, Anastasia Devi, Anna Bannikova, Sobhan Savadkoohi, Omar Masaud Almrhag, Diep Duong within the team, thank you for the company and the times that we have spent together in conferences and discussions to overcome all the difficulties throughout the times when we were together.

I especially want to thank my family, who are overseas for being supportive, understanding and encouraging with my PhD journey.

## PUBLICATIONS AND PRESENTATIONS

### *Publications*

**Chuang, L, Panyoyai, N., Shanks, R. & Kasapis, S. (2015).** Effect of sodium chloride on the glass transition of condensed starch systems.

*Food Chemistry, 184, 65–71. (IF 3.39)*

(This published paper is presented as Chapter 3 in this thesis).

**Chuang, L, Panyoyai, N., Katopo, L., Shanks, R. & Kasapis, S. (2016).** Calcium chloride effects on the glass transition of condensed systems of potato starch. *Food Chemistry, 199, 791-798. (IF 3.39)*

*Food Chemistry, 199, 791-798. (IF 3.39)*

(The published paper is presented as Chapter 4 in this thesis).

*Oral presentations*

Lillian Chuang, Robert Shanks and Stefan Kasapis (2012). Effect of sodium chloride on the glass transition of condensed starch systems, presented at International Conference on Halal Gelling Agents, (5-7<sup>th</sup> December 2012), Penang, Malaysia.

Lillian Chuang, Robert Shanks and Stefan Kasapis (2014). Effect of sodium chloride on the glass transition of condensed starch systems, presented at the 12<sup>th</sup> International Hydrocolloids Conference, Natural Hydrocolloids: A Key to Human Health, (5-9<sup>th</sup> May 2014), Taipei, Taiwan.

Lillian Chuang, Robert Shanks and Stefan Kasapis (2015). Calcium chloride effects on the glass transition of condensed system of potato starch presented at AIFST Food Science Summer School 2015, (28-30<sup>th</sup> January 2015), RMIT University, Melbourne, VIC, Australia.

Lillian Chuang, Robert Shanks and Stefan Kasapis (2016). Counterion effects on the structural properties of starch at low moisture contents, and starch-microcrystalline cellulose mixtures presented at AIFST Food Science Summer School 2016, (27-29<sup>th</sup> January 2016), Charles Sturt University, Wagga Wagga, NSW, Australia.

Lillian Chuang (2013). Effect of sodium chloride on the glass transition of condensed starch systems, presented at 3MT competition, (17<sup>th</sup> June 2013), School of Applied Sciences, Melbourne, VIC, Australia.

*Poster presentations*

Lillian Chuang, Robert Shanks and Stefan Kasapis (2010). Effect of sodium chloride on the glass transition of condensed starch systems presented at 43<sup>rd</sup> Annual AIFST convention, (25-28<sup>th</sup> July 2010), Sebel Albert Park, Melbourne, VIC, Australia.

Lillian Chuang, Robert Shanks and Stefan Kasapis (2011). Effect of sodium chloride on the glass transition of condensed starch systems presented at AIFST Food Science Summer School 2011, (9-11<sup>th</sup> February 2011), St Leo's College, University of Queensland, St Lucia, Brisbane, QLD, Australia.

Lillian Chuang, Robert Shanks and Stefan Kasapis (2012). Effect of sodium chloride on the glass transition of condensed starch systems presented at AIFST Food Science Summer School 2011, (1<sup>st</sup>-3<sup>rd</sup> February 2012), University of Melbourne, VIC, Australia.

Lillian Chuang, Robert Shanks and Stefan Kasapis (2010). Effect of sodium chloride on the glass transition of condensed starch systems presented at Higher Degree Research Student Conference (20<sup>th</sup> October 2010), RMIT University, Melbourne, VIC, Australia.

# TABLE OF CONTENTS

<b>Content</b>	<b>Title</b>	<b>Page</b>
	<b>DECLARATION</b>	i
	<b>ACKNOWLEDGEMENTS</b>	ii
	<b>PUBLICATIONS AND PRESENTATIONS</b>	iv
	<i>Publications</i>	iv
	<i>Oral presentations</i>	v
	<i>Poster presentations</i>	vi
	<b>TABLE OF CONTENTS</b>	vii
	<b>LIST OF FIGURES</b>	xv
	<b>LIST OF TABLES</b>	xxii
	<b>LIST OF ABBREVIATIONS</b>	xxiv
	<b>LIST OF UNITS AND SYMBOLS</b>	xxvi
	<b>EXPLANATORY NOTES</b>	xxviii
	<b>SUMMARY</b>	1
	<b>CHAPTER 1 INTRODUCTION</b>	
1.1	<b>STARCH</b>	5
1.1.1	<i>Composition and structure</i>	5
1.1.2	<i>Functionality</i>	8
1.1.3	<i>Modification</i>	9
1.1.3.1	<i>Chemical modification</i>	9
1.1.3.1.1	<i>Esterification</i>	10
1.1.3.1.2	<i>Etherification</i>	11
1.1.3.1.3	<i>Oxidation</i>	11
1.1.3.1.4	<i>Cross-linking</i>	12
1.1.3.2	<i>Physical modification</i>	12
1.1.3.2.1	<i>Pregelatinisation</i>	13



1.1.3.2.2	<i>Extrusion</i>	13
<b>Content</b>	<b>Title</b>	<b>Page</b>
1.1.3.2.3	<i>Heat-moisture and annealing treatments</i>	14
1.1.4	<i>Potato starch</i>	14
1.1.5	<i>Tapioca starch</i>	15
1.2	CELLULOSE AND DERIVATIVES	16
1.2.1	<i>Composition and structure</i>	16
1.2.2	<i>Microcrystalline cellulose</i>	18
1.2.3	<i>Carboxymethyl cellulose</i>	19
1.2.4	<i>Methylcellulose and methylhydroxypropyl cellulose</i>	20
1.3	WATER IN FOOD	21
1.4	GLASS TRANSITION	23
1.5	BIOPOLYMER MIXTURES	26
1.5.1	<i>Polysaccharide-protein mixtures</i>	28
1.5.2	<i>Polysaccharide-cosolute mixtures</i>	29
1.5.3	<i>Protein-cosolute mixtures</i>	30
1.6	SALTS	31
1.6.1	<i>Hofmeister series</i>	31
1.6.2	<i>Effect of salts on starches</i>	33
1.7	SIGNIFICANCE OF RESEARCH	34
1.8	RESEARCH QUESTIONS	35
1.9	RESEARCH OBJECTIVES	36
1.10	REFERENCES	37
<b>CHAPTER 2 MATERIALS AND METHODS</b>		
2.1	BASIC PRINCIPLES OF INVESTIGATIVE METHODS	51
2.1.1	<i>Rheology analysis-DMA</i>	51
2.1.2	<i>Thermal analysis-DSC</i>	53
2.1.3	<i>Chemical analysis-FTIR</i>	56
2.1.4	<i>Crystallinity analysis-WAXD</i>	57

<b>Content</b>	<b>Title</b>	<b>Page</b>
2.1.5	<i>Structural analysis-SEM</i>	58
2.2	MAJOR EQUIPMENTS	59
2.2.1	<i>Diamond DMA</i>	59
2.2.2	<i>Differential Scanning Calorimeter from TA instrument Model Q2000</i>	60
2.2.3	<i>Fourier transform and spectrophotometry from Perkin Elmer Model Spectrum 100</i>	61
2.2.4	<i>Wide angle X-ray made from Bruker Model-Endeavor D4</i>	62
2.2.5	<i>Energy dispersive X-ray Spectroscopy (EDX)</i>	62
2.2.6	<i>Scanning electron microscope FEI Quanta 200 ESEM</i>	63
2.2.7	<i>Apparatus and auxiliary</i>	64
2.3	SAMPLE PREPARATION	66
2.3.1	<i>Potato starch with co-solutes in the sample formulations</i>	66
2.3.1.1	<i>Potato starch with sodium chloride</i>	66
2.3.1.2	<i>Potato starch with calcium chloride</i>	67
2.3.1.3	<i>Potato starch with MCC</i>	68
2.3.1.4	<i>Relative humidity equilibrium for the potato starch and its co-solutes</i>	68
2.3.2	<i>Tapioca starch with co-solutes in the sample formulations</i>	70
2.3.2.1	<i>Tapioca starch with sodium chloride</i>	70
2.3.2.2	<i>Tapioca starch with calcium chloride</i>	70
2.3.2.3	<i>Relative humidity equilibrium for the tapioca o starch and its co-solutes</i>	71
2.4	EXPERIMENTAL METHODS	71
2.4.1	<i>DMA</i>	71
2.4.2	<i>DSC</i>	71
2.4.3	<i>FTIR</i>	72
2.4.4	<i>WXR</i>	72
2.4.5	<i>EDX</i>	72

2.4.6	<i>SEM</i>	72
<b>Content</b>	<b>Title</b>	<b>Page</b>
2.4.6.1	<i>Potato starch with sodium chloride</i>	72
2.4.6.2	<i>Potato starch with calcium chloride</i>	72
2.4.6.3	<i>Potato starch with MCC</i>	73
2.4.6.4	<i>Tapioca starch with sodium chloride</i>	73
2.4.6.5	<i>Tapioca starch with calcium chloride</i>	73
2.5	REFERENCES	74

### **CHAPTER 3 EFFECT OF SODIUM CHLORIDE ON THE GLASS TRANSITION OF CONDENSED STARCH SYSTEMS**

	ABSTRACT	76
3.1	INTRODUCTION	77
3.2	MATERIALS AND METHODS	79
3.2.1	<i>Materials</i>	79
3.2.1.1	<i>Potato starch</i>	79
3.2.1.2	<i>Sodium chloride</i>	79
3.2.1.3	<i>Millipore water type 2</i>	79
3.2.1.4	<i>Saturated salt solutions</i>	80
3.2.2	<i>Sample preparation</i>	80
3.2.3	<i>Instrumental protocol</i>	81
3.2.3.1	<i>Dynamic mechanical analysis</i>	81
3.2.3.2	<i>Modulated differential scanning calorimetry</i>	81
3.2.3.3	<i>Fourier transform infrared spectroscopy</i>	81
3.2.3.4	<i>Scanning electron microscopy</i>	82
3.2.3.5	<i>Wide angle X-ray diffraction</i>	82
3.3	RESULTS AND DISCUSSION	83
3.3.1	<i>Rheological perspectives for the starch/sodium chloride mixture</i>	83
3.3.2	<i>Calorimetric evidence on the glass transition of starch/sodium chloride mixtures</i>	86

<b>Content</b>	<b>Title</b>	<b>Page</b>
3.3.5	<i>Microscopic examination of the topology in starch/salt composites</i>	92
3.4	CONCLUSIONS	94
3.5	REFERENCES	95

## **CHAPTER 4 CALCIUM CHLORIDE EFFECTS ON THE GLASS TRANSITION OF CONDENSED SYSTEMS OF POTATO STARCH**

	ABSTRACT	98
4.1	INTRODUCTION	99
4.2	MATERIALS AND METHODS	101
4.2.1	<i>Materials</i>	101
4.2.1.1	<i>Potato starch</i>	101
4.2.1.2	<i>Calcium chloride</i>	101
4.2.1.3	<i>Millipore water type 2</i>	101
4.2.1.4	<i>Saturated salt solutions</i>	101
4.2.2	<i>Sample preparation</i>	102
4.2.3	<i>Instrumental protocol</i>	103
4.2.3.1	<i>Dynamic mechanical analysis</i>	103
4.2.3.2	<i>Modulated differential scanning calorimetry</i>	103
4.2.3.3	<i>Fourier transform infrared spectroscopy</i>	103
4.2.3.4	<i>Wide angle X-ray diffraction</i>	104
4.2.3.5	<i>Scanning electron microscopy</i>	104
4.2.3.6	<i>Energy dispersive X-ray spectroscopy</i>	104
4.3	RESULTS AND DISCUSSION	105
4.3.1	<i>Mechanical relaxations in starch/calcium chloride systems as a function of temperature</i>	105
4.3.2	<i>Calorimetric evidence on the vitrification of high-solid starch/calcium chloride systems</i>	108

<b>Content</b>	<b>Title</b>	<b>Title</b>	<b>Page</b>
4.3.3	<i>Infrared spectroscopy for the elucidation of molecular forces in the starch/calcium chloride system</i>		111
4.3.4	<i>X-ray diffraction analysis in high-solid starch/calcium chloride preparations</i>		113
4.3.5	<i>Microscopic examination of the starch/calcium chloride network</i>		115
4.4	CONCLUSIONS		117
4.5	REFERENCES		118

## **CHAPTER 5 EFFECT OF SALT ON THE GLASS TRANSITION OF CONDENSED TAPIOCA STARCH SYSTEMS**

	ABSTRACT		122
5.1	INTRODUCTION		123
5.2	MATERIALS AND METHODS		125
5.2.1	<i>Materials</i>		125
5.2.1.1	<i>Tapioca starch</i>		125
5.2.1.2	<i>Sodium chloride and calcium chloride</i>		125
5.2.1.3	<i>Millipore water type 2</i>		125
5.2.1.4	<i>Saturated salt solutions</i>		125
5.2.2	<i>Sample preparation</i>		126
5.2.3	<i>Instrumental protocol</i>		127
5.2.3.1	<i>Dynamic mechanical analysis</i>		127
5.2.3.2	<i>Modulated differential scanning calorimetry</i>		127
5.2.3.3	<i>Fourier transform infrared spectroscopy</i>		127
5.2.3.4	<i>Wide angle X-ray diffraction</i>		128
5.2.3.5	<i>Scanning electron microscopy</i>		128
5.3	RESULTS AND DISCUSSION		129
5.3.1	<i>Mechanical properties of condensed tapioca starch/salt systems</i>		129
5.3.2	<i>Calorimetric evidence on the vitrification of condensed starch/salt systems</i>		132

<b>Content</b>	<b>Title</b>	<b>Page</b>
5.3.3	<i>FTIR analysis</i>	135
5.3.4	<i>X-Ray analysis</i>	138
5.3.5	<i>Morphology of starch/salt systems</i>	139
5.4	CONCLUSIONS	141
5.5	REFERENCES	142

## **CHAPTER 6 EFFECT OF MICROCRYSTALLINE CELLULOSE ON THE STRUCTURAL PROPERTIES OF CONDENSED POTATO STARCH SYSTEMS**

	ABSTRACT	145
6.1	INTRODUCTION	146
6.2	MATERIALS AND METHODS	148
6.2.1	<i>Materials</i>	148
6.2.1.1	<i>Potato starch</i>	148
6.2.1.2	<i>Microcrystalline cellulose</i>	148
6.2.1.3	<i>Millipore water type 2</i>	149
6.2.1.4	<i>Saturated salt solutions</i>	149
6.2.2	<i>Sample preparation</i>	149
6.2.3	<i>Instrumental protocol</i>	150
6.2.3.1	<i>Dynamic mechanical analysis</i>	150
6.2.3.2	<i>Modulated differential scanning calorimetry</i>	150
6.2.3.3	<i>Fourier transform infrared spectroscopy</i>	151
6.2.3.4	<i>Wide angle X-ray diffraction</i>	151
6.2.3.5	<i>Scanning electron microscopy</i>	151
6.3	RESULTS AND DISCUSSION	152
6.3.1	<i>Mechanical properties of starch/MCC films</i>	152
6.3.2	<i>Thermal stability of starch/MCC films</i>	154
6.3.3	<i>Infrared spectroscopy analysis</i>	157
6.3.4	<i>X-ray diffraction analysis</i>	158

<b>Content</b>	<b>Title</b>	<b>Page</b>
6.3.5	<i>Morphology of starch/MCC films</i>	160
6.4	CONCLUSIONS	161
6.5	REFERENCES	162

## **CHAPTER 7 CONCLUSIONS AND FUTURE WORK**

7.1	CONCLUSIONS	167
7.2	FUTURE WORK	171
7.3	REFERENCES	173

## **APPENDIX**

*Front page of published paper*

Effect of sodium chloride on the glass transition of condensed starch systems 176

*Front page of published paper*

Calcium chloride effects on the glass transition of condensed system of potato starch 177

## LIST OF FIGURES

Figure	Title	Page
<b>CHAPTER 1</b>		
1.1	Schematic diagram of amylose and amylopectin	6
1.2	X-ray diffractometer tracings from various starches	8
1.3	Cellulose molecule and its chair configuration	18
1.4	Moisture sorption isotherm	22
1.5	State diagram of a frozen food; glass transition temperature ( $T_g$ ), melting temperature ( $T_m$ ), glass transition temperature of unfrozen solute-water phase ( $T'_g$ ), and the corresponding solids weight fraction, ( $X'_g$ )	24
1.6	Master curve of viscoelasticity as a function of frequency of oscillation, polymer concentration, molecular weight and temperature, Where $G' = \blacksquare$ , $G'' = \square$ , and $\text{Tan } \delta = \bullet$	25
1.7	Phase diagram of polysaccharide-polysaccharide-water system	28
1.8	Hofmeister series	32
<b>CHAPTER 2</b>		
2.1	A material with sinusoidal stress applied with an oscillating force supplied in DMA	52
2.2	Modes of deformation from DMA	53
2.3	Schematic diagram illustrating the DSC heat fluxes components and corresponding thermal model	54
2.4	DSC thermograms of wheat starch with water content varying from (90%) to (25%) with (a) 2% sodium chloride (% w/w) present and (b) no added salt	55
2.5	FTIR spectra of native (nonirradiated) starches	56
2.6	Diamond DMA from Perkin Elmer	59
2.7	Modulated DSC Q2000 from TA instrument	61
2.8	FTIR Spectrum 100 from Perkin Elmer	61



<b>Figure</b>	<b>Title</b>	<b>Page</b>
<b>2.9</b>	Wide angle X-ray Endeavor D4 from Bruker	62
<b>2.10</b>	FEI Quanta 200 ESEM	63
<b>2.11</b>	Haake Rheomix OS from Thermo Scientific	67
<b>2.12</b>	Hot press	67
<b>2.13</b>	Series of relative humidity chambers (RH11% to 75%) made from DURAN glass desiccators	69

### **CHAPTER 3**

<b>3.1</b>	Heating profiles of tensile storage modulus for potato starch films (a) at a moisture content of 3.6% w/w (RH 11%) and (b) at a moisture content of 18.8% (RH 75%) in the presence of 0.0% (◆), 1.5% (◇), 3.0% (▲), 4.5% (Δ), 6.0% (●) sodium chloride, and variation of tensile storage modulus for potato starch films with different levels of sodium chloride at -100°C (◆; left y axis) and 120°C (■; right y axis) at a moisture content of 3.6% w/w (c) and 18.8% (d) scanned at the rate of 2°C/min, frequency of 1 Hz and strain of 0.1% (error bars denote one standard deviation)	84
<b>3.2</b>	DSC thermograms for potato starch in the presence of sodium chloride at 0.0%, 1.5%, 3.0%, 4.5%, 6.0% with (a) moisture content of 3.6% w/w (RH 11%) and (b) with moisture content of 18.8% w/w (RH 75%) arranged successfully downwards. Table 4.1 Calorimetric markers of the glass transition recorded for potato starch/sodium chloride composites at different levels of relative humidity	87

<b>Figure</b>	<b>Title</b>	<b>Page</b>
<b>3.3</b>	FTIR spectra of potato starch in the presence of sodium chloride at 0.0%, 1.5%, 3.0%, 4.5%, 6.0% arranged upwards with moisture content of a) 3.6% w/w (RH 11%) and b) 18.8% w/w (RH 75%)	90
<b>3.4</b>	X-ray diffractograms for potato starch with sodium chloride at 0.0%, 1.5%, 3.0%, 4.5%, 6% arranged successfully downwards at moisture content of 18.8% w/w (RH 75%)	92
<b>3.5</b>	SEM micrographs for potato starch with moisture content of 3.6% w/w (RH 11%) in the presence of sodium chloride (a) 0.0% and (b) 6.0%, and for moisture content of 18.8% w/w (RH 75%) in the presence of sodium chloride (c) 0.0% and (d) 6.0%	93
 <b>CHAPTER 4</b>		
<b>4.1</b>	Heating profiles of tensile storage modulus for potato starch films at a moisture content of (a) 3.7% w/w (RH 11%) and (b) 18.8% w/w (RH 75%) in the presence of 0.0 (◆), 1.5 (◇), 3.0 (▲), 4.5 (Δ), 6.0% (●) w/w calcium chloride, and variation of tensile storage modulus for potato starch films with different levels of calcium chloride at -100°C (◆, left y axis) and 120°C (■, right y axis) at a moisture content of (c) 3.7 and (d) 18.8% scanned at the rate of 2°C/min, frequency of 1Hz and strain of 0.1%	106

<b>Figure</b>	<b>Title</b>	<b>Page</b>
<b>4.2</b>	Thermograms of potato starch films with a moisture content of (a) 3.7% w/w (RH 11%) and (b) 18.8% w/w (RH 75%) and calcium chloride content arranged successively upwards: 0.0, 1.5, 3.0, 4.5, 6.0% w/w, and $T_g$ values of these samples with moisture content of (c) 3.7% (open symbols) and 18.8% (filled symbols) for sodium chloride (diamonds) and calcium chloride (squares) as a function of salt content (scan rate of 10°C/min)	109
<b>4.3</b>	FTIR spectra showing the absorbance of potato starch in the presence of calcium chloride content of 0.0, 1.5, 3.0, 4.5, 6.0% w/w arranged successfully upwards with moisture content of (a) 3.7% w/w (RH 11%) and (b) 18.8% w/w (RH 75%)	112
<b>4.4</b>	X-ray diffractograms (a) and EDX spectra (b) for potato starch at a moisture content of 18.8% w/w (RH 75%) in the presence of calcium chloride content of 0.0, 1.5, 3.0, 4.5, 6.0% w/w arranged successfully downwards	114
<b>4.5</b>	SEM micrographs of potato starch with moisture and calcium chloride contents of (a) 3.7 and 0.0%, (b) 3.7 and 3.0%, (c) 3.7 and 6.0%, (d) 18.8 and 0.0%, (e) 18.8 and 3.0%, (f) 18.8 and 6.0% w/w, respectively	116
 <b>CHAPTER 5</b>		
<b>5.1</b>	Heating profiles of tensile storage modulus for tapioca starch films in the presence of salt at 0.0% (◆), 1.5% (◇), 3.0% (■), 4.5% (□), 6.0% (▲) at a moisture content of 7.34% w/w (RH 23%) with (a) calcium chloride and (b) sodium chloride, and at a moisture content of 19.52% (RH 75%) with (c) calcium	130

<b>Figure</b>	<b>Title</b>	<b>Page</b>
	chloride and (d) sodium chloride	
<b>5.2</b>	Variation of tensile storage modulus for tapioca starch films with different levels of salt at -100°C (◆; left y axis) and 100°C (■; right y axis) at a moisture content of 7.34% w/w (RH 23%) with (a) calcium chloride (b) sodium chloride, and at a moisture content of 19.52% w/w (RH 75%) with (c) calcium chloride (d) sodium chloride (scan rate is 2°C/min, frequency is 1 Hz, and error bars denote one standard deviation)	131
<b>5.3</b>	DSC thermograms of tapioca starch films in the presence of salt at 0.0% 1.5%, 3.0%, 4.5%, and 6.0% arranged successfully upwards at a moisture content of 7.34% w/w (RH 23%) with (a) calcium chloride and (b) sodium chloride, and at a moisture content of 19.52% (RH 75%) with (c) calcium chloride and (d) sodium chloride.	133
<b>5.4</b>	FTIR spectra of tapioca starch films in the presence of salt at 0.0% 1.5%, 3.0%, 4.5%, and 6.0% arranged successfully upwards at a moisture content of 7.34% w/w (RH 23%) with (a) calcium chloride and (b) sodium chloride, and at a moisture content of 19.52% (RH 75%) with (c) calcium chloride and (d) sodium chloride	137
<b>5.5</b>	X-ray diffractograms of tapioca starch films in the presence of salt at 0.0% 1.5%, 3.0%, 4.5%, and 6.0% arranged successfully downwards at a moisture content of 7.34% w/w (RH 23%) with (a) calcium chloride and (b) sodium chloride, and at a moisture content of 19.52% (RH 75%) with (c) calcium chloride and (d) sodium chloride	139

<b>Figure</b>	<b>Title</b>	<b>Page</b>
<b>5.6</b>	SEM micrographs for tapioca starch systems with moisture content of 7.34% (RH 23%) in the presence of (a) 0% salt, (c) 6.0% CaCl <sub>2</sub> , (e) 6.0% NaCl, and for moisture content of 19.52% w/w (RH 75%) in the presence of (a) 0% salt, (d) 6.0% CaCl <sub>2</sub> and (f) 6.0% NaCl	140

## **CHAPTER 6**

<b>6.1</b>	Heating profiles of tensile storage modulus for potato starch films (a) at a moisture content of 4.15% w/w (RH 11%) and (b) at a moisture content of 17.48% (RH 75%) in the presence of 0.0% (◆), 1.5% (▲), 3.0% (□), 4.5% (■), 6.0% (◇) MCC, and variation of tensile storage modulus for potato starch films with different levels of MCC at -100°C (◆) and 60°C (■) at a moisture content of 4.15% w/w (c) and 17.48% w/w (d) scanned at the rate of 2°C/min, frequency of 1 Hz (error bars denote one standard deviation)	153
<b>6.2</b>	DSC thermograms for potato starch in the presence of MCC at 0.0%, 1.5%, 3.0%, 4.5%, 6.0% with (a) moisture content of 4.18% w/w (RH 11%) and (b) with moisture content of 17.48% w/w (RH 75%) arranged successfully downwards	155
<b>6.3</b>	FTIR spectra of potato starch in the presence of MCC at 0.0%, 1.5%, 3.0%, 4.5%, 6.0% and MCC alone arranged upwards with moisture content of (a) 4.15% w/w (RH 11%) and (b) 17.48% w/w (RH 75%)	157

<b>Figure</b>	<b>Title</b>	<b>Page</b>
<b>6.4</b>	X-ray diffractograms of potato starch with MCC at 0.0%, 1.5%, 3.0%, 4.5%, 6% and MCC only and arranged successfully upwards with moisture content of (a) 4.15 % w/w (RH 11%) and (b) 17.48% w/w (RH 75%)	159
<b>6.5</b>	SEM micrographs for potato starch with moisture content of 4.15% w/w (RH 11%) in the presence of MCC (a) 0.0% and (b) 6.0%, and for moisture content of 17.48% w/w (RH 75%) in the presence of MCC (c) 0.0% and (d) 6.0%	160

## LIST OF TABLES

Table	Title	Page
<b>CHAPTER 1</b>		
1.1	Food and medical uses of starch	6
1.2	Commercial food applications of cellulose and its derivatives	17
<b>CHAPTER 2</b>		
2.1	Specification for Diamond DMA in tension mode	60
2.2	Descriptions of instrumentation and equipment	64
2.3	Tabulated apparatus and auxiliary	64
2.4	Ingredients information	65
2.5	Information of preparation of the saturated salt solution	69
2.6	Relative humidity with moisture contents measured from the starch/co-solute samples	70
<b>CHAPTER 3</b>		
3.1	Calorimetry markers of the glass transition recorded for potato starch/sodium chloride composites at different levels of relative humidity	88
<b>CHAPTER 4</b>		
4.1	$T_g$ values at moisture contents from 3.7% w/w (RH11%) to 18.8% w/w (RH75%) for potato starch with calcium chloride contents between 0.0% to 6.0% (w/w)	110
<b>CHAPTER 5</b>		
5.1	$T_g$ values determined from DSC for tapioca starch with sodium chloride and calcium chloride content at different relative humidity values	146

<b>Table</b>	<b>Title</b>	<b>Page</b>
<b>CHAPTER 6</b>		
<b>6.1</b>	$T_g$ values determined from DSC for potato starch and MCC content up at different relative humidity values	169



## LIST OF ABBREVIATIONS

<b>AGU</b>	Anhydroglucose unit
<b>BSE</b>	Back Scattered Electron
<b>CMC</b>	Carboxymethyl Cellulose
<b>DS</b>	Degree of Carboxymethyl
<b>DP</b>	Degree of Polymerisation
<b>DM</b>	Dry Matter
<b>DSC</b>	Differential Scanning Calorimeter
<b>DMA</b>	Dynamic Mechanical Analysis
<b>DMTA</b>	Dynamic Mechanical Thermal Analysis
<b>EDX</b>	Energy Dispersive X-ray Spectroscopy
<b>FTIR</b>	Fourier Transform Infrared Spectrometer
<b>Ltd.</b>	Limited
<b>LVR</b>	Linear Viscoelastic Region
<b>M</b>	Magnification
<b>Max</b>	Maximum
<b>MC</b>	Methyl Cellulose
<b>HPMC</b>	Methylhydroxypropyl Cellulose
<b>MCC</b>	Microcrystalline Cellulose
<b>MDSC</b>	Modulated Differential Scanning Calorimeter
<b>NSW</b>	New South Wales
<b>PSD</b>	Position Sensitive Detector
<b>QLD</b>	Queensland
<b>RMIT</b>	Royal Melbourne Institute of Technology
<b>RMMF</b>	RMIT Microscopy and Microanalysis Facility
<b>RH</b>	Relative Humidity
<b>Salt</b>	Sodium Chloride (Na <sup>+</sup> Cl <sup>-</sup> )
<b>St</b>	Saint
<b>SEM</b>	Scanning Electron Microscope
<b>NIST</b>	The National Institute of Standards and Technology

## **LIST OF ABBRIVATRIONS (CONT.)**

<b>USA</b>	The United State of America
<b>VIC</b>	Victoria
<b>WAXD</b>	Wide Angle X-ray Diffraction

## LIST OF UNITS AND SYMBOLS

<b>AU</b>	Absorbance
$-\phi$	Binding energy
$\Delta H$	Change in enthalpy
$\Delta T$	Change in temperature
<b>CFU/g</b>	Colony Forming Unit per gram
$E^*$	Complex modulus
$X'_g$	Corresponding solids weight fraction
<b>Da</b>	Dalton
°	Degree
°C	Degree Celsius
°C/min	Degree Celsius per minute
$\varnothing$	Diameter
$E'$	Elastic/storage modulus
$E$	Energy
$T_g$	Glass transition temperature
$T'_g$	Glass transition temperature of unfrozen solute-water phase
<b>g/mol</b>	Gram per mole
$C_p$	Heat capacity
<b>Hz</b>	Hertz
<b>kV</b>	Kilo Volt
<b>L</b>	Litre
$E''$	Loss/viscous modulus
<b>X</b>	Magnification
$T_m$	Melting temperature
$\mu\text{m}$	Micro metre
$\mu\text{W}/^\circ\text{C}$	Micro Watt per degree Celsius
$\mu\text{W}$	Micro Watt

## LIST OF UNITS AND SYMBOLS (CONT.)

<b>mA</b>	Milliampere
<b>mg</b>	Milligram
<b>mg/kg</b>	Milligram per kilogram
<b>mm</b>	Millimetre
<b>mm<sup>2</sup></b>	Square millimetre
<b>mN</b>	Milli Newton
<b>mL</b>	Milli Litre
<b>mL/min</b>	Milli Litre per minute
<b>min</b>	Minute
<b>M</b>	Molar (Mol L <sup>-1</sup> )
<b>ppm</b>	Part per million
<b>N</b>	Newton
<b>Pa</b>	Pascal
<b>cm<sup>-1</sup></b>	Per centimeter
<b>tan δ</b>	Phase angle
<b>pH</b>	$-\log_{10} [\text{H}^+]$ ; ie $[\text{H}^+] = 10^{-\text{pH}}$ M
<b>rpm</b>	Revolution per minute
<b>s</b>	Second
<b>Bar, Torr</b>	Units of pressure
<b>a<sub>w</sub></b>	Water activity
<b>W/g</b>	Watt per gram
<b>w/w</b>	Weight for weight

## EXPLANATORY NOTES

These notes briefly describe the approaches adopted during the preparation of this thesis. They relate to the expression of spelling, units of measurement and the referencing of scientific literature sources:

(i) Where alternative spellings are in common use then the British rather than the American style has been adopted in the text. Example includes words ending with –ise (rather than –ize) and some technical terms. In addition where a lengthy name or expression is repeated, abbreviated symbols have been used instead of the full name (eg glass transition temperature as  $T_g$ ), and chemical symbols for elements have been used.

(ii) In expressing results, SI units have generally been used wherever possible throughout this thesis. Symbols for Units used follow the recent recommendations of The National Institute of Standards and Technology (NIST).

(iii) The format, citation and list of reference and information sources follow the current recommendations to authors for *Food Chemistry* (published by Elsevier).

## SUMMARY

Apart from cellulose, starch is the main carbohydrate found in grains, plant roots or tubers, and as such is widely used as a functional ingredient in snacks and a myriad of other manufactured foods. The main components of starch are amylose and amylopectin together with several minor substances including lipids, proteins, and minerals. In terms of industrial food applications, starch is utilised for modifying texture, extrudability, viscosity, gelation, and mouthfeel. In the case of potato starch, which is the main material of interest in this PhD thesis, there is bound phosphate (800 ppm) capable of increasing viscosity, and by giving solutions a slightly anionic character is able, as will be documented in this work, to influence the glass transition properties of condensed preparations.

The central idea behind this PhD project was to examine the techno-functionality of starch in condensed materials (>70% solid in formulations), which include snacks, a rapidly growing sector of the food manufacturing industry assisted by advances in processing technology in the area of low-moisture materials. In the USA for example, the Centre for Disease Control and Prevention reported in 2013 that 21% of Americans obtain their daily calorie intake from snack foods and beverages. The major ingredient in snacks is gelatinised starch, an inert granule that has been converted *via* heat treatment to a polymeric material, and different sources or concentrations of the ingredient result in distinct physical properties of the final product including structure and expansion ratio during thermal processing.

Along with starch type, increasing use of other ingredients, particularly salts, to achieve a variety of textures and sensory profiles can have unexpected effects on the organoleptic consistency of commercial formulations. To date, molecular studies on these systems are scant in the literature, but the subject has important technological implications and affects the overall quality of preparations. Therefore, this PhD research innovates in the sense that although there is a great number of studies examining the effect of hydrocolloid type and chemical conformation, molecular weight distribution and concentration, and addition of plasticizer in the form of

moisture or sugars (sucrose, lactose, etc.) on the glass transition temperature ( $T_g$ ) of high-solid systems, there is very little work on materials that vary the amount, or type, of added counter cations, according to their electric charge (like sodium ( $\text{Na}^+$ ) or calcium ( $\text{Ca}^{2+}$ ) ions), to monitor glassy phenomena.

Given the above, this PhD study examined the structural properties of condensed starch obtained from slightly anionic potato starch, and comparisons were made with the non-phosphorylated, hence neutral, tapioca (cassava) starch. In detail, experimental samples were condensed potato starch–sodium chloride, potato starch – calcium chloride, tapioca starch – sodium chloride, and tapioca starch – calcium chloride. Sample preparation included hot pressing at 120°C for 7 min to cause granule disruption, leaching of amylose and extensive starch gelatinisation. The materials examined covered a range of moisture contents from 3.6 to 18.8%, which corresponded to relative humidity values of 11 and 75%. Salt addition in the form of sodium chloride or calcium chloride, with sodium and calcium ions being at opposite ends of the Hofmeister series, was up to 6.0% in model formulations. Instrumental work was carried out with dynamic mechanical analysis in tension within the linear viscoelastic region (LVR) of the polymeric network, modulated differential scanning calorimetry, Fourier transform infrared spectroscopy, scanning electron microscopy and wide angle X-ray diffraction.

It was found that experimental conditions ensured the development of amorphous starch matrices undergoing a temperature initiated glass transformation, thus imitating textural consistency in commercial products. Moisture content variation affects dramatically the characteristics of the  $T_g$  of the macromolecule. Sodium ions interact with potato starch hydroxyl and phosphate groups to alter considerably the mechanical properties of high-solid preparations. These become softer than starch-water systems at conditions of elevated temperatures governed by molecular mobility. In contrast, salt addition creates hard matrices at conditions of low temperature, which are characteristic of the mechanical glassy state according to the master curve of viscoelasticity. Densely packed salt-polysaccharide segments in the

glassy state have a high energy resistance to molecular mobility that raises the  $T_g$  with increasing counterion content.

Dissolved calcium ions in these systems, as opposed to solid crystalline calcium chloride, forms specific electrostatic interactions with the polar and negatively charged sequences of the potato starch molecule (the  $\text{Ca}^{2+}$  ion has almost twice the charge density of the  $\text{Na}^+$  ion), inducing an antiplasticising (rigidifying) effect on potato starch that stabilises the polymeric matrix in the glassy state. Strikingly, such effects were minimal in the non-phosphorylated amylopectin sequences of tapioca starch. Where both the  $\text{Na}^+$  and  $\text{Ca}^{2+}$  containing formulations exhibited similar structural behaviour and, in addition, there was no statistically valid variation in the values of the  $T_g$  (at the same moisture-content) for samples of cassava starch upon addition of calcium or sodium chloride of equal percentage levels. This result reinforces the significance of electrostatic interaction in determining the  $T_g$  behavior of starch.

The final chapter of Results and Discussion deals with the effect of addition of microcrystalline cellulose (MCC), up to 6.0% w/w, on the physicochemical properties of potato starch based films. This system has been selected based on fundamental considerations spanning the range of conformation type from  $\alpha(1-4)$  in starch amylose to  $\beta(1-4)$  in cellulose molecules, and the capacity for network formation ranging from non-gelling MCC to gelation at intermediate concentrations of potato starch. Composite materials were treated as for single starch systems and revealed that the inclusion of MCC increases the mechanical strength of the starch films. In contrast to salt addition, both moisture content and the presence of MCC have a plasticising effect producing a reduction in the  $T_g$ . Overall, the results indicate that there were no specific interactions between starch and MCC, with the elongated fibres acting as an inert filler in the polymeric composite. This final piece of research is a prelude to future work that should examine the effect of addition of cations as electric-charge carriers on the structural behaviour of mixtures made of



biopolymers with disparate conformational fingerprints, an area which is well developed in protein biochemistry.

# CHAPTER 1

## INTRODUCTION

In this chapter, the relevant scientific literature on the four keywords of this thesis, i.e. starch, microcrystalline cellulose, salt and moisture are critically reviewed. The chapter covers the theories behind the glass transition and their significance, the interactions in biopolymer mixtures and the behavior of ions based on the Hofmeister series. In addition, the various hydrocolloids utilized in the development of the matrices are briefly reviewed.

### 1.1 STARCH

#### *1.1.1 Composition and structure*

Starch is the primary carbohydrate in various higher plants and is mainly found in cereal grains, legume seeds, roots, and tubers. It exists in the form of granules that range in size from 1 to 100 $\mu$ m, is relatively dense, and insoluble in cold water. Native granular starch has limited applications; however, modified starch has been applied in a wide range of products (Liu, 2005). Examples of industrial applications of starch are given in Table 1.1.

The two major molecular entities of starch are amylose and amylopectin, illustrated in Figure 1.1, with the content of the former usually between 15 to 25% for most starches. Amylose is fundamentally made up from the helical arrangement of  $\alpha$ -glucans  $\alpha$ -(1 $\rightarrow$ 4)-linked linearly, whilst amylopectin is made with  $\alpha$ -glucans  $\alpha$ -(1 $\rightarrow$ 4)-linked linearly as the backbone structure with branch points of  $\alpha$ -(1 $\rightarrow$ 6)-links. The latter is the larger molecule, with a molecular weight of  $10^7$ - $10^9$  Da, compared to amylose of  $10^5$ - $10^6$  Da (Perez, Baldwin, & Gallant, 2009).

**Table 1.1** Food and medical uses of starch (adapted from Ellis et al., 1998)

Industry	Use of starch/modified starch
Food	Viscosity modifier, glazing agent
Medical	Plasma extender/replacers, transplant organ preservation, absorbent sanitary products
Pharmaceuticals	Diluent, binder, drug delivery
Plastics	Biodegradable filler

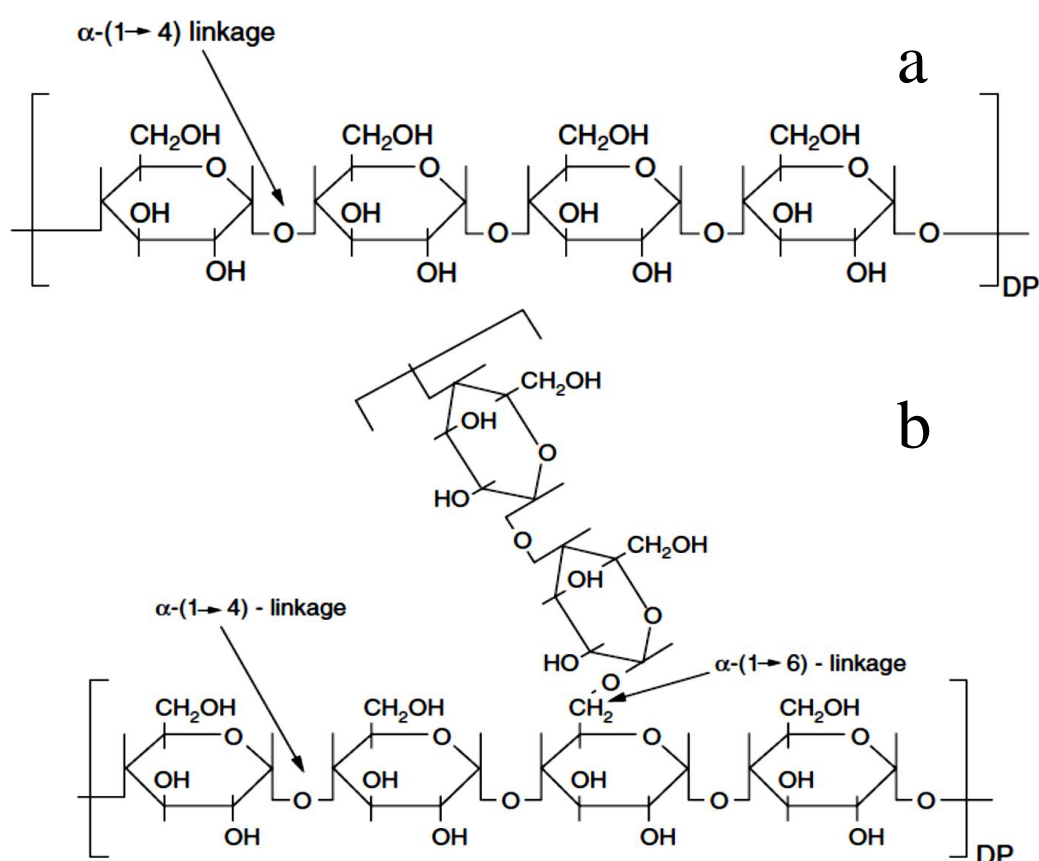


**Figure 1.1** Schematic diagram of amylose (a) and amylopectin (b) (Liu, 2005).

In addition to amylose and amylopectin, starch granules contain other materials, such as lipids (including phospholipids and free fatty acids), phosphate monoesters, and proteins (Jane, 2009). Although these substances are present at low levels in granules, they have a significant effect on the physicochemical properties of starch. For example, lipids and phospholipids can form stable complexes with amylose and the long branched chains of amylopectin, which can restrict the swelling of granules

(Batres & White, 1986; Medcalf, Youngs, & Gilles, 1968; Morrison, Law, & Snape, 1993; Morrison, Tester, Gidley, & Karkalas, 1993). Further, protein can promote Maillard reactions between free amino acid groups and reducing sugars, which lead to undesirable flavours or colours in starch or starch hydrolysis products (Liu, 2005).

In general, native starches possess a semi-crystalline structure, having a crystallinity of about 15 to 45% (Zobel, 1988a). The semi-crystalline structure of native starches can be characterised into four types, A, B, C, and V, through x-ray diffraction patterns (Figure 1.2). Starches of cereal origin commonly give the A-type pattern; the characteristic of potato is a B-type, as well as other retrograded starches, root starches, and amyloomaized starches; generally most of bean starches and smooth pea is the C-type. Starch complexing and gelatinization with lipid or related compounds in the amylose helical complex give the type-V pattern (Zobel, 1988b). The x-ray diffraction patterns indicate the packing arrangement of double helices on the amylopectin side-chain. A closely packed arrangement of double helices is a typical trait of A-type structure, whereas more open packing of helices occurs in the structure of B-type containing a large number of inter-helical water molecules (Wu & Sarko, 1978a, 1978b). It has been shown that A-type starch has a higher melting temperature, thus, is more thermally stable than the B-type (Gidley, 1987).

It is reported that based on the level of crystallinity, most starch granules are in an amorphous state (Oostergetel & van Bruggen, 1993). The amorphous regions are prone to chemical reaction; hence, they can react with functional groups or can be removed using acid. These regions influence the water absorption of starch due to the crystallites possessing a defined water content (Liu, 2005).

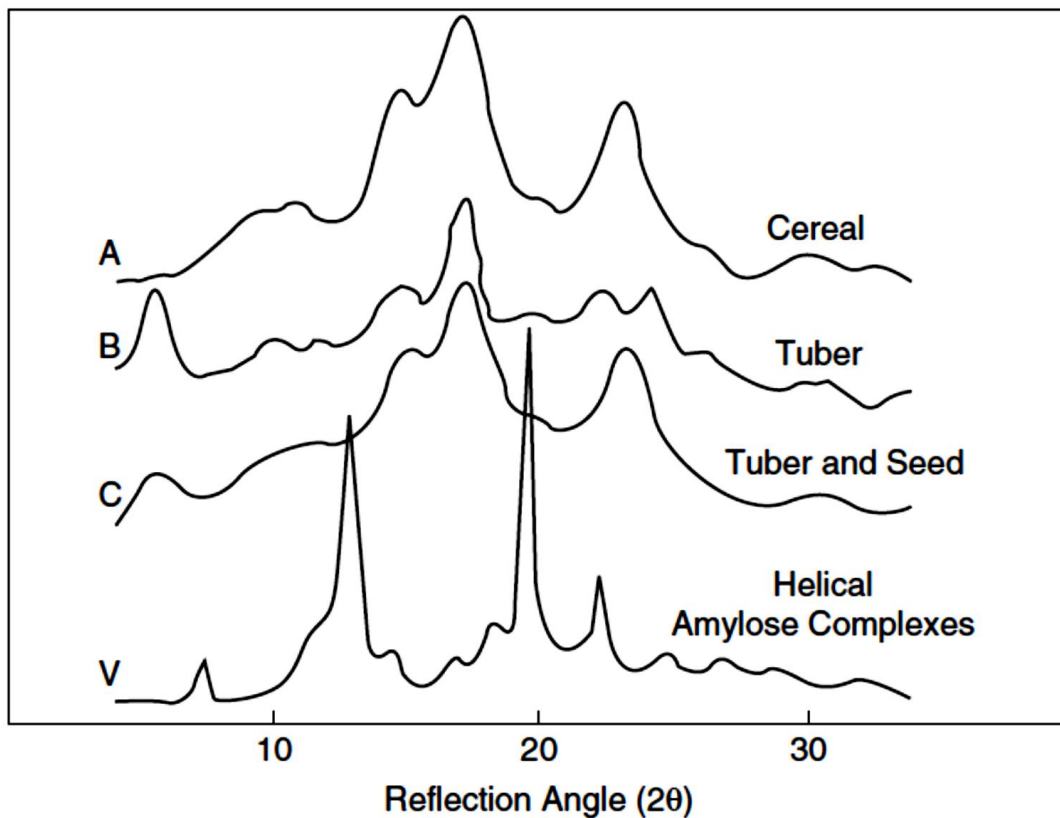


**Figure 1.2** X-ray diffractometer tracings from various starches (adapted from Zobel, 1988b).

### 1.1.2 Functionality

Important aspects in starch applications are granule swelling, pasting, gelatinization, and retrogradation. Native starch granules swell in warm water, although they are insoluble in cold water. Gelatinisation occurs within the granule disrupting the molecular order and leading to irreversible behaviour, such as swelling of the granule, melting of the crystallite, birefringence loss, development of viscosity, and solubilisation (Biliaderis, 2009). Conditions that affect gelatinization include environmental factors such as pressure, mechanical damage, starch sources, small molecular solutes presence, moisture content, physical modifications, chemical modifications, and hydrophilic hydrocolloids.

Starch pasting is a processing behavior whereby the granule slurry substantially changes as the suspended granules swell to dispersion followed by the granule

disruption, then decomposition molecular. Pasting is defined as the state following gelatinisation of starch. Based on their gelatinised paste viscosity profiles, starches can be categorised into four types, I, II, III, and IV (Schoch & Maywald, 1968). Starches have high swelling characteristics with a viscosity at a high peak then later, during heating, a rapid thinning in viscosity can be observed, for example type I potato and tapioca starch. Starches that have modest swelling power are of type II which generally are the cereal starches, which exhibit the peak viscosity at a lower level than type I. Starches with restrained swelling power are the type III and IV, for example, modified starches which are structurally cross-linked and highly restrained starch, such as maize starch with a high amylose content, respectively.

Starch retrogradation is a process occurring when the reassociation of the starch molecules and the ordered double helices reform during storage. The process consists of two stages, the retrograded amylose creates crystalline regions, and within the amylopectin an ordered structure forms. Starch retrogradation is a process which is kinetically controlled (Slade & Levine, 1987); therefore, significant processing changes based on time, temperature, and water content can affect the final product.

### *1.1.3 Modification*

The application of native starch in foods is limited by its physical and chemical properties. One of the main shortcomings is the high viscosities that characterise the dispersions formed when native starches are dispersed in water and cooked. Further, it has been observed that the viscosity and thickening power of native starches decreases upon cooking, particularly in an acidic environment or under retort conditions (Otto, 2006). As a result, native starches are often enhanced with chemical and/or physical treatments to give the best performance.

#### *1.1.3.1 Chemical modification*

Chemical modifications of the hydroxyl groups on the  $\alpha$ -D-glucopyranosyl units in starch include esterification, etherification and oxidation (Chiu & Solarek, 2009).

These modifications are generally performed to enhance resistance to mechanical shearing, and acidic environments (Xie et al., 2005).

#### *1.1.3.1.1 Esterification*

Starch esters can be categorised into three types, starch acetates, starch succinate and alkenylsuccinate, and starch phosphate. The esterification is expressed as average degree of substitution (DS), with a maximum value of 3.0 (Xie et al., 2005).

Starch acetates are prepared by reacting starch with acetic anhydride at alkaline pH. Tapioca and waxy maize starch with acetylated cross-links have been prepared with exceptional product thickening and stability, which is desirable for baby foods application (Jarowenko, 1986).

Starch succinates and alkenylsuccinates are formed by reacting starch with succinic anhydride or alkenyl substituted succinic anhydride. The former contains a free carboxylate group that enhances the water holding power and tendency to swell in cold water which provides excellent clarity, and freeze-thaw stability. The viscosity of starch succinate is markedly influenced by the presence of salt in the solution. A study by Trubiano (1986) showed that in the presence of sodium chloride the peak of viscosities of corn starch succinate were greatly reduced and granule swelling limited, allowing it to be used in soups, and canned and refrigerated food.

Starch alkenylsuccinates possess hydrophobic and hydrophilic groups, which makes them suitable for application in emulsion systems. Such starch molecules bind at the water-oil interface via their hydrophilic group to water and their hydrophobic group to the oil. Hence, they reduce the occurrence of coalescence and separation in the dispersed phase. These properties of balanced hydrophilic and hydrophobic groups make them suitable to stabilize emulsions and encapsulate flavours (King, Trubiano, & Perry, 1976). Starch octenylsuccinate derivatives have been utilized as a gum arabic replacement for stabilization of carbonated beverages due to their superior emulsion stabilizing properties (Xie et al., 2005).

Starch phosphates are anionic polymers that produce high viscosity and stable systems with long term cohesive structure and resistance to retrogradation (Code of Federal Regulations Title 21, 2001). The addition of salt to the dispersions decreases their viscosities. The polymers are good emulsifiers due to their ionic properties (Rutenberg & Solarek, 1984). Dispersions of starch phosphate also exhibit superior freeze-thaw stability to other modified starches (Albrecht, Nelson, & Steinberg, 1960; Kerr & Cleveland, 1962). These modified starches can be utilised as emulsion stabilisers in emulsion for oil in water phase and as an excellent freeze-thaw stabilising thickening agent.

#### *1.1.3.1.2 Etherification*

Etherification produces starch with excellent viscosity stability. Starch ethers are relatively stable at high pH, compared to the ester counterparts, such as starch acetate. Examples of starch ethers for food applications are hydroxyethyl and hydroxypropyl. The latter are compared under alkaline conditions, by combining starch with propylene oxide, which is the major form used in the food industry (Xie et al., 2005). The hydroxypropyl groups disrupt starch granule retrogradation and limit gelation, as well as syneresis (Seib, 1996). Bjorck, Gunnarson, and Ostergard (1989) also found that enzymatic attack may be hindered by the hydroxypropyl group on the starch chain.

Cross-linking agents are usually combined with these starches to improve the processing properties. They are extensively applied as thickening agents in fillings for fresh or frozen desserts, stock gravies, various sauces, and dressings for salads (Xie et al., 2005) as well as in frozen puddings (D'Ercole, 1972). Hydroxypropyl high-amylose starch makes an exceptional coating on foods (Mitan & Jokay, 1969).

#### *1.1.3.1.3 Oxidation*

The oxidation of starch uses various oxidising agents, for instance, hypochlorite, hydrogen peroxide, periodate, persulfate, and chlorite (Rutenberg & Solarek, 1984).



Oxidised starch for food applications is commonly made by reacting starch with sodium hypochlorite. This modification occurs mainly in the amorphous regions of the granule because the oxidised starches exhibit the same x-ray diffraction patterns as that of their native counterparts (Rutenberg & Solarek, 1984). Oxidised starches can be used as binding agents in foods, for example batters applied to fish or meats before frying.

#### *1.1.3.1.4 Cross-Linking*

Cross-linked starches are prepared by reaction of the starch hydroxyls with reagents such as sodium trimetaphosphate, phosphoryl chloride, a mixed adipic acetic anhydride, and composites of sodium trimetaphosphate and tripolyphosphates (Seib, 1996). The modification is performed to hamper the swelling of the polymer granules during heating or to impede the gelatinisation of starch.

High levels of cross-links effectively hinder the granule from swelling; as a result, the starch is unable to be gelatinised in hot water, even under autoclave circumstances (Srivastava & Patel, 1973). The rubbery, stringy texture associated with heated native starches, notably waxy and root starches, can be eliminated with a low level of cross-linking.

These starches are employed in salad dressings because of their thickening properties, and they are the preferred starches for retort products (Evans, Kruger, & Szymanski, 1969; Rutenberg & Solarek, 1984; Rutenberg, Tessler, & Kruger, 1975).

#### *1.1.3.2 Physical modification*

Physical modifications include pregelatinisation, extrusion, heat-moisture, and annealing treatments. This modification is done to transform native starch into small crystallite or cold-water soluble counterpart. The production of cold-water soluble starch involves pregelatinisation of a native starch preparation followed by drum drying, which destroys the grain and reduces the pasting viscosity (Xie et al., 2005).

Small granular starches can be prepared by stirring the native starch at a high shear supplemented by low pH condition (Jane, Shen, Wang , & Maningat, 1992).

#### *1.1.3.2.1 Pregelatinisation*

Typical pregelatinised starches are generally prepared by drum drying, spray drying or extrusion. The unique characteristic of these type of starches is their ability to convert into dispersions and swell in the presence of water at ambient temperature (Xie et al., 2005).

The common applications of these starches are pie fillings, sauces, and puddings. Cross-linked starches can be processed with drying and milling to a particular particle size in order to create soft and stringy texture. Such starches are employed to alter the physical properties of soups and sauces (Marotta & Trubiano, 1969; Trubiano & Marotta, 1971).

#### *1.1.3.2.2 Extrusion*

This modification is used to produce pregelatinised starches and for use in snacks, ready-to-eat cereals, confectionary products, and pet foods (Harper, 1989). In addition, extruders can behave as chemical reactors to form chemically modified starches, such as starch phosphates, anionic starch (an ester of various dicarboxylic acids), and oxidised starches (Chang & Lii, 1992;Tomasik, Wang, & Jane, 1995; Wing & Willett, 1997).

Extrusion consists of mixing, kneading, shearing, heating, cooling, shaping, and forming operations. Such processes cause the starch polymers to be degraded into smaller molecules. Neither short oligosaccharide nor glucose is formed during extrusion; however, there is formation of amylose-lipid complexes (Mercier, Charbonniere, Gallant, & Delagueriviere, 1980).

Extrusion increases the water solubility of starch, but lowers its water absorption capacity, thus, reduces its capability to produce a gel. Nevertheless, extruded starch readily produces a paste at ambient temperature.

#### *1.1.3.2.3 Heat-moisture and annealing treatments*

In heat-moisture treatment, starches are treated at various moisture levels (<35%) at a temperature above the  $T_g$  but below the gelatinisation temperature. These treatments cause displacement of the amylose moieties in the matrix to create intermolecular association between amylose and/or amylopectin chains. Such treatment raises the gelatinisation temperature giving products which display excellent freeze-thaw stability for use in pie fillings (Hoover & Manuel, 1996). Further, heat-moisture treated potato starch is suitable to replace maize starch amid a shortage of corn starch (Lorenz & Kulp, 1981; Stute, 1992).

Annealing treatment involves incubation of starch at water levels from 40 to > 60% w/w at a temperature between the  $T_g$  and the gelatinisation temperature (Jacobs & Delcour, 1998; Tester & Debon, 2000). It alters the physicochemical properties of starch such as, gelatinisation temperature and gelatinisation range without destroying the granule structure.

#### *1.1.4 Potato starch*

Tuber starch granules, such as potato starch, are usually voluminous and oval shaped with an eccentric hilum. The size of potato starch granules are generally larger than other starches, ranging from 2 to 100  $\mu\text{m}$  in diameter (Mishra & Rai, 2006; Pomeranz, 1985). Potato starch has an amylose to amylopectin ratio of 1:3 and contains more phosphate ester groups compared to other starches (Luallen, 2002; Mishra & Rai, 2006). This contributes to lower pasting temperature, higher viscosity, improved clarity (due to small amount of lipids and protein), and allows easier access of water during gelatinisation (Kearsley & Sicard, 1989; Roller, 1996).

Ester and ether modifications to potato starch are performed to obtain the properties desired for particular applications. In the food industry, potato starch is preferred starch because it has a neutral flavor and its pastes possess good clarity due to the small quantity of lipids and protein present (Glicksman, 1969).

#### *1.1.5 Tapioca starch*

Tapioca starch contains high molecular weight amylose and amylopectin but only low levels of residual fat, protein, ash and a lower amylose content than other amylose containing starches (Swinkels, 1985).

Tapioca starch generally has an amylose content between 17 and 20%. The starch granules are typically smooth and spherical in shape, with diameters ranging from 4 to 35  $\mu\text{m}$ . The hilum is off-centre and there are usually noticeable fissures that cross the hilum (Breuninger, Piyachomkwan, & Sriroth, 2009). Retrogradation is less noticeable in tapioca starch due to a lower amylose content and higher molecular weight amylose compared to other starches.

Tapioca starch is a popular choice as a thickening and stabilising agent due to its lack of flavour and it has been used widely in the production of Asian-style noodles in combination with other ingredients. For example, tapioca starch was incorporated in noodle dough of durum semolina in order to achieve an instant cooking noodle (Ishigaki, Saito, & Fujita, 1994). It was found that tapioca starch moderated water uptake during noodle rehydration. Starches from other tuber and grain sources, with higher levels of amylose, possess the disadvantage of more difficult rehydration because of retrogradation in the noodle.

The properties of tapioca starch are markedly influenced by the presence of other ingredients, such as sucrose and salts. The inclusion of sucrose and sodium chloride has been shown to increase the gelatinisation temperature of tapioca starch, but does not affect the gelatinisation enthalpy.

## **1.2 CELLULOSE AND DERIVATIVES**

### *1.2.1 Composition and Structure*

Cellulose, the world's most abundant naturally occurring polysaccharide with an annual biomass production of 50 billion tonnes (Carlin, 2008), is the main structural polysaccharide in the cell walls of higher plants (Marchessault & Sundararajan, 1983). It is a major component of wood (40-50%), jute (60-70%), flax (80%), and cotton (85-97%) (Cash & Caputo, 2010; Izydorczyk, Cui, & Wang, 2005). Cellulose can also be found in the cell walls of green algae, as well as in the membranes of fungi. Cellulose, together with some other inert polysaccharides, compose the indigestible carbohydrate of plant food (vegetables, fruits, or cereals), known as dietary fibre.

The polysaccharide has been used extensively in diverse industries, such as paper, mining and food, and as an alternative source of renewable energy. Typical applications of cellulose and its derivatives in food products are shown in Table 1.2. The physically modified celluloses, such microcrystalline cellulose (MCC), are commonly utilised in reduced or low calorie foods where bulking fillers (agents) are desirable (Setser & Racette, 1992). The major functions of chemically modified cellulose derivatives are the governance of viscosity, surface texture, control of ice crystal development and water-binding capability.

**Table 1.2** Commercial food applications of cellulose and its derivatives (adapted from Coffey, Bell, & Henderson, 2006)

<b>Cellulose/cellulose derivatives</b>	<b>Applications</b>
Hydroxypropyl cellulose HPC Hydroxypropylmethyl cellulose	Whipped toppings, mousses, extruded foods, baked goods, bakery fillings, icings, fried foods, sauces, dressings, frozen desserts, reduced-fat foods
Methylcellulose Methylethyl cellulose	Sauces, soups, breads, tortillas, fried foods, restructured (matrix) foods, reduced-fat foods, foams, whipped toppings, mousses, egg white substitute
Microcrystalline cellulose (MCC) Powdered cellulose Sodium carboxymethyl cellulose (CMC)	Dressings, sauces, baked goods, beverages, whipped toppings, reduced-fat foods, breads, cookies, pastries, pasta, imitation cheeses, cereals, canned meats, frozen desserts, baked goods, dressings, sauces, syrups, beverages, extruded foods, animal foods, reduced-calorie foods

In contrast to amylose and amylopectin which contain  $\alpha$ -D-glucopyranose units, the structure of cellulose contains  $\beta$ -D-glucopyranose residues (Figure 1.3) which adopt an extended ribbon-like conformation due to the  $\beta(1\rightarrow4)$  linkages (French, Bertoniere, Battiste, Cuculo, & Gray, 1993; Klemm, Heublein, Fink, & Bohn, 2005). The tertiary structure is stabilised by intermolecular H-bonds and van der Waals forces which create three-dimensional fibrous bundles (Izydorczyk et al., 2005), that strengthen the plant structure and lead to its virtual insolubility in common solvents, particularly water (Coffey et al., 2006). Nevertheless, it does swell in water, dilute acids, and most solvents (Belitz, Grosch, & Schieberle, 2009a; Coffey et al., 2006). Solubility in concentrated acids can be obtained (Rorrer & Hawley, 1993) but only via hydrolytic degradation of the glycosidic bonds. Alkaline solutions cause swelling and dissolution of the hemicelluloses present.

Cellulose is a linear-chain polymer with a large number of hydroxyl groups (three per anhydroglucose unit, AGU). The chain length of cellulose is defined by the number of constituent AGUs expressed as the degree of polymerization (DP), which

varies with the origin and treatment of the raw material. For example, the DP values for wood pulp are in the range of 300 to 1700, whereas cotton and other plant fibres possess DP values between 800 and 10000 (Klemm et al., 2005).

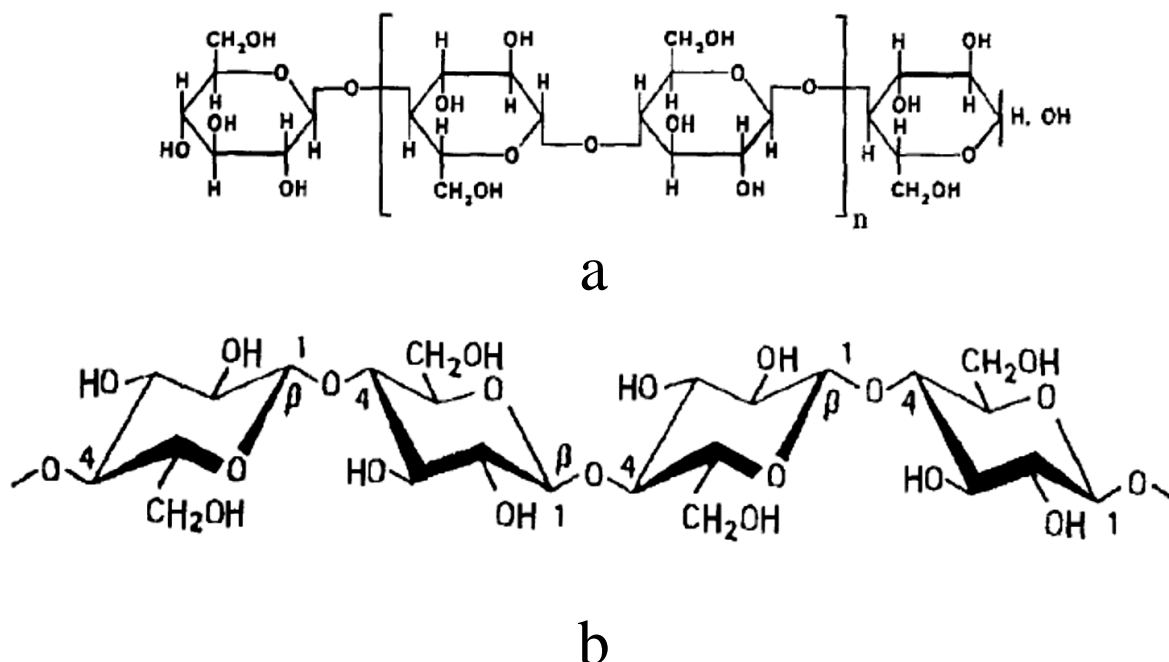


**Figure 1.3** Cellulose molecule Haworth structure (a) and its chair configuration (b) (Hon, 1994).

### 1.2.2 Microcrystalline cellulose

Microcrystalline cellulose (MCC) is obtained by treating natural cellulose with hydrochloric acid in order to partially dissolve and remove the less organised amorphous regions (BeMiller & Huber, 2008). It is a partially purified depolymerised fraction of  $\alpha$ -cellulose. MCC is used extensively in the pharmaceutical, paper, and food industries (Samir, Alloin, & Dufresne, 2005), for example, as a stabiliser in foams and emulsions, as a bulking agent to alter food textures, and as a fat replacer in emulsion based products. It is a common ingredient in reduced fat ice cream and other frozen dessert products (BeMiller & Huber, 2008).

MCC can be obtained in two forms, powdered MCC and colloidal MCC. The former is insoluble, chemically inert, crystalline in nature and very porous (Tuason, Krawczyk, & Buliga, 2010) and is utilised as a flavour carrier and an anticaking agent for shredded cheese. In contrast, colloidal MCC is water soluble and possess functionality which is similar with the properties of hydrocolloids. When the colloidal MCC is fully dispersed in water, the MCC particles form a network which is thermally stable and exhibits thixotropic behavior. The gel that is formed possesses the elastic properties of a solid that exhibits relatively high yield stress (Tuason et al., 2010) and this behaviour is the key to the unique properties of colloidal microcrystalline cellulose as a stabiliser in low-fat systems (Imeson & Humphreys, 1997).

### *1.2.3 Carboxymethyl cellulose*

Carboxymethyl cellulose (CMC), commonly known as cellulose gum, is formed through chloroacetic acid treatment of alkaline cellulose. It has a light tan to white appearance and is a tasteless powder that is fairly hygroscopic. Both the degree of polymerisation (DP) and degree of carboxymethyl (DS) substitution, as well as uniformity of substitution affect the solution properties of the polymer. Commercial grade CMC generally has a DS value between 0.4 and 1.5 (Zecher & Gerrish, 1997). The material is insoluble in water at  $DS < 0.4$ .

The chain length (or DP) of the polysaccharide influences the viscosity of a cellulose gum. Solutions of cellulose gum tend to exhibit pseudoplastic behaviour; however, at low concentrations they demonstrate Newtonian-like flow behaviour. The pseudoplasticity of CMC typically declines with higher DS; at DS value  $\geq 1.0$ , systems have limited interchain cooperation that displays little or no hysteresis during increasing or decreasing physical force (Coffey et al., 2006). Thixotropic behaviour, which is observed in low DS or nonuniformly substituted cellulose gum solutions (Cash & Caputo, 2010), is a product of the intermolecular hydrogen bonding between neighbouring segments of mostly unsubstituted anhydroglucose molecules.



The polymer solutions maintain their viscosity over a wide range of pH, although the maximum viscosity and stability is seen at near neutral pH. Low pH systems, i.e. below pH 4.0, cause precipitation of the polymer, while above pH 10.0 the viscosity decreases.

The impact of solutes, such as salt, on viscosity varies with salt type and concentration, as well as the order of addition. Generally, the maximum viscosity can be achieved if the cellulose gum is fully hydrated prior to the addition of solute. During hydration of the CMC, water molecules bind to the anionic carboxylate groups, partially shielding them from cations that are added later. Upon addition of monovalent salts (e.g.  $\text{Na}^+$ ,  $\text{K}^+$ ) at low to moderate levels the solution properties of CMC, such as haze, viscosity, and clarity, remain unaffected (Mulchandani & Mahmoud, 1997). Whilst divalent salts, e.g. calcium ( $\text{Ca}^{2+}$ ) inhibit hydration of cellulose gum, thus, reducing the solution quality. Trivalent cations (eg  $\text{Fe}^{3+}$ ,  $\text{Al}^{3+}$ ) cause precipitation of the polysaccharide.

CMC has been widely utilised as a thickening agent to improve or alter the texture of food products, such as jellies, paste fillings, salad dressings, spreadable processed cheeses, and cake fillings. It is known for its excellent performance in heat-shock protection by controlling ice crystal growth in ice cream. The polysaccharide also improves the stability and rehydration characteristics in many dehydrated food products (Belitz et al., 2009a).

#### *1.2.4 Methyl cellulose and methylhydroxypropyl cellulose*

Methyl cellulose (MC) and methylhydroxypropyl cellulose (HPMC) are non-ionic water-soluble cellulose ethers, with thickening, surface activity (due to hydrophobic groups), and film forming properties. The former is obtained by treating alkali cellulose with methyl chloride, in alkali whereas methyl chloride and propylene oxide are used to prepare the latter. The cellulose derivatives have an appearance of light-coloured free-flowing powders with neutral taste and odour, but less

hygroscopic than CMC. MC and HPMC commonly have DS values in the range of 1.4-2.2 and 1.0-2.3 respectively (Cash & Caputo, 2010; Izydorczyk et al., 2005).

The aqueous solutions of these cold water soluble polymers generally exhibit pseudoplastic behaviour; which increases with concentration and molecular weight (Coffey et al., 2006). However, low concentrations of the polysaccharide in water demonstrate Newtonian behaviour. Two particular characteristics of MC and HPMC are their inverse temperature solubility and thermal gelation properties. It was found that the gelling of MC was a two-step process, an initial melting of structures found in solution, and a reordering to allow a different structure at high temperature (Haque & Morris, 1993). Gel formation occurs at elevated temperature as a result of hydrophobic interactions between highly substituted regions, which consequently stabilise intermolecular hydrogen bonding (Izydorczyk et al., 2005). This phenomenon is reversible and the gel returns to the initial solution viscosity upon cooling. The MC typically gels at lower temperature compared to HPMC (Coffey et al., 2006). The former produces hard and brittle gels, whereas the latter gels are softer (Cash & Caputo, 2010).

The presence of solutes, such as salt and sucrose, reduces the thermal gelling temperature of the polymers. For example, inclusion of 2% sodium chloride in a 2% solution of cellulose derivative lowers the gel temperature by 10 to 15°C. However, care needs to be taken, as the addition of higher levels of salt may cause a “salting out” effect. Further, incorporation of 10% sucrose decreases the thermal gelling temperature by up to 10°C (Coffey et al., 2006).

### **1.3 WATER IN FOOD**

The amount of water and its interaction with food ingredients greatly influences the physical, chemical and microbiological stability of food. Water is capable of acting as a solvent and plasticiser for a large number of food components, as well as the fact that it may exist in solid, liquid, and gaseous states at common food processing and storage temperatures. The effect of water on the physical state of food materials

is often noticed as a lowering of the melting temperature of water-soluble food solids and structural changes that are dependent on water activity and water content (Belitz, Grosch, & Schieberle, 2009b). The relationship between water content and water activity in a food is characterised by its water sorption isotherm, which is used to establish storage and processing conditions (Rahman & Labuza, 1999).

Figure 1.4 depicts a typical moisture sorption isotherm of a low moisture food. Minor changes in water content lead to significant changes in water activity ( $a_w$ ). The desorption isotherm, which corresponds to a drying process, is located above the adsorption isotherm. The symmetry of the hysteresis loop changes when the hydration and drying processes are repeated (Belitz et al., 2009b).

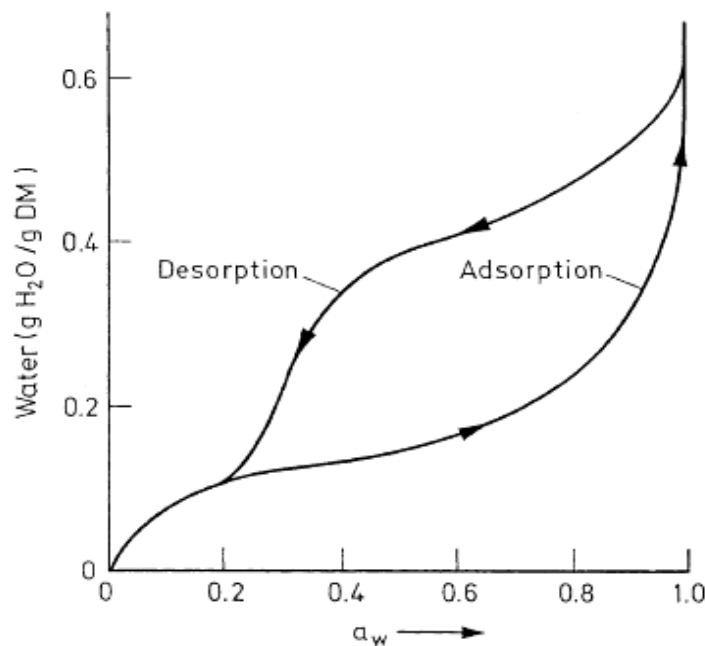


**Figure 1.4** Moisture sorption isotherm (Labuza, Tannenbaum, & Karel, 1970).

Water activity has limited use as an indicator for the storage life of foods with a low moisture content. This is because water activity indicates a state that applies only to ideal systems, i.e. very dilute solutions that are at thermodynamic equilibrium. Foods with low moisture content are non-ideal systems, and as such do not follow change thermodynamical changes during storage, but according to kinetic principles (Belitz et al., 2009b).

## 1.4 GLASS TRANSITION

In food, it has been found that water activity alone is not sufficient to understand the change in food quantity, and instead both water activity and glass transition needs to be considered to estimate the storage stability of a food product. Work by Rockland and Nishi (1980) argued that a product is most stable at its monolayer moisture content, i.e. an  $a_w$  of about 0.1-0.3. Correspondingly, it has been noted that food products are stable at or below their corresponding  $T_g$ .

The glass transition, or vitrification process, is a second-order time and temperature dependent transition in which the material undergoes a change in state but not in phase. This process is characterised by a discontinuity in the physicochemical properties of a material (Rahman, 2006). Food stability alters as a food passes through the glass transition because the water in the concentrated phase becomes kinetically immobilized and not available for reactions (Rahman, 1999; Slade & Levine, 1991b).

A glassy material is produced when an amorphous structure is cooled promptly, thus, the molecules of the liquid have no time to reorganise and enter into regular (crystalline) regions (Hutchinson, 1995). The molecules become “frozen” in the molecular arrangement of a liquid with a very high viscosity, which, however, prevents them from flowing like a liquid (Jiang, Kasapis, & Kontogiorgos, 2012). Further cooling of the system demonstrates a change in physio-chemical features at the glass transition region (Kasapis, 2005). Examples of partial/total glassy materials include biscuits, pasta, ice cream, and carbohydrate or protein samples in aqueous environments or in mixtures high in sugars (Slade & Franks, 2002).

The glass transition behaviour, along with the freezing curve and solubility line, has been used to construct a state diagram of food as a function of solids content and temperature. Figure 1.5 illustrates a typical phase/state diagram for a frozen food, with the region below the  $T_g$  curve representing a glassy state (Rao, 2003). Depending on  $T_g$ , a material behaves as a super-cooled melt when it is above  $T_g$ ,

whilst, below  $T_g$  it is known as an amorphous solid or glass. A material with low  $T_g$  is soft and relatively elastic at room temperature. In contrast, a material with high  $T_g$  is hard and brittle at room temperature (Kasapis, 2005).

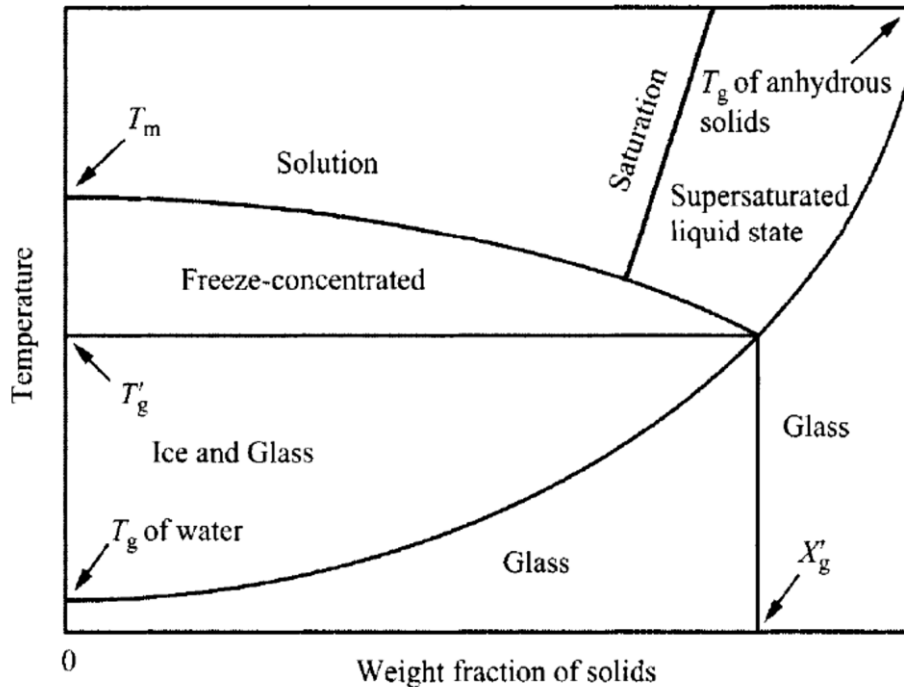


**Figure 1.5** State diagram of a frozen food; glass transition temperature ( $T_g$ ), melting temperature ( $T_m$ ), glass transition temperature of unfrozen solute-water phase ( $T'_g$ ), and the corresponding solids weight fraction, ( $X'_g$ ). Adapted from Rao (2003).

The most common method used to measure the  $T_g$  is differential scanning calorimetry (DSC). The technique detects the change in heat capacity accompanying the glass transition (Rahman, 2006). Besides DSC, dynamic mechanical analysis (DMA), dynamic mechanical thermal analysis (DMTA), and dynamic oscillation methods have been utilised to investigate the glass transition phenomenon. These methods examine changes in storage modulus ( $G'$ ) and loss modulus ( $G''$ ) as a function of the frequency of oscillation, as illustrated in Figure 1.6. Regions I and II correspond to flow and rubbery plateau regions, respectively: Region I is a result of the predominance of molecular flow in the biopolymer solution and a concentrated preparation of the co-solute. Therefore, the values of  $G''$  are higher than  $G'$ ; Region II portrays a crossover of  $G'$  and  $G''$ , with  $G'$  values

greater than  $G''$  values, due to the formation of a rubbery or elastic network within the system. Region III is known as the glass transition region, which is characterised by the second crossover of  $G'$  and  $G''$  with the viscous component being dominant. Finally, in Region VI, the elastic and viscous moduli cross over for a third time, thus, producing a glassy zone (Ong, Whitehouse, Abeysekera, Al-Ruqaie, & Kasapis, 1998).

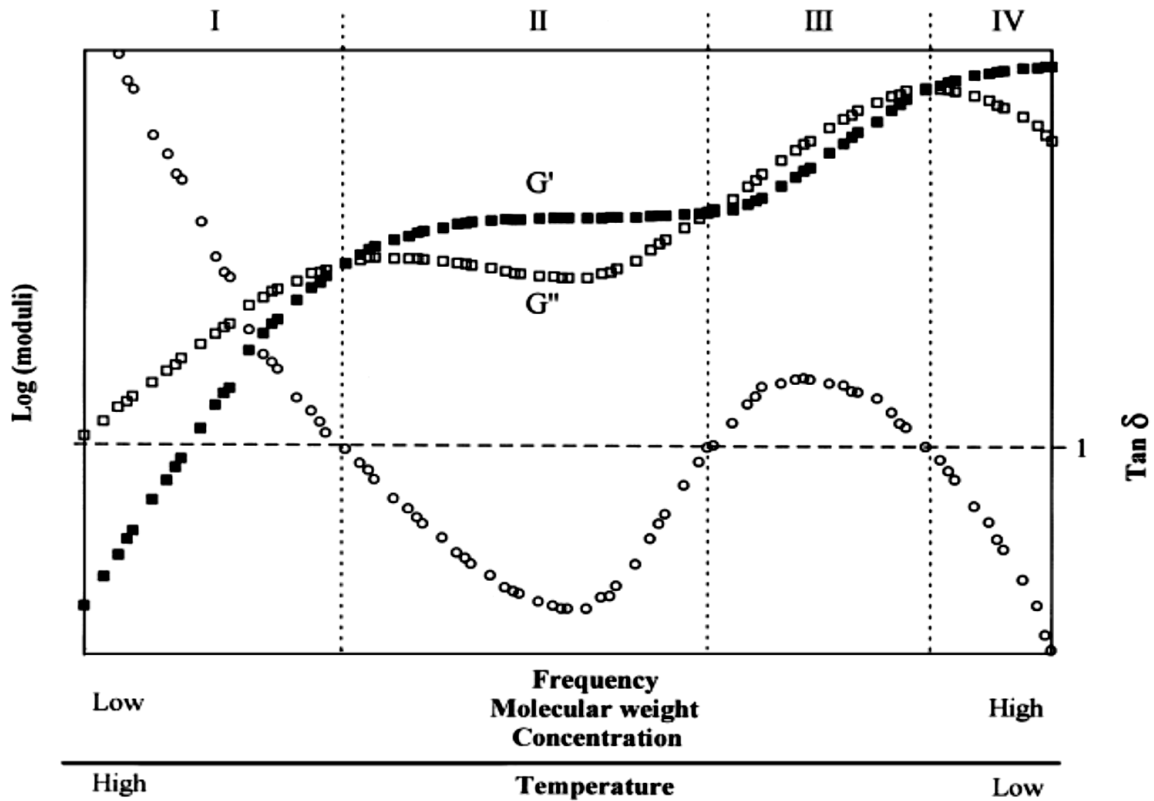


**Figure 1.6** Master curve of viscoelasticity as a function of frequency of oscillation, polymer concentration, molecular weight and temperature (Ong et al., 1998). Where  $G' = \blacksquare$ ,  $G'' = \square$ , and  $\text{Tan } \delta = \circ$ .

Plasticisers increase a material's workability, flexibility or extensibility by allowing increased segmental motion in the system chain (Kasapis, 2005). It has been established that water and other low molecular weight solvents exert a plasticizing effect on many polymers and decrease the  $T_g$ . This arises as a result of the average molecular weight of the homogenous polymer-plasticiser decreasing and its free volume increasing (Ferry, 1980).

Water is a very effective plasticiser and modifies the  $T_g$  of amorphous materials as well as the  $T_g$  and  $T_m$  (melting temperature) of partially crystalline materials (Rowland, 1980; Slade & Levine, 1991a, 1991b). Atkins (1987) observed that water molecules act as plasticizer to reduce the  $T_g$  of most biomaterials from around 200°C (for dehydrated systems, e.g. starch, gelatin) to around -10°C or so for the hydrated counterparts. Further work by Slade and Levine (1991a) found that although initial swelling caused by water uptake of the starch is plasticizing, it does not occur at the same time.

Sugars are also used to plasticise biopolymers. In the case of starch, two opposite effects are observed during gelatinization; in a high moisture system (i) where sugar and water act as co-solvents, with starch as the sole solute, its  $T_g$  is increased in the presence of sugar, in contrast, in low moisture systems, (ii) sugar and starch act as co-solutes with water acting as the sole solvent, and its  $T_g$  is decreased in the presence of sugar (Slade & Levine, 1994). Such behaviour of sugars is also evident in other polysaccharide- and protein-containing systems (Levine & Slade, 1989; Slade & Levine, 1989).

## **1.5 BIOPOLYMER MIXTURES**

Two possible interactions may take place upon mixing different biopolymers in food, namely, associative and segregative. The former occurs in a limited number of systems and is characterised by the formation of ordered heterotypic junctions which form gels, often called “synergistic gels” (Morris 2009). The mechanism of associative interaction generally involves an ionic interaction between polyanions (e.g. negatively charged polysaccharides) and polycations (e.g. proteins below their isoelectric point) (Chilvers, Gunning, & Morris, 1988; Chilvers & Morris, 1987; Galazka, Smith, Ledward, & Dickinson, 1999; Gilsenan & Morris, 2003; Imeson, Ledward, & Mitchell, 1977; Michon, Cuvelier, Launay, Parker, & Takerkart, 1995; Muchin, Wajnermann, & Tolstogusow, 1976; Stainsby, 1980; Tschumak, Wajnermann, & Tolstogusow, 1976; Ye, 2008). This type of electrostatic

interaction can lead to co-precipitation of the two polymers, as a “complex coacervate”. Alternately, it may leads to gel formation via a “coupled network” (Morris, 1986).

The more common segregative interactions occur in most biopolymer mixtures where there is no significant inter-chain electrostatic bonding. This characteristic is often called “thermodynamic incompatibility” (Syrbe, Fernandes, Dannenberg, Bauer, & Klostermeyer, 1995), and can be attributed to differences in the polarity and composition structural features of the hydrocolloids (Schorsch, Jones, & Norton, 1999; Zeman & Patterson, 1972). The thermodynamic incompatibility of biopolymers in mixtures often leads to phase separation.

In the liquid state, phase separation can commonly be identified by the creation of opacity upon mixing leading to a “water-in-water emulsion” (Grinberg & Tolstoguzov, 1972, 1997; Polyakov, Grinberg, & Tolstoguzov, 1997). However, for gelling biopolymers, the result is not so clear because the structure of the water-in-water system can be immobilised by the formation of a network. This will produce a composite gel where one hydrocolloid will form the continuous phase with the second component being dispersed as the discontinuous filler. Kasapis (2008) argued that the classic description of demixing in the liquid state will give rise to thermodynamic equilibrium in solution between the two macromolecules, which will not be reestablished in the gel upon controlled cooling. This is because the formation of a composite gel is attained by coil-helix transitions and possible polymeric agglomeration that entraps the two components in a state of kinetic equilibrium.

The incompatibility of biopolymers in mixtures can be shown quantitatively by phase diagrams, which portray the phase behaviour and phase equilibrium in a given system. A typical phase diagram of ‘polysaccharide (A) concentration’ versus ‘polysaccharide (B) concentration’ is illustrated in Figure 1.7. The region below the hyperbolic curve (the solid line, BEFGD) corresponds to a single-phase of mixed polysaccharide solutions, while the region above it describes the biphasic systems.



The tie-line (DE) connect points corresponding to the compositions of the coexisting equilibrium phases (Tolstoguzov, 2006). At the critical point (F), the two co-existing phases have the same volume and composition. The phase separation threshold, i.e. the minimal bulk biopolymer concentrations at which phase separation occurs, is shown as point G (Tolstoguzov, 2000).

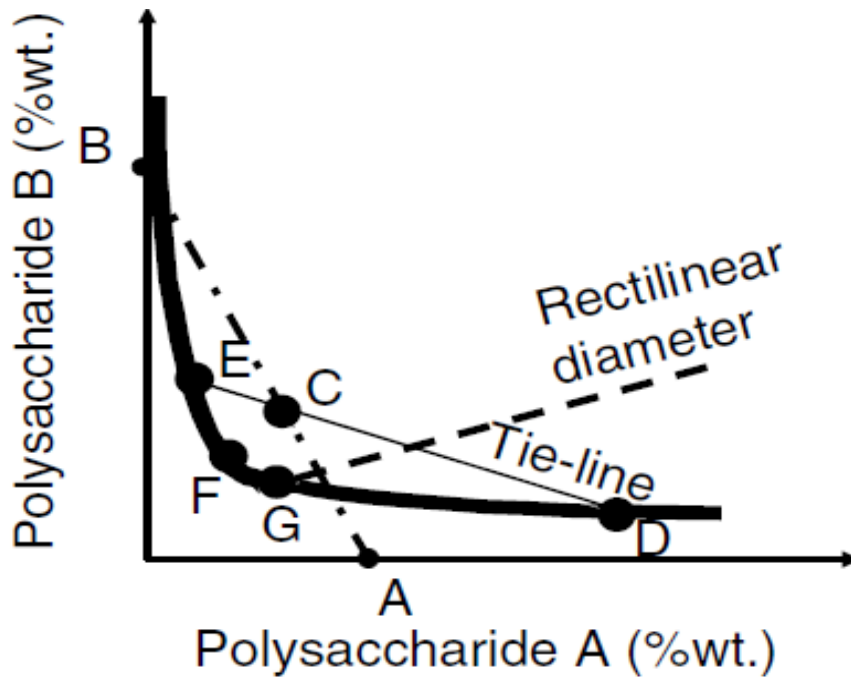


**Figure 1.7** Phase diagram of polysaccharide-polysaccharide-water system (Tolstoguzov, 2006).

### 1.5.1 Polysaccharide-protein mixtures

Early work by Kasapis, Morris, Norton, and Brown (1993) displayed a classic phase separation in concentrated mixtures of gelatin with maltodextrin at a temperature of 45°C, above the onset of conformational ordering and gelation of either component. Further, Katopo, Kasapis, and Hemar (2012) examined the influence of changing thermal treatment and pH on the structural properties of agarose/whey protein systems. They observed the formation of a range of two-phase materials, from continuous agarose matrices perforated by liquid-like whey protein inclusions, in cooled only systems, to phase inverted systems where a soft protein matrix, in

thermally treated preparations, suspends hard agarose-filler particles upon subsequent cooling. The findings were interpreted as a classic phase separation in solution, transforming to a kinetically controlled “equilibrium” between the two phases in the gel state (Kasapis, 2008). Distinct dependence of water holding patterns between agarose and whey protein phases was predicted as a function of changing pH in mixtures.

Detailed accounts regarding mixtures of milk proteins with starch have been widely reported. Indeed, a mixture of anionic potato starch and milk is a common example of an associative interaction (Grega et al., 2003). However, the majority of studies suggest that the properties of milk protein and non-ionic starch mixtures arise from segregative interactions (Bont, Kempen, & Vreeker, 2002; Considine et al., 2011; Corredig, Sharafbafi, & Kristo, 2011; Matser & Steeneken, 1997; Yang, Liu, Ashton, Gorczyca, & Kasapis, 2013).

Phase separation between amylopectin and whey protein occurs at high levels of amylopectin compared to other matrices, for instance, casein-guar gum or casein-locust bean gum requiring 5% casein and 0.02% or 0.04% of the non-starchy polysaccharide, respectively. Amylose and amylopectin, which leach from disrupted starch granules during pasting at elevated temperatures, cause phase separation in milk proteins, and the source of starch influences the rheological properties of these composite systems (Noisuwan, Hemar, Wilkinson, & Bronlund, 2009). Inclusion of cross-linked waxy maize starch in skim milk has been shown to produce a higher final storage modulus compared to a system with water at the same level of starch, indicating that the milk components influence the storage modulus of the binary mixture (Matser & Steeneken, 1997).

### *1.5.2 Polysaccharide-cosolute mixtures*

The phase behaviour of polysaccharide/co-solute systems has been extensively investigated. Incorporation of co-solutes such as sucrose, glucose, glucose syrup or polydextrose up to 40% in mixtures produce structures that are stronger and more

thermally stable (Almrhag, George, Bannikova, Katopo, & Kasapis, 2012; Chaudhary, Small, & Kasapis, 2013; Kasapis, Al-Marhoobi, Deszczynski, Mitchell, & Abeysekera, 1993). This stiffening effect is ascribed to H-bonding between the different components, since hydrogen bond disruptors (e.g. urea or guanidine hydrochloride) decrease the network strength (Nishinari, Watase, Miyoshi, Takaya, & Oakenfull, 1995; Nishinari, Watase, Williams, & Phillips, 1990).

Chaudhary et al. (2013) reported a drop in the value of storage modulus in the deacylated gellan matrices at intermediate levels of co-solute (40-70%). This decline in modulus values was accompanied by a decrease in the enthalpy of the coil-to-helix transition (Almrhag et al., 2012; Chaudhary et al., 2013). Results from electron microscopy showed the polysaccharides disaggregating and dissolving in the saturated sugar environment.

In a condensed agarose system (total solids content >70%), the addition of polydextrose prevents full helix development of the polysaccharide, with the system appearing to be amorphous. However, a condensed pectin system exhibited a double structuring functionality in the presence of polydextrose, which is due to its double mode of gelation, involving a hydrophobic ordering at high temperatures and a hydrophilic interaction at sub-ambient temperature. Polydextrose addition results in the formation of rubbery pectin gels at ambient temperature, which, upon controlled cooling to subzero temperatures, converts rapidly to a clear glass (Almrhag et al., 2012).

### *1.5.3 Protein-cosolute mixtures*

Co-solutes, such as sugars and polyols, are often incorporated in solutions of globular proteins to stabilize them against denaturing induced by temperature, mechanical stress or dehydration treatments. Examples of stabilising co-solutes are sucrose, glucose, raffinose, trehalose and glycerols. The stabilisation of proteins by simple sugars has been shown to proceed primarily through a steric exclusion mechanism (McClements, 2002). Studies have shown that co-solutes can

successfully increase the thermal transition temperature of fish and meat proteins (Carvajal, MacDonald, & Lanier, 1999; MacDonald, Lanier, & Giesbrecht, 1996).

Co-solutes can exert a significant effect on the functional characteristics of globular proteins, for instance, water solubility leading to protein stabilisation and subsequent gelation or emulsification. The effect of co-solutes on the water solubility of a protein complex depends on protein type, co-solute type, concentration, pH and temperature, since they can both increase, or decrease the protein solubility depending on the actual solution conditions.

Cosolutes are capable of altering the observed physicochemical properties of protein gels; First, they change the temperature at which the protein molecules unfold; Second, they alter the magnitude of the attractive and repulsive forces between protein molecules and Third, cosolutes enhance the viscosity of aqueous protein solutions (McClements, 2002).

## **1.6 SALT**

Salt, sodium chloride ( $\text{Na}^+\text{Cl}^-$ ) has been used extensively as a food additive in the food industry due to its low cost and functional properties. It has a preservative effect because of its ability to reduce the water activity in foods, which hinders vital microbial processes, and high levels of salt exert an osmotic effect, which is detrimental to spoilage organisms. However, essential water-soluble components, such as vitamins and minerals may be lost. Salt has also been identified in some reactions responsible for the development of the organoleptic characteristics of many foods. (Albarracin, Sanchez, Grau, & Barat, 2011). Salt can also improve flavor, and may assist water absorption (Lawrence, Dikeman, Stephens, Obuz, & Davis, 2004; Silva, Morais, & Silvestre, 2003).

### *1.6.1 Hofmeister series*

Ion-specific salt-induced interactions play an important role in biopolymer interactions in aqueous solutions at biological and higher concentrations, i.e. at all

concentrations relevant for protein precipitation (Boström, Williams, & Ninham, 2003). The Hofmeister series is an arrangement of ionized molecules based on their physicochemical properties in relation to aqueous processes, ranging from protein denaturation to colloidal assembly (Zhang & Cremer, 2006). The effect of ions on the solubility of proteins was first studied by Lewith and Hofmeister during the 1880s and 1890s (Kunz, Henle, & Ninham, 2004). They demonstrated that the precipitation of proteins in salt solutions depends not only on the protein concentration, but also on the nature of the salt and its concentration (Hofmeister, 1888; Lewith, 1888).

The order of anions and cations in the Hofmeister series is illustrated in Figure 1.8. The ions on the left side are capable of stabilising the native folded structure of a protein and reduce its solubility, whereas the ions on the right tend to encourage protein denaturation and increase its solubility (Kunz et al., 2004). The anions generally have a more pronounced effect than the cations at relatively hydrophobic interfaces, such as protein surfaces, and therefore are easier to monitor (Zhang & Cremer, 2006). These phenomena can also be used to investigate the effect of ions or salts on a colloidal starch-water system.

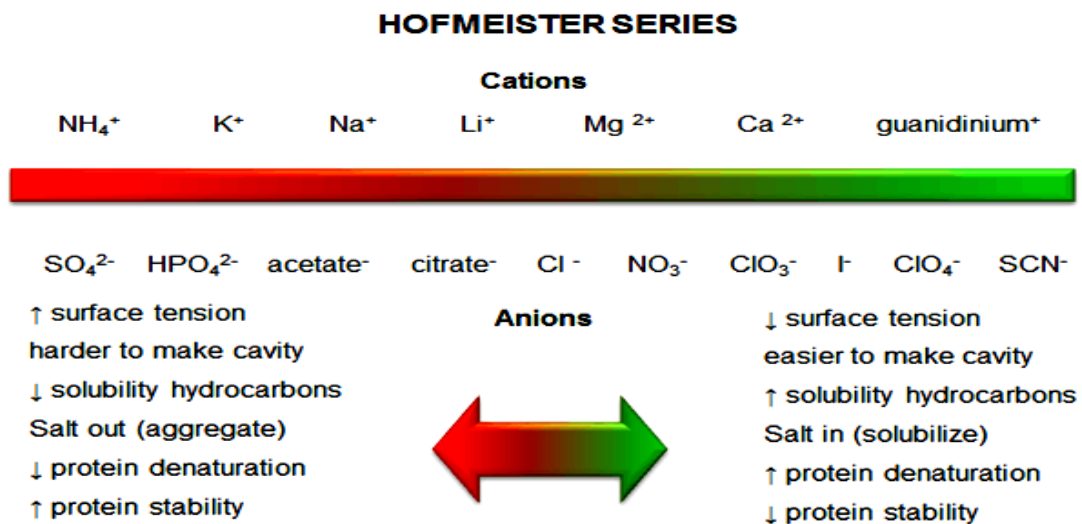


**Figure 1.8** Hofmeister series (Jakubowski, 2013).

### *1.6.2 Effect of salts on starches*

Numerous researchers have published accounts of the effect of salt on the physicochemical properties of starch. For instance, Oosten (1982) suggested that salt could act as a weak-acid based ion-exchanger, with the cations tending to protect and stabilise the starch granule structure. In contrast, it was suggested that the anions acted as the gelatinising agents and disrupted the hydrogen bonds. Jane (1993) postulated that the mechanism of starch gelatinisation in salt solutions was a result of the structure-making and structure-breaking effect of the ions on water aggregates and the electrostatic interactions between salts and the hydroxyl groups on starch. Zhou et al. (2014) investigated the effect of salting-out and salting-in ions on the properties of potato starch. It was argued that salting out ions, such as  $F^-$  and  $SO_4^{2-}$ , reduced the swelling power and increased the peak temperature ( $T_p$ ) as well as the gelatinisation enthalpy ( $\Delta H$ ) of potato starch. In contrast, the study showed a reverse trend with the addition of salting-in ions, such as  $I^-$  and  $SCN^-$ .

Larsson (2002) showed that addition of NaCl, at levels up to 2%, enhanced the elastic modulus of wheat flour dough as measured in a rotational rheometer. This behaviour can be attributed to the influence of salt on the gluten and protein fraction with the salt strengthening the gluten network (Salovaara, 1982). Other work has demonstrated that the inclusion of salt has a plasticisation effect. Indeed, Farahnaky, Farhat, Mitchell, and Hill (2009) concluded that addition of NaCl decreased markedly the  $T_g$  of potato and cassava starches, and  $CaCl_2$  had a similar plasticising effect on starch/poly vinyl alcohol films (Jiang et al., 2012).

## 1.7 SIGNIFICANCE OF RESEARCH

Snacks are a rapidly growing sector of the food industry assisted by technological advances in the area of low-moisture materials. In the USA, for example, the Centre for Disease Control and Prevention reported in 2013 that 21% of Americans obtain their daily calorie intake from snack foods and beverages. The major ingredient in snacks is starch, and different sources of the ingredient result in distinct physical properties of the final product including structure and expansion ratio during thermal processing.

Along with starch type, increasing use of other ingredients, particularly salts, to achieve a variety of sensory profiles can have unexpected effects on the textural performance of commercial formulations. To date, molecular studies on these systems are scant in the literature, although the subject has important technological implications and affects the overall quality of preparations. Given the above, the significance of the current research is summarised in the following paragraphs:

- (i) There is a great number of studies examining the effect of hydrocolloid type and chemical conformation, hydrocolloid molecular weight distribution and concentration, and addition of plasticizer, in the form of moisture or sugars (sucrose, lactose, etc.) on the glass transition temperature of high-solid systems.
- (ii) However, there is very little work on materials that vary the amount, or type, of added counterions, according to their electric charge (like sodium  $\text{Na}^+$  or calcium  $\text{Ca}^{2+}$  ions), to monitor glassy phenomena, although these have clear commercial benefits and are of scientific interest.
- (iii) This research utilises experimental conditions and sample composition to develop materials in relation to high-solid systems that would allow direct scaling up in product concepts of industrial exploitation.

- (iv) A study of the parameters, such as variation in starch concentration, starch type (potato or tapioca), salt type (sodium or calcium chloride) and concentration, as implemented in this work, has important technological implications since it can inform manufacturers of the overall quality and performance of industrial preparations.

## **1.8 RESEARCH QUESTIONS**

- i) What is the role of phosphorylated amylopectin sequences in potato starch in relation to the effect of calcium ions, as compared to that of the sodium ions?
- ii) Do calcium ions plasticise or antiplasticise starch preparations, and how does this compare with the corresponding effect of sodium ions on the glass transition temperature and mechanical strength of high-solid potato preparations?
- iii) Since tapioca starch is a non-phosphorylated material, is there a corresponding plasticising or antiplasticising effect of sodium and calcium ion addition on the vitrification characteristics of condensed preparations?
- iv) Are there any direct or specific molecular interactions between potato starch and microcrystalline cellulose, or does microcrystalline cellulose act as inert filler within the starch matrix?
- v) Is the effect of microcrystalline cellulose, in terms of the glass transition temperature and reinforcement of the mechanical strength in the continuous phase of condensed potato starch, comparable to that of salt addition?



## 1.9 RESEARCH OBJECTIVES

- i) Examine the plasticising or antiplasticising effect of the calcium ion, as compared to that of the sodium ion, in relation to the role of phosphorylated amylopectin sequences in potato starch.
- ii) Identify the effect of calcium ions, as high charge density cations in comparison to that of low charge density sodium cations, on the physicochemical behaviour of potato and tapioca starch, so as to focus discussion on the added cations, as opposed to the chloride anions.
- iii) Monitor the glass transition temperature of tapioca starch in the presence of sodium or calcium chloride at equal levels of cation addition in order to assess the influence, and importance, of a phosphorylation-free starch sequence.
- iv) Develop an experimental protocol that examines the phase behaviour of microcrystalline cellulose and potato starch in terms of mechanical strength and glass transition temperature.
- v) Explore the effect of moisture content and the presence of microcrystalline cellulose on the vitrification patterns of potato and tapioca starch, in relation to salt addition.

## 1.10 REFERENCES

- Albarracin, W., Sanchez, I., Grau, R., & Barat, J. M. (2011). Salt in Food Processing: Usage and Reduction - A Review. *International Journal of Food Science and Technology*, *46*, 1329-1336.
- Albrecht, J. J., Nelson, A. I., & Steinberg, M. P. (1960). Chrematistics of corn starch and starch derivatives as affected by freezing, storage, and thawing. *Food Technology*, *14*, 57-68.
- Almrhag, O., George, P., Bannikova, A., Katopo, L., & Kasapis, S. (2012). Networks of polysaccharides with hydrophilic and hydrophobic characteristics in the presence of co-solute. *International Journal of Biological Macromolecules*, *51*, 138-145.
- Batres, L. V., & White, P. J. (1986). Interaction of amylopectin with monoglycerides in model systems. *Journal of the American Oil Chemists' Society*, *63*, 1537-1540.
- Belitz, H. D., Grosch, W., & Schieberle, P. (2009a). Carbohydrates. In H. D. Belitz, W. Grosch & P. Schieberle (Eds.), *Food Chemistry* (4th ed.). Heidelberg: Springer.
- Belitz, H. D., Grosch, W., & Schieberle, P. (2009b). Water and phase transitions. In H. D. Belitz, W. Grosch & P. Schieberle (Eds.), *Food Chemistry* (4th ed.). Heidelberg: Springer.
- BeMiller, J., & Huber, K. C. (2008). Carbohydrates. In S. Damodaran, K. L. Parkin & O. R. Fennema (Eds.), *Fennema's Food Chemistry* (4th ed., pp. 83-151). Boca Raton: Taylor & Francis.
- Biliaderis, C. G. (2009). Structural transitions and related physical properties of starch. In J. BeMiller & R. Whistler (Eds.), *Starch: Chemistry and Technology* (3rd ed.). San Diego, CA: Academic Press.
- Bjorck, L., Gunnarson, A., & Ostergard, K. (1989). A study of native and chemically modified potato starch. Part II. Digestibility in the rat intestinal tract. *Starch - Stärke*, *41*, 128-134.

- Bont, P. W. d., Kempen, G. M. P. v., & Vreeker, R. (2002). Phase separation in milk protein and amylopectin mixtures. *Food Hydrocolloids*, *16*, 127-138.
- Boström, M., Williams, D. R. M., & Ninham, B. W. (2003). Specific Ion Effects: Why the Properties of Lysozyme in Salt Solutions Follow a Hofmeister Series. *Biophysical Journal*, *85*, 686-694.
- Breuninger, W. F., Piyachomkwan, K., & Sriroth, K. (2009). Tapioca/cassava starch: production and use. In J. BeMiller & R. Whistler (Eds.), *Starch: Chemistry and Technology* (3rd ed.). San Diego, CA: Academic Press.
- Carlin, B. (2008). Direct compression and the role of filler-binders. In L. L. Augsburger & S. W. Hoag (Eds.), *Pharmaceutical Dosage Forms: Tablets* (pp. 173-216): Informa.
- Carvajal, P. A., MacDonald, G. A., & Lanier, T. C. (1999). Cryostabilisation mechanism of fish muscle proteins by maltodextrin. *Cryobiology*, *38*, 16-26.
- Cash, M. J., & Caputo, S. J. (2010). Cellulose derivatives. In A. Imeson (Ed.), *Food Stabilisers, Thickeners and Gelling Agents* (pp. 95-115). United Kingdom: Blackwell Publishing Ltd.
- Chang, Y. H., & Lii, C. Y. (1992). Preparation of starch phosphates by extrusion. *Journal of Food Science*, *57*, 203-205.
- Chaudhary, V., Small, D. M., & Kasapis, S. (2013). Structural studies on matrices of deacylated gellan with polydextrose. *Food Chemistry*, *137*, 37-44.
- Chilvers, G. R., Gunning, A. P., & Morris, V. J. (1988). Coacervation of gelatin–XM6 mixtures and their use in microencapsulation. *Carbohydrate Polymers*, *8*, 55-61.
- Chilvers, G. R., & Morris, V. J. (1987). Coacervation of gelatin–gellan gum mixtures and their use in microencapsulation. *Carbohydrate Polymers*, *7*, 111-120.
- Chiu, C.-w., & Solarek, D. (2009). Modification of starches. In J. BeMiller & R. Whistler (Eds.), *Starch: Chemistry and Technology* (3rd ed.). San Diego, CA: Academic Press.

- Code of Federal Regulations Title 21. (2001). Paragraph 172.892. Food Starch-Modified. Washington, D.C.: US Government Printing Office.
- Coffey, D. G., Bell, D. A., & Henderson, A. (2006). Cellulose and cellulose derivatives. In A. M. Stephen, G. O. Phillips & P. A. Williams (Eds.), *Food Polysaccharides and Their Applications* (2nd ed., pp. 147-179). Boca Raton: CRC Press.
- Considine, T., Noisuwan, A., Hemar, Y., Wilkinson, B., Bronlund, J., & Kasapis, S. (2011). Rheological investigations of the interactions between starch and milk proteins in model dairy systems: A review. *Food Hydrocolloids*, 25, 2008-2017.
- Corredig, M., Sharafbafi, N., & Kristo, E. (2011). Polysaccharide-protein interactions in dairy matrices, control and design of structures. *Food Hydrocolloids*, 25, 1833-1841.
- D'Ercole, A. D. (1972). Process of Preparing Frozen Pudding Composition: US Patent 3669687.
- Ellis, R. P., Cochrane, M. P., Dale, M. F. B., Duffus, C. M., Lynn, A., Morrison, I. M., . Tiller, S. A. (1998). Starch production and industrial use. *Journal of the Science of Food and Agriculture*, 77, 289-311.
- Evans, R. B., Kruger, L., & Szymanski, C. D. (1969). Inhibited Starch Products: US Patent 3463668.
- Farahnaky, A., Farhat, I. A., Mitchell, J. R., & Hill, S. E. (2009). The effect of sodium chloride on the glass transition of potato and cassava starches at low moisture contents. *Food Hydrocolloids*, 23, 1483-1487.
- Ferry, J. D. (1980). *Viscoelastic Properties of Polymers* (3rd ed.). New York: John Wiley.
- French, A. D., Bertoniere, N. R., Battiste, O. A., Cuculo, J. A., & Gray, D. L. (1993). Cellulose. In K. Othmer (Ed.), *Kirk-Othmer Encyclopedia of Chemical Technology* (5th ed.). New Jersey: John Wiley & Sons.

- Galazka, V. B., Smith, D., Ledward, D. A., & Dickinson, E. (1999). Complexes of bovine serum albumin with sulphated polysaccharides: effects of pH, ionic strength and high pressure treatment. *Food Chemistry*, *64*, 303-310.
- Gidley, M. J. (1987). Factors affecting the crystalline type (A-C) of native starches and model compounds: a rationalisation of observed effects in terms of polymorphic structures. *Carbohydrate Research*, *161*, 301-304.
- Gilsenan, P. M. R., R.K., & Morris, E. R. (2003). Associative and segregative interactions between gelatin and low-methoxy pectin: Part 1 – Associative interactions in the absence of Ca<sup>2+</sup>. *Food Hydrocolloids*, *17*, 723-737.
- Glicksman, M. (1969). *Gum Technology in the Food Industry*. New York, NY: Academic Press.
- Grega, T., Najgebauer, D., Sady, M., Baczkowicz, M., Tomasik, P., & Faryna, M. (2003). Biodegradable complex polymers from casein and potato starch. *Journal of Polymers and the Environment*, *11*, 75-83.
- Grinberg, V. Y., & Tolstoguzov, V. B. (1972). Thermodynamic compatibility of gelatin with some D-glucans in aqueous media. *Carbohydrate Research*, *25*, 313-321.
- Grinberg, V. Y., & Tolstoguzov, V. B. (1997). Thermodynamic incompatibility of proteins and polysaccharides in solutions. *Food Hydrocolloids*, *11*, 145-158.
- Haque, A., & Morris, E. R. (1993). Thermogelation of methylcellulose. Part I: molecular structures and processes. *Carbohydrate Polymers*, *22*, 161-173.
- Harper, J. M. (1989). Food extruders and their applications. In C. Mercier & J. M. Harper (Eds.), *Extrusion Cooking* (pp. 1-15). St. Paul, MN: American Association of Cereal Chemists, Inc.
- Hofmeister, F. (1888). Zur lehre der wirkung der salze. Zweite mittheilung. *rch Exp Pathol Pharmakol.*, *24*, 247–260.
- Hon, D. N. S. (1994). Cellulose: a random walk along its historical path. *Cellulose*, *1*, 1-25.
- Hoover, R., & Manuel, H. (1996). The effect of heat-moisture treatment on the structure and physicochemical properties of normal maize, waxy maize, dull

- waxy maize and amylo maize V starches. *Journal of Cereal Science*, 23, 153-162.
- Hoover, R., & Vasanathan, T. (1994). Effect of heat-moisture treatment on the structure and physicochemical properties of cereal, legume, and tuber starches. *Carbohydrate Research*, 252, 33-53.
- Hutchinson, J. M. (1995). Physical aging of polymers. *Progress in Polymer Science*, 20(703-760).
- Imeson, A. P., & Humphreys, W. (1997). Microcrystalline cellulose. In A. P. Imeson (Ed.), *Thickening and Gelling Agents for Food* (2nd ed., pp. 180-197). United Kingdom: Chapman & Hall.
- Imeson, A. P., Ledward, D. A., & Mitchell, J. R. (1977). On the nature of the interaction between some anionic polysaccharides and proteins. *Journal of the Science of Food and Agriculture*, 28, 661-668.
- Ishigaki, T., Saito, H., & Fujita, A. (1994). Process for producing extruded noodle capable of being instantly cooked. US Patent 5332592: Ishigaki Foods Company Limited.
- Izydorczyk, M., Cui, S. W., & Wang, Q. (2005). Polysaccharide gums: structures, functional properties, and applications. In S. W. Cui (Ed.), *Food Carbohydrates: Chemistry, Physical Properties, and Applications*. Boca Raton: Taylor & Francis.
- Jacobs, H., & Delcour, J. A. (1998). Hydrothermal modifications of granular starch, with retention of the granular structure: A review. *Journal of Agriculture and Food Chemistry*, 46, 2895-2905.
- Jakubowski, H. (2013). Protein Structure. Retrieved 23 April 2015, from <http://employees.csbsju.edu/hjakubowski/classes/ch331/protstructure/olhydrophobprot.html>
- Jane, J.-I. (1993). Mechanism of starch gelatinisation in neutral salt solutions. *Starch - Stärke*, 45, 161-166.

- Jane, J.-I. (2009). Structural features of starch granules II. In J. BeMiller & R. Whistler (Eds.), *Starch: Chemistry and Technology* (3rd ed.). San Diego, CA: Academic Press.
- Jane, J.-I., Shen, L., Wang, L., & Maningat, C. C. (1992). Preparation and properties of small-particle corn starch. *Cereal Chemistry*, *69*, 280-283.
- Jarowenko, W. (1986). Acetylated starch and miscellaneous organic esters. In O. B. Wurzburg (Ed.), *Modified Starches: Properties and Uses* (pp. 55-78). Boca Raton, FL: CRC Press.
- Jiang, B., Kasapis, S., & Kontogiorgos, V. (2012). Fundamental considerations in the effect of molecular weight on the glass transition of the gelatin/cosolute system. *Biopolymers*, *97*(5), 303-310.
- Jiang, X., Jiang, T., Gan, L., Zhang, X., Dai, H., & Zhang, X. (2012). The plasticizing mechanism and effect of calcium chloride on starch/poly(vinyl alcohol) films. *Carbohydrate Polymers*, *90*, 1677-1684.
- Kasapis, S. (2005). Glass Transition Phenomena in Dehydrated Model Systems and Foods: A Review. *Drying Technology*, *23*(4), 731-757.
- Kasapis, S. (2008). Phase Separation in Biopolymer Gels: A Low- to High-Solid Exploration of Structural Morphology and Functionality. *Critical Reviews in Food Science and Nutrition*, *48*(4), 341-359.
- Kasapis, S., Al-Marhoobi, I. M., Deszczynski, M., Mitchell, J. R., & Abeysekera, R. (1993). Gelatin vs. polysaccharide in mixture with sugar. *Biomacromolecules*, *4*, 1142-1149.
- Kasapis, S., Morris, E. R., Norton, I. T., & Brown, C. R. T. (1993). Phase-Equilibria and gelation in gelatin maltodextrin systems .3. phase-separation in mixed gels. *Carbohydrate Polymers*, *21*, 261-268.
- Katopo, L., Kasapis, S., & Hemar, Y. (2012). Segregative phase separation in agarose/whey protein systems induced by sequence-dependent trapping and change in pH. *Carbohydrate Polymers*, *87*, 2100-2108.

- Kearsley, M. W., & Sicard, P. J. (1989). The chemistry of starches and sugars present in food. In J. Dobbing (Ed.), *Dietary Starches and Sugars in Man: A Comparison* (pp. 1-34). London: Springer.
- Kerr, R. W., & Cleveland, F. C. (1962). Thickening Agent and Method of Making the Same: US Patent 3021222.
- King, W., Trubiano, P. C., & Perry, P. (1976). Modified starch encapsulating agent offer superior emulsification, film forming, and low surface oil. *Food Product Development, Dec*, 54-57.
- Klemm, D., Heublein, B., Fink, H.-P., & Bohn, A. (2005). Cellulose: Fascinating Biopolymer and Sustainable Raw Material. *Angewandte Chemie International Edition*, 44(22), 3358-3393.
- Kunz, W., Henle, J., & Ninham, B. W. (2004). 'Zur Lehre von der Wirkung der Salze' (about the science of the effect of salts): Franz Hofmeister's historical papers. *Current Opinion in Colloid and Interface Science*, 9, 19-37.
- Labuza, T. P., Tannenbaum, S. R., & Karel, M. (1970). Water Content and stability of low-moisture and intermediate-moisture foods. *Food Technology*, 24.
- Larsson, H. (2002). Effect of pH and sodium chloride on wheat flour dough properties: ultracentrifugation, and rheological measurements. *Cereal Chemistry*, 79, 544-545.
- Lawrence, T. E., Dikeman, M. E., Stephens, J. W., Obuz, E., & Davis, J. R. (2004). In situ investigation of the calcium-induced proteolytic and salting-in mechanisms causing tenderization in calcium-enhanced muscle. *Meat Science*, 66, 69-75.
- Levine, H., & Slade, L. (1989). A food polymer science approach to the practice of cryostabilization technology. *Comments on Agricultural and Food Chemistry*, 1, 315-396.
- Lewith, S. (1888). Zur lehre der wirkung der salze. Erste mittheilung. *Arch Exp Pathol Pharmacol.*, 24, 1-16.



- Liu, Q. (2005). Understanding starches and their role in foods. In S. W. Cui (Ed.), *Food Carbohydrates: Chemistry, Physical Properties, and Applications*. Boca Raton: Taylor & Francis
- Lorenz, K., & Kulp, K. (1981). Heat-moisture treatment of starches. II. Functional properties and baking potential. *Cereal Chemistry*, 58, 49-52.
- Luallen, T. E. (2002). A comprehensive review of commercial starches and their potential in foods. In A. L. Branen, P. M. Davidson, S. Salminen & J. H. Torngate (Eds.), *Food Additives* (pp. 757-807). New York: Marcel Dekker.
- MacDonald, G. A., Lanier, T. C., & Giesbrecht, F. G. (1996). Interaction of sucrose and zinc for cryoprotection of surimi. *Journal of Agriculture and Food Chemistry*, 44, 113-118.
- Marchessault, R. H., & Sundararajan, P. R. (1983). Cellulose. In G. O. Aspinall (Ed.), *The Polysaccharides* (Vol. 2, pp. 11). New York: Academic Press.
- Marotta, N. C., & Trubiano, P. C. (1969). Pulpy Textured Food Systems Containing Inhibited Starches: US Patent 3443964.
- Matser, A. M., & Steeneken, P. A. M. (1997). Rheological properties of highly cross-linked waxy maize starch in aqueous suspensions of skim milk components. Effects of the concentration of starch and skim milk components. *Carbohydrate Polymers*, 32, 297-305.
- McClements, D. J. (2002). Modulation of Globular Protein Functionality by Weakly Interacting Cosolvents. *Critical Reviews in Food Science and Nutrition*, 42, 417-471.
- Medcalf, D. G., Youngs, V. L., & Gilles, K. A. (1968). Wheat Starches. II. Effect of Polar and Nonpolar Lipid Fractions on Pasting Characteristics. *Cereal Chemistry*, 45, 88-95.
- Mercier, C., Charbonniere, R., Gallant, D. J., & Delagueriviere, J. F. (1980). Formation of amylose-lipid complexes by twin-screw extrusion cooking of manioc starch. *Cereal Chemistry*, 57, 4-9.
- Mercier, C., Charbonniere, R., Gallant, D. J., & Guilbot, A. (1979). Structural modifications of various starches by extrusion cooking with twin-screw

- French extruder. In J. M. V. Blanshard & J. R. Mitchell (Eds.), *Polysaccharides in Food* (pp. 153-170). London: Butterworths.
- Michon, C., Cuvelier, G., Launay, B., Parker, A., & Takerkart, G. (1995). Study of the compatibility/incompatibility of gelatin/iota-carrageenan/water mixtures. *Carbohydrate Polymers*, 28, 333-336.
- Mishra, S., & Rai, T. (2006). Morphology and functional properties of corn, potato and tapioca starches. *Food Hydrocolloids*, 20(5), 557-566.
- Mitan, F. J., & Jokay, L. (1969). Process of Coating Food: US Patent 3427951.
- Momany, F. A., & Willett, J. L. (2002). Molecular dynamics calculations on amylose fragments. I. Glass transition temperatures of maltodecaose at 1, 5, 10, and 15.8% hydration. *Biopolymers*, 63(2), 99-110.
- Morris, E. R. (2009). Functional interactions in gelling biopolymer mixtures. In S. Kasapis, I. T. Norton & J. B. Ubbink (Eds.), *Modern Biopolymer Science* (pp. 167-198). Oxford: Elsevier.
- Morris, V. J. (1986). Multicomponent gels. In G. O. Phillips, D. J. Wedlock & P. A. Williams (Eds.), *Gums and Stabilisers for the Food Industry 3* (pp. 87-99). London: Elsevier.
- Morrison, W. R., Law, R. V., & Snape, C. E. (1993). Evidence for Inclusion Complexes of Lipids with V-amylose in Maize, Rice and Oat Starches. *Journal of Cereal Science*, 18, 107-109.
- Morrison, W. R., Tester, R. F., Gidley, M. J., & Karkalas, J. (1993). Resistance to acid hydrolysis of lipid-complexed amylose and lipid-free amylose in lintnerised waxy and non-waxy barley starches. *Carbohydrate Research*, 245, 289-302.
- Muchin, M. A., Wajnermann, E. S., & Tolstogusow, W. B. (1976). Complex gels of proteins and acidic polysaccharides. *Die Nahrung*, 20, 313-319.
- Nishinari, K., Watase, M., Miyoshi, E., Takaya, T., & Oakenfull, D. (1995). Effects of sugar on the gel-sol transition of agarose and  $\kappa$ -carrageenan. *Food Technology*, October, 90-96.

- Nishinari, K., Watase, M., Williams, P. A., & Phillips, G. O. (1990).  $\kappa$ -Carrageenan gels: Effect of sucrose, glucose, urea and guanidine hydrocolloid on the rheological and thermal properties. *Journal of Agriculture and Food Chemistry*, *38*, 1188-1193.
- Noisuwan, A., Hemar, Y., Wilkinson, B., & Bronlund, J. E. (2009). Dynamic Rheological and Microstructural Properties of Normal and Waxy Rice Starch Gels Containing Milk Protein Ingredients. *Starch-Starke*, *61*, 214-227.
- Ong, M. H., Whitehouse, A. S., Abeysekera, R., Al-Ruqaie, I. M., & Kasapis, S. (1998). Glass transition-related or crystalline forms in the structural properties of gelatin/oxidised starch/glucose syrup mixtures. *Food Hydrocolloids*, *12*, 273-281.
- Oostergetel, G. T., & van Bruggen, E. F. J. (1993). The crystalline domains in potato starch granules are arranged in a helical fashion. *Carbohydrate Polymers*, *21*, 7-12.
- Otto, B. W. (2006). Modified Starches *Food Polysaccharides and Their Applications* (2nd ed., pp. 87-118): CRC Press.
- Perez, S., Baldwin, P. M., & Gallant, D. J. (2009). Structural features of starch granules I. In J. BeMiller & R. Whistler (Eds.), *Starch: Chemistry and Technology* (3rd ed.). San Diego, CA: Academic Press.
- Polyakov, V. I., Grinberg, V. Y., & Tolstoguzov, V. B. (1997). Thermodynamic incompatibility of proteins. *Food Hydrocolloids*, *11*, 171-180.
- Pomeranz, Y. (1985). *Functional Properties of Food Components*. Orlando, FL.: Academic Press.
- Rahman, M. S. (1999). Glass transitions and other structural changes in foods. In M. S. Rahman (Ed.), *Handbook of food preservation* (pp. 75-93). New York: Marcel Dekker.
- Rahman, M. S. (2006). State diagram of foods: Its potential use in food processing and product stability. *Trends in Food Science and Technology*, *17*, 129-141.

- Rahman, M. S., & Labuza, T. P. (1999). Water activity and food preservation. In M. S. Rahman (Ed.), *Handbook of food preservation* (pp. 339-382). New York: Marcel Dekker.
- Rao, M. A. (2003). Phase transitions, food structure and texture. In B. M. McKenna (Ed.), *Texture in Food Volume 1: Semi-solid Foods* (pp. 36-62). Cambridge, UK: Woodhead Publishing Ltd.
- Rockland, L. B., & Nishi, S. K. (1980). Influence of water activity on food product quality and stability. *Food Technology*, 34, 42-51.
- Roller, S. (1996). Starch-derived fat mimetics: Maltodextrins. In S. Roller & S. A. Jones (Eds.), *Handbook of Fat Replacers* (pp. 99-118). Boca Raton: CRC Press.
- Rorrer, G. L., & Hawley, M. C. (1993). Vapor-phase HF solvolysis of cellulose: Modification of the reversion oligosaccharide distribution by in-situ methanolysis. *Carbohydrate Polymers*, 22, 9-13.
- Rowland, S. P. (1980). *Water in Polymers* (Vol. 127): American Chemical Society.
- Rutenberg, M. W., & Solarek, D. (1984). Starch derivatives: production and uses. In R. Whistler, J. N. BeMiller & E. F. Paschall (Eds.), *Starch: Chemistry and Technology* (pp. 314-388). New York: Academic Press Inc.
- Rutenberg, M. W., Tessler, M. M., & Kruger, L. (1975). Inhibited Starch Products Containing Labile and Non-Labile Cross-Links: US Patent 3899602.
- Salovaara, H. (1982). Effect of partial sodium chloride replacement by other salts on wheat flour dough rheology and breadmaking. *Cereal Chemistry*, 59, 422-426.
- Samir, M. A. S. A., Alloin, F., & Dufresne, A. (2005). Review of recent research into cellulosic whiskers, their properties and their application in nanocomposite field. *Biomacromolecules*, 6(2), 612-626.
- Schoch, T. J., & Maywald, E. C. (1968). Preparation and properties of various legume starches. *Cereal Chemistry*, 45, 564-573.

- Schorsch, C., Jones, M. G., & Norton, I. T. (1999). Thermodynamic incompatibility and microstructure of milk protein locust bean gum sucrose systems. *Food Hydrocolloids*, *13*, 89-99.
- Seib, P. A. (1996). *Starch Chemistry and Technology, Syllabus*. Manhattan, KS: Kansas State University.
- Setser, C. S., & Racette, W. L. (1992). Macromolecule replacers in food products. *Critical Reviews in Food Science and Nutrition*, *32*, 275-297.
- Silva, J. G., Morais, H. A., & Silvestre, M. P. C. (2003). Comparative study of the functional properties of bovine globin isolates and sodium caseinate. *Food Research International*, *36*, 73-80.
- Slade, L., & Franks, F. (2002). Appendix I: Summary report of the discussion symposium on chemistry and application technology of amorphous carbohydrates. In H. Levine (Ed.), *Amorphous Food and Pharmaceutical Systems*. Cambridge: The Royal Society of Chemistry.
- Slade, L., & Levine, H. (1987). Recent advances in starch retrogradation. In S. S. Stilva, V. Crescenzi & I. C. M. Dea (Eds.), *Industrial Polysaccharides* (pp. 387-430). New York: Gordon and Breach Sci.
- Slade, L., & Levine, H. (1989). A food polymer science approach to selected aspects of starch gelatinisation and retrogradation. In R. P. Millane, J. N. BeMiller & R. Chandrasekaran (Eds.), *Frontiers in Carbohydrate Research. I. Food applications* (pp. 215-270). London: Elsevier Applied Science.
- Slade, L., & Levine, H. (1991a). Beyond water activity - Recent advances based on an alternative approach to the assessment of food quality and safety *Critical Reviews in Food Science and Nutrition*, *30*, 115-360.
- Slade, L., & Levine, H. (1991b). A Food Polymer Science Approach to Structure-Property Relationships in Aqueous Food Systems: Non-Equilibrium Behavior of Carbohydrate-Water Systems. In H. Levine & L. Slade (Eds.), *Water Relationships in Foods* (Vol. 302, pp. 29-101): Springer US.
- Slade, L., & Levine, H. (1994). Water and the glass transition — Dependence of the glass transition on composition and chemical structure: Special implications

- for flour functionality in cookie baking. *Journal of Food Engineering*, 22, 143-188.
- Srivastava, H. C., & Patel, M. M. (1973). Viscosity stabilization of tapioca starch. *Starch - Stärke*, 25, 17-21.
- Stainsby, G. (1980). Proteinaceous gelling systems and their complexes with polysaccharides. *Food Chemistry*, 6, 3-14.
- Stute, R. (1992). Hydrothermal modification of starches: the difference between annealing and heat-moisture treatment. *Starch - Stärke*, 6, 205-214.
- Swinkels, J. J. M. (1985). Composition and Properties of Commercial Native Starches. *Starch - Stärke*, 37, 1-5.
- Syrbe, A., Fernandes, P. B., Dannenberg, F., Bauer, W., & Klostermeyer, H. (1995). Whey protein and polysaccharide mixtures: polymer incompatibility and its applications. In E. Dickinson & D. Lorient (Eds.), *Food Colloids and Macromolecules*. Cambridge, UK: The Royal Society of Chemistry.
- Tester, R. F., & Debon, S. J. J. (2000). Annealing of starch - a review. *International Journal of Biological Macromolecules*, 27, 1-12.
- Tolstoguzov, V. (2000). Phase behaviour of macromolecular components in biological and food systems. *Die Nahrung*, 5, 299-308.
- Tolstoguzov, V. (2006). Phase behaviour in mixed polysaccharide systems. In A. M. Stephen, G. O. Phillips & P. A. Williams (Eds.), *Food Polysaccharides and Their Applications* (2nd ed., pp. 589-627). Boca Raton: CRC Press.
- Tomasik, P., Wang, Y. J., & Jane, J.-l. (1995). Facile route to anionic starches. Succinylation, maleination and phthalation of corn starch on extrusion. *Starch - Stärke*, 47, 96-99.
- Trubiano, P. C. (1986). Succinate and substituted succinate derivatives of starch. In O. B. Wurzburg (Ed.), *Modified Starches: Properties and Uses* (pp. 131-148). Boca Raton, FL: CRC Press.
- Tschumak, G. J., Wajnermann, E. S., & Tolstogusow, W. B. (1976). Structure and properties of complex gels of gelatin and pectin. *Die Nahrung*, 20, 321-328.

- Tuason, D. C., Krawczyk, G. R., & Buliga, G. (2010). Microcrystalline Cellulose. In A. Imeson (Ed.), *Food Stabilisers, Thickeners and Gelling Agents* (pp. 218-236). United Kingdom: Blackwell Publishing Ltd.
- Wing, R. E., & Willett, J. L. (1997). Water soluble oxidised starches by reactive extrusion. *Industrial Crops and Products*, 7, 45-52.
- Wu, H. C. H., & Sarko, A. (1978a). The double-helical molecular structure of crystalline A-amylose. *Carbohydrate Research*, 61, 27-40.
- Wu, H. C. H., & Sarko, A. (1978b). The double-helical molecular structure of crystalline B-amylose. *Carbohydrate Research*, 61, 7-25.
- Xie, S. X., Liu, Q., & Cui, S. W. (2005). Starch modification and applications. In S. W. Cui (Ed.), *Food Carbohydrates: Chemistry, Physical Properties, and Applications*. Boca Raton: Taylor & Francis
- Yang, N., Liu, Y., Ashton, J., Gorczyca, E., & Kasapis, S. (2013). Phase behaviour and in vitro hydrolysis of wheat starch in mixture with whey protein. *Food Chemistry*, 137, 76-82.
- Ye, A. (2008). Complexation between milk proteins and polysaccharides via electrostatic interaction: principles and applications – a review. *International Journal of Food Science and Technology*, 43, 406-415.
- Zecher, D., & Gerrish, T. (1997). Cellulose derivatives. In A. Imeson (Ed.), *Thickening and Gelling Agents for Food* (pp. 60-85). London: Blackie Academic & Professional.
- Zeman, L., & Patterson, D. (1972). Effect of the Solvent on Polymer Incompatibility in Solution. *Macromolecules*, 5, 513-516.
- Zhang, Y., & Cremer, P. S. (2006). Interactions between macromolecules and ions: the Hofmeister series. *Current Opinion in Chemical Biology*, 10, 658-663.
- Zobel, H. F. (1988b). Starch Crystal Transformations and Their Industrial Importance. *Starch - Stärke*, 40, 1-7.

## CHAPTER 2

# MATERIALS AND METHODS

The purpose of this chapter is to describe the instrumentation, ingredients, chemicals, equipment and methodologies applied to this study. This includes the assessment of glass transition temperature ( $T_g$ ) by techniques such as dynamic mechanical analysis (DMA) and modulated differential scanning calorimetry (DSC). In addition, the characterisation of the physico-chemical properties of the materials utilised Fourier transform infrared spectrometry (FTIR), wide angle X-ray diffraction (WAXD), and scanning electron microscopy (SEM).

### 2.1 BASIC PRINCIPLES OF INVESTIGATIVE METHODS

#### 2.1.1 Rheological analysis –Dynamic Mechanical Analysis (DMA)

DMA is a technique that applies a small deformation in a periodic manner to a sample and then examines the material's response to stress, temperature, and frequency (Figure 2.1. and Menard, 1999). In this analysis, the material's response to an applied force is related to its stiffness. Thus, DMA provides information in regard to the modulus of the material. In DMA, an oscillation force is applied while a sample is being heated and this provides information on variation in stress response with temperature (Menard, 2008).

Young's modulus can be obtained from the slope of the stress-strain curve in the linear region, while applying a load to a material during mechanical analysis. The response of a material to a sinusoidal oscillating force can be determined from the complex modulus ( $E^*$ ) calculation, which consists of an elastic (storage) modulus ( $E'$ ) and a loss modulus ( $E''$ ) as expressed in Equation 2.1 (Menard, 2008).

$$E^* = E' + iE'' \quad (2.1)$$

$$\tan \delta = E''/ E' \quad (2.2)$$



The elastic response of a material is commonly defines as  $E'$  which is the storage modulus.  $E''$  is the energy stored within the material during the measurement cycle, which is the loss modulus, and is described as a material's viscous response. Hence, viscous flow with energy lost or heat dissipation is the loss modulus as illustrated in Figure 2.1.

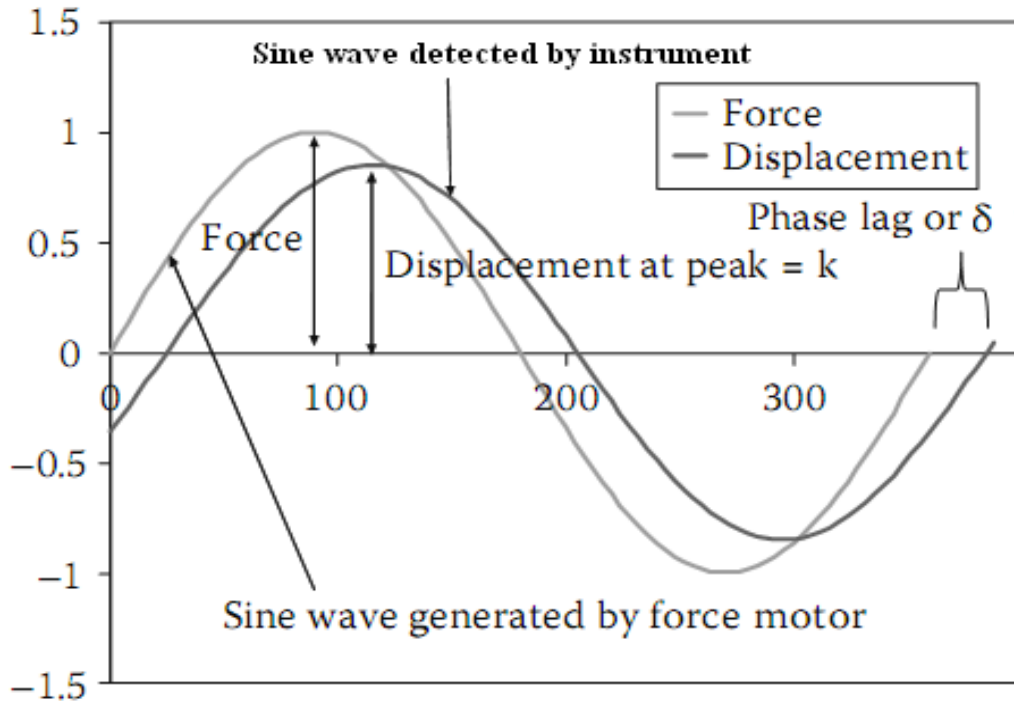


**Figure 2.1** A material with sinusoidal stress applied with an oscillating force supplied in DMA (Menard, 2008).

There are several geometric arrangements that can be used to apply stress to a material, and these are illustrated in Figure 2.2. All the geometric arrangements are stationary apart from the bulk compression where it is three dimensional, which moving is restrained with the sides. In this thesis chapter the tensile/ extensive geometry was used for all the analyses.

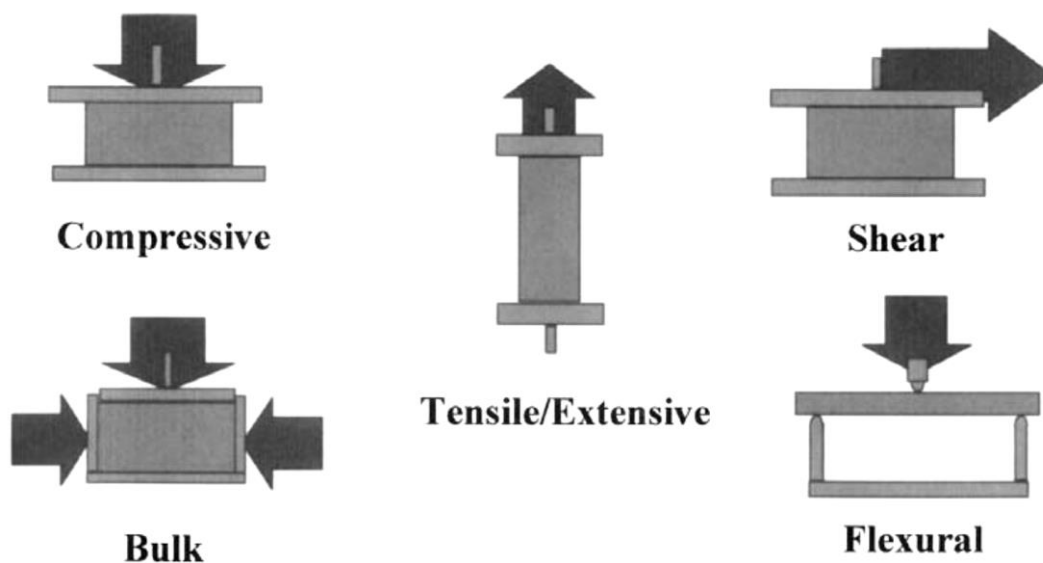


**Figure 2.2** Modes of deformation for DMA (Menard, 1999).

### 2.1.2 Thermal analysis – Modulated Differential Scanning Calorimetry (MDSC)

Modulated differential scanning calorimetry was used to analyse the enthalpy change occurring with the sample during heating and cooling. The enthalpy change can be determined as an endo- or/and exothermic outcome in the energy differentiates the materials nature. The glass transition was determined by the total heat flow which was a combination of the reverse and non-reverse heat flow during scanning. In a typical calorimetric analysis, a chemical change occurs in a sealed container which is isolated from the outside environment (Coleman, & Craig, 1996) and knowing the heat capacity ( $C_p$ ) of the container and the sample, and also any change in temperature ( $\Delta T$ ) of the system, the change in enthalpy for the process can be calculated from:

$$\Delta H = \Delta T C_p \quad (2.3)$$

Conventional DSC is a technique measuring the heat flow differences between a sample and an inert sample subject to time, and a function of temperature, with time, temperature, atmospheric and pressure conditions carefully controlled. It can differentiate between two types of thermal processes namely, exothermic by

measuring loss of heat energy and endothermic by measuring gain in heat energy. The area under the exo- or endothermic peaks is proportional to the heat energy released or absorbed by the sample during a particular process (Rahman, Machado-Velasco, Sosa-Morales, and Velez-Ruiz, 2009). In conventional DSC, the temperature regime experienced by the sample and reference is linear and the heating or cooling rates can be as fast as 200 °C/min or as slow as 0 °C/min (isothermal). Equation 2.4 can be used to describe either DSC or MDSC (Thomas, 2005) and Figure. 2.3 depicts the schematic diagram of a heat flux type DSC which operates accordingly the relation:

$$dQ/dt = Cp\beta + f(T,t) \tag{2.4}$$

where  $dQ/dt$  represents the heat flow,  $Cp$  is the heat capacity,  $\beta$  denotes heating rate and  $f(T,t)$  is the heat flow from kinetic processes.

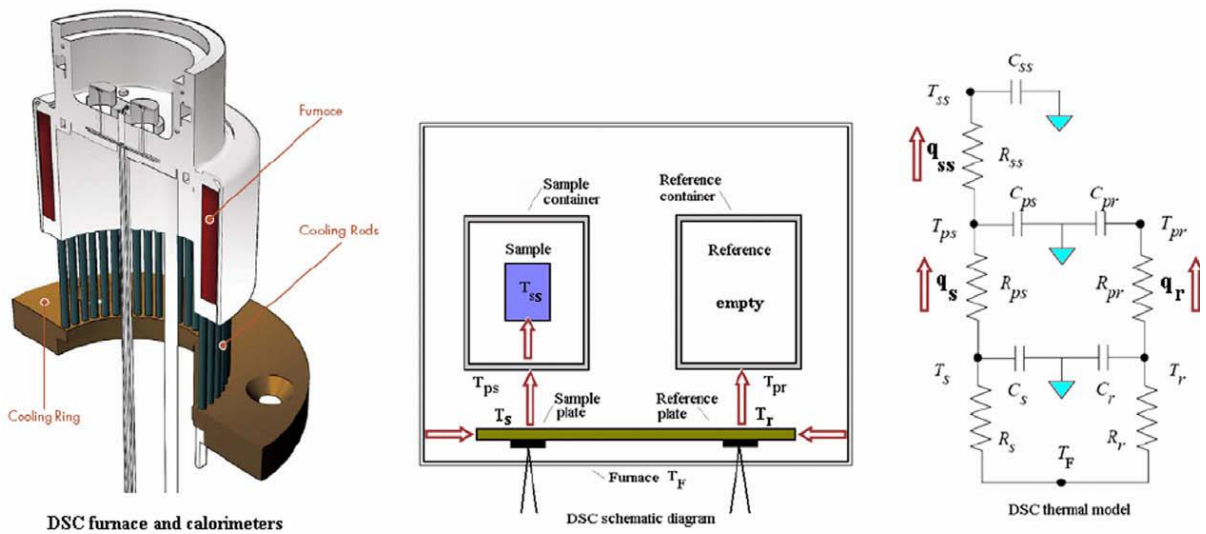


**Figure 2.3** Schematic diagram illustrating the DSC heat fluxes components and corresponding thermal model (Rady, 2009).

The use of a Modulated DSC signal enables the determination of the total and the two individual components thus leading to a better understanding of the complex and overlapping thermal transitions that may occur in materials. This is possible in modulated DSC as it uses two heating rates: average heating rate providing information on total heat flow and sinusoidal heating rate giving information on

heat capacity. The heat capacity component ( $Cp\beta$ , reversing heat flow) and kinetic component ( $f(T,t)$ , non-reversing heat flow) help to resolve complex transitions associated with a material. Reversing heat flow exhibits second order phase transition behavior such as glass transition whereas non-reversing heat flow represents first order phase transitions like melting, gelation etc. (TA Instruments, 2010).

In amorphous materials, moisture can act as a plasticiser, therefore, lower glass transition values have been observed. Broad endotherms typically in a heating profile typically indicate the loss of moisture (Rabel, Jona, Maurin, 1999). Figure 2.4 shows a series of MDSC thermogram from native wheat starch with excess (90%) water content and limited water content (25%) in the presence of sodium chloride 2% w/w total (Day et al, 2013).

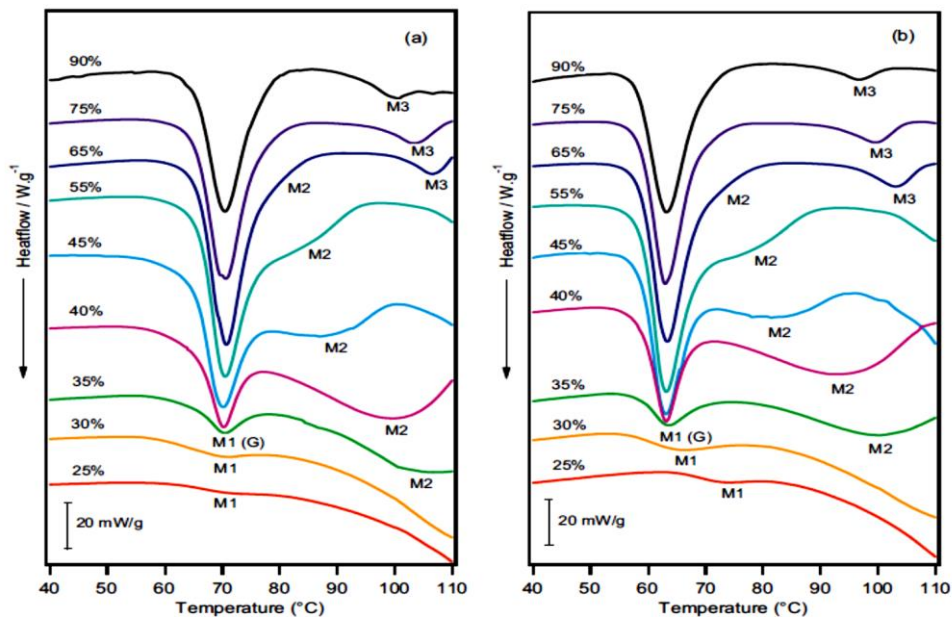


**Figure 2.4** DSC thermograms of wheat starch with water content varying from (90%) to (25%) with (a) 2% sodium chloride (% w/w) present and (b) no added salt (Day et al, 2013).

### 2.1.3 Chemical analysis – Fourier Transform Infra-Red Spectroscopy (FTIR)

Fourier Transform Infra-red Spectroscopy was used to gain information about the chemical structure of starch materials prepared in this work. In particular, the absorption peaks correspond to the vibration frequencies of the chemical bonds of the atoms making up the sample. In most systems, the wavelength normally ranges within the mid-infrared region ( $600\text{-}4000\text{cm}^{-1}$ ) which is recorded using either dispersive infrared analysis or FTIR. In most cases FTIR is preferred as it is faster and has a better signal to noise ratio (Yang & Zhang, 2011). Figure 2.5 illustrates the FTIR spectrum of a typical native starch sample (Kizil, Irudayaraj, & Seetharaman, 2002).

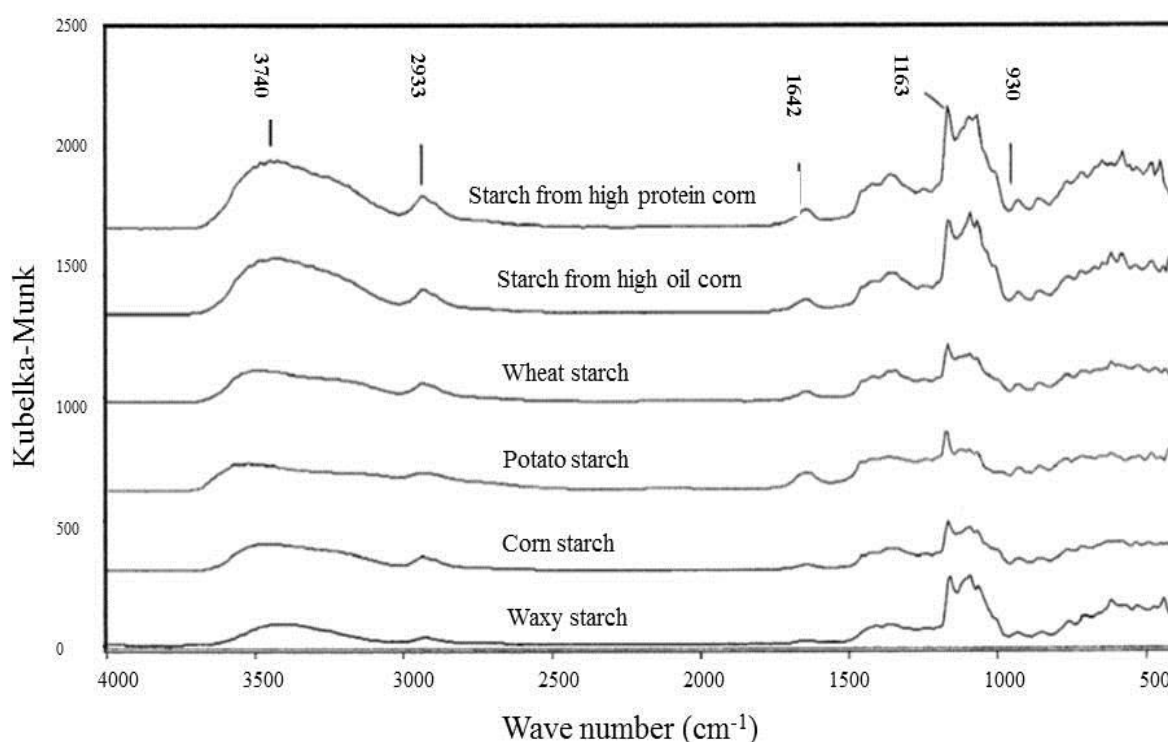


**Figure 2.5** FTIR spectra of native (non-irradiated) starches (Kizil, Irudayaraj, & Seetharaman, 2002).

#### *2.1.4 Crystallinity analysis – Wide Angle X-ray Diffraction (WAXD)*

When an incoming X-ray beam of a given frequency hits an atom, the electrons around the atom start to oscillate and re-emit X-rays at the same frequency in all directions. This results in both constructive and destructive interference effects such that ordered molecules in samples produce well-defined X-ray beams in particular directions according to the distance between molecular planes and lead to  $2\theta$  angles that can be estimated (Jenkins & Snyder, 1996, He, 2009). The X-ray diffraction measurement is usually taken at a particular scan rate, and the relative intensities of each peak within the  $2\theta$  range is calculated by dividing the area of a peak by the total area of all of the peaks observed from the relative crystallinity (Rindav-Westling, Standing, Hermansson and Gatenholm, 1998).

Thus, the fundamental principle of all X-ray diffraction phenomena is scattering of X-rays (Liebhafsky, Pfeiffer, Winslow and Zeman, 1966), and this is used to provide structural information regarding the structural of the materials at atomic resolution (I’Ason, Bacon, Lambart, Miles, Morris, Wright and Nave, 1987). WAXD scattering is a measure used for the determination of the degree of crystallinity and as well as assessing the unit cell dimensions in comparison to the small angle scattering which indicates information at the lamellar level (Mano, 2007).

The X-ray diffractograms can then be interpreted as exhibiting crystalline or amorphous behavior for material under investigation (Jenkins & Snyder, 2000). In the present work, this technique was used to investigate the crystallinity of the various starch samples prepared by admixture of sodium chloride, calcium and microcrystalline cellulose.

### *2.1.5 Structural analysis – Scanning Electron Microscope (SEM)*

The technique was employed to investigate the surfaces of the composite starch samples after heat treatment and the addition of co-solute. It was used to give tangible evidence for the uniformity, or otherwise, of the micro-structure of a sample depending on the manner in which it was prepared.

SEM produces an image of a material surface by scanning it with a beam of electrons that possess high-energy. The electrons interact with the molecules that constitute the material yielding signals containing information about the characteristics of the sample. These include surface morphology, sample conductivity and its composition. Secondary electrons, back scattered electrons (BSE), characteristic X-rays, specimen current and transmitted electrons are the different categories of outputs generated by SEM.

Secondary electron imaging is the common detection mode employed in SEM, and such mode can generate high-resolution images of a material's surface, with details ranging from 1 to 5nm in size. SEM also can produce a three-dimensional observation making it a valuable tool in characterizing the surface of a material. Such technique has a wide range of magnifications, i.e. from 25 to 250,000 times, with 250 times corresponding to the upper limit of the finest optical microscope.

## 2.2 MAJOR EQUIPMENT

### 2.2.1 *Diamond Dynamic Mechanical Analysis (DMA)*

The Diamond DMA from Perkin Elmer as illustrated in Figure 2.6 covers a wide modulus range from  $10^3$  up to  $10^{12}$  Pa. and uses Fourier Transform (FT) technology, which reduces signal noise. By increasing the numbers of measurement data points, more accurate viscoelastic data can be obtained (U.S.A. Patent 5287749, 5452614 by Perkin Elmer, 2003).



**Figure 2.6** Diamond DMA from Perkin Elmer (Perkin Elmer, 2003).



**Table 2.1** Specification for Diamond DMA in tension mode (Perkin Elmer, 2003)

<b>Deformation Range</b>	<b>Tension</b>
Measurement Range	$10^5$ - $10^{12}$ Pa
Maximum sample Size (Length x thickness x width)	5-35 x 3 x 10 mm
Probes	Metal
Application Mode	Dynamic measurement: Single wave Oscillation, Synthetic Oscillation Static Measurement: Program Stress Control, Program Strain Control
Frequency	Sine Wave Oscillation: 0.01-100 Hz (Max. 13 Frequencies) Synthetic Oscillation: Max. 5 Frequencies
Temperature Range	-150°C to 600°C
Automatic Cooling Accessory	Forced air or liquid nitrogen vaporisation method
Scanning Rate	0.01 – 20°C/min
Sample Length	Automated measurement
Atmosphere	Air, inlet gas, Swelling**, Humidity Control**
Maximum Load	Static: $\pm 10$ N Dynamic: $\pm 8$ N

\*Optional measuring systems

\*\*Optional

### 2.2.2 Differential scanning calorimeter from TA instrument, Model Q2000

The TA Instrument DSC Q2000 is shown in Figure 2.7. The Q2000 instrument has high performance features, especially the baseline flatness, and it is fitted with Advanced Tzero® technology.

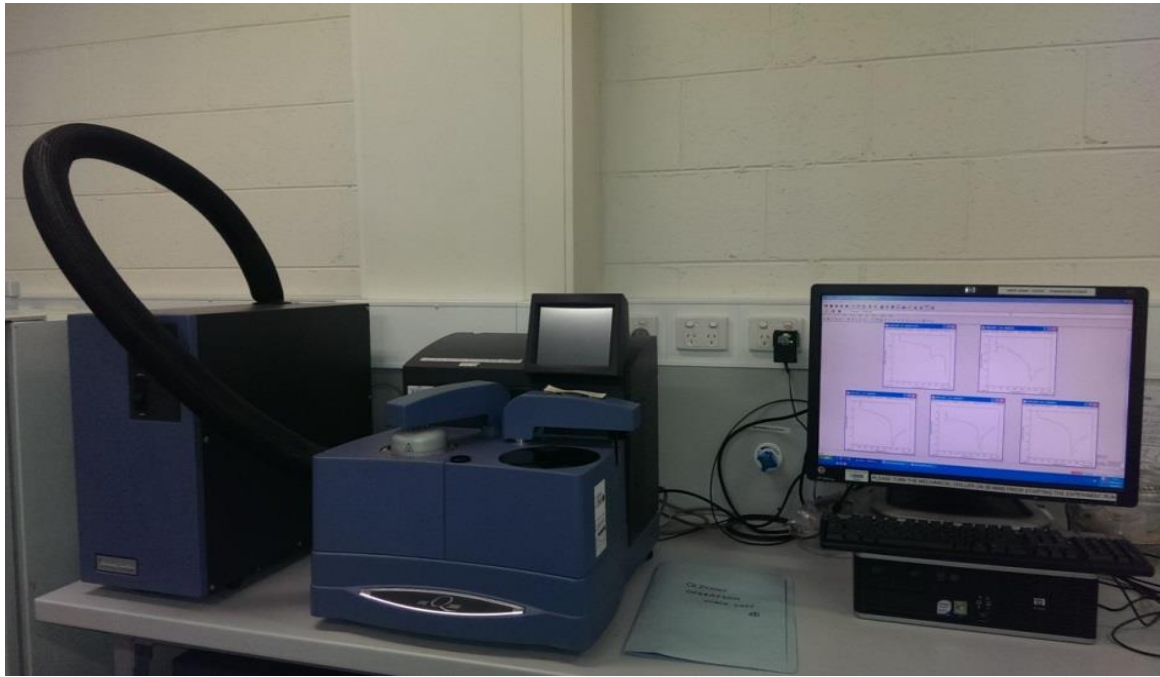


**Figure 2.7** Modulated DSC Q2000 from TA Instrument.

### *2.2.3 Fourier transform infrared spectrometry from Perkin Elmer Model Spectrum 100*

The Spectrum 100 FTIR spectrum is illustrated in Figure. 2.8. It is a highly sensitive instrument with advanced digital signal processing that reduces signal artefacts and improves response linearity.



**Figure 2.8** FTIR Spectrum 100 from Perkin Elmer (Antolasic, 2014).

#### *2.2.4 Wide angle X-ray instrument from Bruker Model - Endeavor D4*

This instrument (Figure 2.9) features a high precision 2 circle goniometer, modern X-ray optics and detectors which yield excellent analytical results. It can handle a wide variety of samples of different dimensions and consistency which can be loaded at the same time and can be analysed differently.

This work utilised the D4 Endeavor unit available within the Integrated Victorian X-ray structural Determination and Material Characterisation Facility located at RMIT University. It was equipped with a 66 position auto-sampler and innovative 1-dimensional X-ray detector Lynweye – which significantly reduces measurement time per sample.



**Figure 2.9** Wide angle X-ray Endeavor D4 from Bruker.

#### *2.2.5 Energy dispersive X-ray spectroscopy (EDX)*

A Philips XL30 SEM (Sussex, England) was used to determine the elemental composition of starch films. The non-conductive specimens were attached to sample holders followed by carbon coating with a thickness of 5nm. The specimens were irradiated excited with a 20kV electron beam and the emitted X-ray spectrum

recorded with an Oxford Instruments X-Max 20mm<sup>2</sup> detector (Oxford Instruments, Scott's valley, California, USA). The results were processed using Aztec software v3.1 (Oxford Instruments Nano analysis) to plot the EDX spectra and determine the element composition.

#### 2.2.6 Scanning electron microscope FEI Quanta 200 ESEM

Figure 2.10 illustrated the SEM used in this study, which is located the RMIT Microscopy and Microanalysis Facility (RMMF) and features three imaging modes – high-vacuum, low-vacuum and ESEM<sup>TM</sup>, hence accommodating the widest range of samples of any SEM system. It minimises the amount of sample preparation as low and ESEM vacuum capabilities enable charge-free imaging and analysis of non-conductive specimens and/or hydrated specimens.



**Figure 2.10** FEI Quanta 200 ESEM.

**Table 2.2** Description of instrumentation and equipment

<b>Equipment</b>	<b>Manufacturer/supplier</b>	<b>Model Number</b>
MDSC	TA Instruments	DSC Q2000
DMA	Perkin Elmer, MA, USA	DMA Diamond
FTIR	Perkin Elmer, MA, USA	Spectrum 100
SEM	FEI	FEI Quanta 200 ESEM
	Philips, Sussex, England	Philips XL30 SEM
WAXD	Germany	Bruker Endeavor D4

### *2.2.7 Apparatus and auxiliary systems*

**Table 2.3** Tabulated apparatus and auxiliary systems

<b>Apparatus</b>	<b>Maker</b>	<b>Model number</b>
Haake Rheomix OS	Haake	OS
Hot press	RMIT PolyLab Building 7	N/A
a <sub>w</sub> meter	Novasina	Set aw -1
Gravity and forced convection oven	SEM	18
Analytical balance	Mettler Toledo	AE200
Karl Fisher titrator	Mettler Toledo	EasyPlus
Desiccator	Duran	24 781 61
Type two water system	Millipore	Elix ® 10 – control Filter – Progard ® 2W/O polyphosphate

**Table 2.4** Ingredients information

<b>Ingredients</b>	<b>Supplier</b>	<b>Country of origin</b>	<b>Item number</b>	<b>Batch code</b>
Potato starch	Penford	Europe	Potato starch	TDI-474-01
Cassava starch	Scalzo	Thailand	TAPFLR05	
Sodium chloride (co-solute in the potato starch)	Sigma Aldrich	USA	S7653	038K0097
Calcium chloride	Sigma Aldrich	USA	C1016	109K1483
Microcrystalline cellulose Avicel ® PH-101	Sigma Aldrich	Ireland	11363	BCBD6133
Lithium chloride (RH11%)	LabChem	Australia	-	-
Potassium acetate (RH23%)	BDH	England	-	K20357982 350
Magnesium chloride (RH33%)	Merck	Germany	-	-
Sodium bromide (RH58%)	BDH	England	-	-
Magnesium acetate (RH65%)	Merck	Germany	-	-
Sodium chloride (RH75%)	Merck	France	-	7581KVKL-2
Type 2 water	Millipore	France	Elix ® 10 – control Filter – Progard ® 2W/O polyphosphate	Type 2 water

## **2.3 SAMPLE PREPARATION**

### *2.3.1 Potato starch with the co-solutes in the sample formulations*

#### *2.3.1.1 Potato starch with sodium chloride*

Potato starch powder with an original moisture content of 18.34% w/w was analysed by the oven method using an oven temperature of 102°C overnight. It was then carefully weighed out with the required amount of sodium chloride in the formulation from 0.0% w/w up to 6.0% w/w. A sufficient amount of Millipore type 2 water was added to each sodium chloride/potato starch mixture to achieve a total moisture content of 35.0% w/w. Each sample was transferred to the Haake Rheomix OS (refer to Figure 2.11) at a screw mixing speed of 200 rpm for 2 min at ambient temperature, and then transferred to a stainless steel metal frame to produce a potato composite sheet.

To prevent the starch sheet sticking to the hot press, a heat proof plastic film was placed on the top and bottom of the stainless steel frame with the starch composite sandwiched between. Then, a flat stainless steel metal sheet was placed on the top and bottom of the plastic film with the previous items inside. The assembled sample was then transferred to the hot press (refer to Figure 2.12) for heat treatment at 120°C for 7 min, under a pressure of 59 Bar.

The sample was then cooled to between 40-50°C before being taken out of the hot press. The starch sample was then removed from the stainless steel frame with the plastic films still adhering on the top and the bottom of the sample, and the sandwiched sample transferred into a clean air, and moisture/gas impermeable vacuum bag. The bag was then sealed with a handheld heat sealer and transferred into a refrigerator at 4°C until further experimentation.



**Figure 2.11** Haake Rheomix OS from Thermo Scientific.

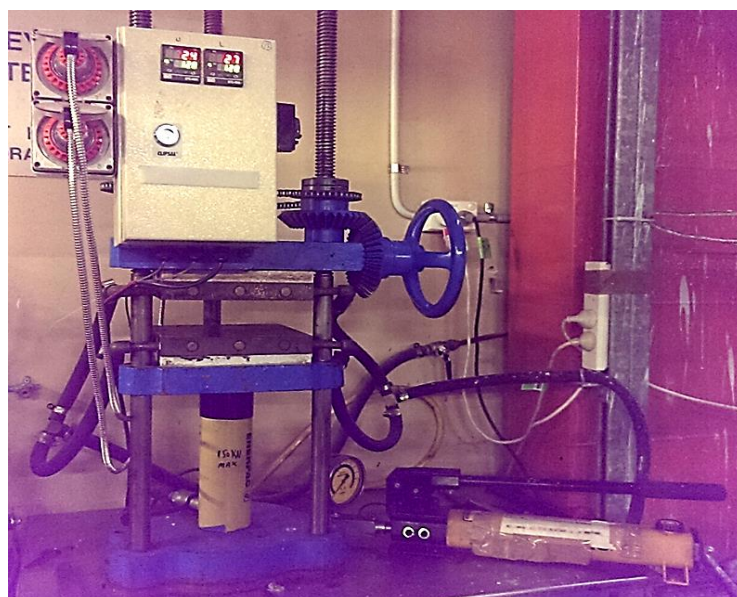


**Figure 2.12** Hot press used in this work

### *2.3.1.2 Potato starch with calcium chloride*

The same potato starch, as for the sodium chloride experiments, was used in this part of the work. Apart from the moisture content being changed slightly to 15.08% w/w, it was also analysed for its moisture content by the oven method and then the co-solute, calcium chloride, was added to the composite up to 6.0% w/w, whilst maintaining the initial moisture content at 35.0% w/w. The rest of the preparation



protocol is identical to the one described in the preceding section for sodium chloride.

### *2.3.1.3 Potato starch with MCC*

The original moisture content of the potato starch was the same as for the moisture content used for the potato starch used in the earlier work; as confirmed with the oven method as described previously. The moisture content of the MCC sample was determined by the Karl Fisher titrator instrument from Mettler Toledo (Model Easy Plus) and it was found to be 4.1% w/w. The actual part of the experimental sample preparation was as before with a moisture content of 35.0% w/w and the concentration of the co-solute MCC ranging from 0.0% w/w up to 6.0% w/w being added to the starch.

### *2.3.1.4 Relative humidity equilibration for the potato starch and its co-solutes*

Potato starch samples with the desired amount and type of co-solute were removed from the fridge to warm to room temperature before were cut, using a sharp stainless steel surgical knife, into shapes of 40mm x 1mm x 40mm for DMA analysis, 10mm x 1mm x 10mm for X-ray, FTIR, SEM analysis, and small granules for DSC analysis. They were then stored in each saturated salt solution desiccator: lithium chloride (RH 11%), potassium acetate (RH 23%), magnesium chloride (RH 33%), sodium bromide (RH 58%), magnesium acetate (RH 65%) and sodium chloride (RH 75%) as per Table 2.5. This lists the water-to-salt ratio to reach saturation for each preparation and the levels of RH achieved.

The moisture level in each sample was analysed with the oven method at 102°C overnight for each material and Table 2.6 summarizes moisture contents and relative humidity for each experimental combination: potato starch with co-solute (sodium chloride, calcium chloride, microcrystalline cellulose), and tapioca starch with co-solute (sodium chloride, calcium chloride). A series of RH chambers made for this work is illustrated in Figure 2.13. An equilibration period of at least 4-8

weeks before instrumental analysis was employed to ensure adequate RH levels had been reached within the samples before instrumental analysis was undertaken. These were checked with the Novasina water activity meter weekly to ensure adequate equilibration in each material had been reached before instrumental work was finally carried out.

**Table 2.5** Information on the preparation of saturated salt solution known as the “solubility table”

Salt	Chemical formulation for the salts	Amount of salt to reach saturation at 20°C/100mL of water	Relative humidity (%) at 20°C
Lithium chloride	LiCl	83.5	11
Potassium acetate	CH <sub>3</sub> COOK	256	23
Magnesium chloride	MgCl <sub>2</sub> ·6H <sub>2</sub> O	54.3	33
Sodium bromide	NaBr	90.8	58
Magnesium acetate	Mg(CH <sub>3</sub> COO) <sub>2</sub> ·4H <sub>2</sub> O	53.4	65
Sodium chloride	NaCl	35.9	75



**Figure 2.13** Series of relative humidity chambers (RH11% to RH75%) made with DURAN glass desiccators.

**Table 2.6** Relative humidity with moisture content measured from the starch/co-solute samples

<b>Salt</b>	<b>Relative humidity (%)</b>	<b>Potato starch/ NaCl/CaCl<sub>2</sub> moisture content (%<sub>w/w</sub>)</b>	<b>Tapioca starch/ NaCl/CaCl<sub>2</sub> moisture content (%<sub>w/w</sub>)</b>	<b>Potato starch/ MCC moisture content (%<sub>w/w</sub>)</b>
Lithium chloride	11	3.57	-	4.15
Potassium acetate	23	8.01	7.34	6.51
Magnesium chloride	33	11.63	-	8.22
Sodium bromide	58	13.56	10.44	14.26
Magnesium acetate	65	15.66	-	15.80
Sodium chloride	75	18.83	19.52	17.48

### 2.3.2 Tapioca starch with co-solutes in the sample formulations

#### 2.3.2.1 Tapioca starch with sodium chloride

Tapioca starch with an original moisture content of 12.1% w/w was obtained from Thailand, and was weighed out with the co-solute of sodium chloride co-solute according to the concentration required, with samples ranging from 0.0% w/w up to 6.0% w/w salt. The moisture content was taken up to 35.0% w/w as per the previous potato starch/co-solutes and the remaining experimentation was as described earlier.

#### 2.3.2.2 Tapioca starch with calcium chloride

The same sample preparation was performed for the tapioca starch with the co-solute of calcium chloride instead of sodium chloride. The concentration of calcium

chloride ranged from 0.0% w/w up to 6.0% w/w, and the final total moisture was constant at 35.0% w/w of the composite, which was followed by the aforementioned standard routine of experimentation.

### *2.3.2.3 Relative humidity equilibration for the tapioca starch and its co-solutes*

Relative humidity chambers were prepared for 23% (potassium chloride), 58% (sodium bromide) and 75% (sodium chloride). The moisture contents were measured periodically over 4-8 weeks until each chamber was equilibrated to the expected relative humidity.

## **2.4 EXPERIMENTAL METHODS**

### *2.4.1 DMA*

DMA analysis was carried out with a heating profile from -110°C to +180°C at 2°C/min, L amplitude at 10µm, minimum compression force gain at 0.01mN, tension (sinusoidal oscillation) measuring mode at 1Hz. The measuring volume of the sample was 10mm x 10mm x 1mm.

### *2.4.2 DSC*

DSC samples were equilibrated at 40°C for 2 minutes, modulate at  $\pm 0.53^\circ\text{C}$  every 40s, ramped from +40°C to +200°C, cooled from +200°C to -90°C then heated up again from -90°C to +200°C at a 10°C/min heating/cooling rate for both sodium chloride and calcium chloride with either potato or tapioca starch samples. The potato starch/microcrystalline cellulose samples were examined according to the same experimental protocol. The samples ranged in mass from 2-6 mg depending on the moisture content, and were carefully weighed out using an empty pan to serve as the reference sample.

### 2.4.3 FTIR

Each sample was scanned over the wave number range 650 to 4500 $\text{cm}^{-1}$  with a scan frequency of 32 times to give a clear image, with the sample being analysed at ambient temperature.

### 2.4.4 WXR

WXR analysis was done at a scan rate of 0.1° from 5 to 90° angle at 2 $\theta$  degree scaling at ambient temperature.

### 2.4.5 EDX

The carbon coated specimens with a thickness of 5nm were excited with an electron beam at 20kV and the emitted specific X-rays at different energy levels were recorded with a detector. This was only used for the calcium chloride with potato starch to confirm its ionisation in the samples.

### 2.4.6 SEM

#### 2.4.6.1 Potato starch with sodium chloride

Images were taken of samples with the dimensions of 10mm x 1mm x 10mm for all RH conditions. Samples were placed on a clean aluminum stud with a round platform and a double sided carbon sticky tape to prevent excess noise creation during scanning. The measuring chamber parameters were: low vacuum, 30kV, with spot size of 5.0 and an LFD detector used for imaging. The measuring magnification was taken at 1600X and the working distance was between 6.8 to 7.7 mm.

#### 2.4.6.2 Potato starch with calcium chloride

Images were taken of samples with the dimensions of 10mm x 1mm x 10mm for the whole series of the RH conditions. Samples were placed on a clean round platform

with double sided carbon sticky tape in between to avoid excess noise created from the beam. The measuring chamber's condition was set at 20kV, with a spot size of 2.5 and the LFD detector LFD used for imaging. Measuring magnification was at 2400X for all samples and the working distance was between 10.0 to 12.2 mm.

#### *2.4.6.3 Potato starch with MCC*

To obtain images for starch/MCC, samples were shaped to 10mm x 10mm x 1mm prior to loading into the SEM. Each sample was attached with double sided carbon sticky tape to prevent excess noise generated with the electron beam. Images were taken of the cross sections of the material with conditions set at 20kV, with spot size of 5.0, LFD detector and at the low vacuum mode of 0.50Torr. The measuring magnification was at 3000X for all samples and the working distance was between 10.5 to 11.1mm.

#### *2.4.6.4 Tapioca starch with sodium chloride*

SEM images were taken of samples with 10mm x 10mm x 1mm dimensions in cross section. The measurements in the chamber were performed in low vacuum mode at 0.05 Torr, spot size of 5.0, LFD detector, and a 20kV high voltage beam. The magnification of the image was taken at 2400X for all samples and the working distance was between 10 to 11mm.

#### *2.4.6.5 Tapioca starch with calcium chloride*

SEM images were taken of the sample's cross section, with a sample size of 10mm x 10mm x 1mm. Image taking conditions inside the sample chamber were set to a high voltage beam at 20kV, LFD detector, and spot size at 5.0 and a low vacuum condition of 0.05 Torr. The working distance to the sample was between 10 to 11mm at a magnification of 2400X for all images.

## 2.5 REFERENCES

- Antolasic F. (2014). FTIR Spectrum 100. Retrieved on 30 March 2015.  
<http://minyos.its.rmit.edu.au>
- Coleman, N. J., & Craig, D. Q. M. (1996). Modulated temperature differential scanning calorimetry: a novel approach to pharmaceutical thermal analysis. *International Journal of Pharmaceutics*, 135, 13-29.
- Day, L., Fayet, C., & Homer, S. (2013). Effect of NaCl on the thermal behaviour of wheat starch in excess and limited water. *Carbohydrate Polymers*, 94, 31-37.
- FEI.Quanta™ Scanning Electron Microscope (2006). Retrieved on 30 March 2015.  
[http://mtrmika.technion.ac.il/wp-content/uploads/2013/12/2006\\_06\\_Quanta200\\_pb1.pdf](http://mtrmika.technion.ac.il/wp-content/uploads/2013/12/2006_06_Quanta200_pb1.pdf)
- I'Ason, K. J., Bacon, J. R., Lambart, N., Miles, M. J., Morris, V. J., Wright, D. J., & Nave, C. (1987). Synchrotron radiation wide-angle X-ray scattering studies of glycinin solutions. *International Journal of Biological Macromolecules*, 9, 386-370.
- Jenkins, R. (2000). X-ray Techniques: Overview Encyclopedia of Analytical Chemistry. John Wiley & Sons. Retrieved on 27 April 2015.  
[https://facultystaff.richmond.edu/~jbell2/sb36801\\_EAC.pdf](https://facultystaff.richmond.edu/~jbell2/sb36801_EAC.pdf).
- Kizil, R., Irudayaraj, J., & Seetharaman, K. (2002). Characterisation of irradiated starches by using FT-Raman and FTIR spectroscopy. *Journal of Agricultural and Food Chemistry*, 50, 3912-2918.
- Liebhafsky, H. A., Pfeiffer, H. G., Winslow, E. H., & Zeman, P. D. (1966). X-ray absorption and emission in Analytical chemistry. 2nd ed, John Wiley & Sons, INC. p 24.
- Mano, J. F. (2007). Structural evaluation of amorphous phase during crystallisation of poly(L-lactic acid): A synchrotron wide-angle X-ray scattering study. *Journal of Non-Crystalline Solids*, 353, 2567-2572.
- Menard, K. P. (1999). Dynamic mechanical analysis: a practical introduction. CRC Press, Boca Raton.

- Menard, K. P. (2008). *Dynamic mechanical analysis: a practical introduction*. 2nd edition, CRC Press, Boca Raton.
- Brochure TMA DMA, (2003). Perkin Elmer. Retrieved on 28 April 2015.
- Rabel, S. R., Jona, J. A., Maurin, M. B. (1999). Applications of modulated differential scanning calorimetry in preformulation studies. *Journal of Pharmaceutical and Biomedical Analysis*, 21, 339-345.
- Rahman, M. S., Machado-Velasco, K. M., Sosa-Morales, M. E., & Velez-Ruiz, J. F. (2009). Freezing Point: Measurement, Data, and Prediction. In M. S. Rahman (Ed.), *Food Properties Handbook* (2nd ed., pp 153-192). Boca Raton: CRC.
- Rindav-Westling, A., Standing, M., Hermansson, A., & Gatenholm, P. (1998). Structure mechanical and barrier properties of amylose and amylopectin films. *Carbohydrate Polymers*, 36, 217-224.
- Solubility table, (2015). Retrieved on 29 April 2015.  
[http://en.wikipedia.org/wiki/Solubility\\_table](http://en.wikipedia.org/wiki/Solubility_table)
- TA Instruments (2010). (n.d.-b). *Differential Scanning Calorimeters*. Retrieved on 8 April 2015.  
<http://www.tainstruments.com/product.aspx?id=10&n=1&siteid=11>
- Thermo-Nicolet. (2001). *Introduction to Fourier Transform Infrared Spectrometry*. Retrieved on 8 April 2015. <http://mmrc.caltech.edu/FTIR/FTIRintro.pdf>.
- Yang, B., & Zhang, B. (2011). *Analytical methods in combinatorial chemistry*. 2nd ed. CRC Press. P 56.



# CHAPTER 3

## EFFECT OF SODIUM CHLORIDE ON THE GLASS TRANSITION OF CONDENSED STARCH SYSTEMS

*Based on a Journal article published in Food Chemistry as:  
“Effect of sodium chloride on the glass transition of condensed starch systems”*

### ABSTRACT

The present investigation deals with the structural properties of condensed potato starch-sodium chloride systems undergoing a thermally induced glass transition. Sample preparation included hot pressing at 120°C for 7min to produce extensive starch gelatinisation. The materials examined covered a range of moisture contents from 3.6 to 18.8%, which corresponded to relative humidity values of 11 and 75%. Salt addition was up to 6.0% in formulations. Instrumental work was carried out with dynamic mechanical analysis in tension, modulated differential scanning calorimetry, Fourier transform infrared spectroscopy, environmental scanning electron microscopy and wide angle X-ray diffraction. Experimental conditions ensured the development of amorphous matrices that exhibited thermally reversible glassy consistency. Both moisture content and addition of sodium chloride affected the mechanical strength and glass transition temperature ( $T_g$ ) of polymeric systems. Sodium ions interact with chemical moieties of the polysaccharide chain to alter considerably structural properties, as compared to the starch-water matrix.

**Keywords:** glass transition, sodium chloride, starch, high-solid systems

### 3.1 INTRODUCTION

Starch, from cereals, tubers and roots, is commonly used as the major food reserve to provide, at low cost, a bulk nutrient and energy source in the diet of man. In terms of techno-functionality, starch is able to impart thickening and gelling properties to processed foods where relatively small amounts of the material can bind large quantities of water bringing about a desirable change in textural consistency (Mishra, & Rai, 2006). Its biocompatibility and degradability afford additional application in pharmaceuticals, thermoplastics, paper, textile, etc. (Copeland, Blazek, Salman, & Tang, 2009).

In the main, starch has two major components, i.e. amylose, which is essentially a linear polymer of variable molecular size (approximately  $10^5$ - $10^6$ Da) comprising (1→4)-linked  $\alpha$ -D-glucopyranosyl units, and amylopectin, the major component of starch, which is a larger molecule than amylose with molecular weight of  $10^7$ - $10^9$  Da. The latter is a highly branched fraction, with the structure being built from chains of  $\alpha$ -D-glucopyranosyl residues linked together mainly by  $\alpha$ -(1→4) and 5-6%  $\alpha$ -(1→6) linkages (Considine, Noisuwan, Hemar, Wilkinson, Bronlund, & Kasapis, 2011).

Potato starch has an amylose-to-amylopectin ratio of 1:3 and contains large oval spherical granules, with their size ranging between 5 and 100 $\mu$ m (Zobel, & Stephen, 2006). It can be produced in a refined grade containing a minimal protein (0.2% Max) or fat (0.1% Max) content. This gives the starch powder a clear white colour and the cooked material characteristics of neutral taste, long texture and clarity with minimal tendency to solution yellowing (Alvani, Qi, & Tester, 2012). Phosphate is bound to the molecule of potato starch, as opposed to other botanical sources, giving the solution a slightly anionic character, high swelling power and a relatively low gelatinisation temperature of around 60°C, which is accompanied by high viscosity (Singh, Singh, Kaur, Sodhi, & Gill, 2003).

Sodium chloride (NaCl) is the most widely used salt in the food industry as preservative and flavour enhancer (Albarracín, Sánchez, Grau, & Barat, 2011). Sodium cation is the counterion for the chloride anion and *vice versa* in order to maintain electric neutrality. In the Hofmeister or lyotropic series, the order of cations is given as:  $\text{NH}_4^+ > \text{K}^+ > \text{Na}^+ > \text{Li}^+ > \text{Mg}^{2+} > \text{Ca}^{2+} > \text{Guanidinium}$  (Hofmeister, 1888; Kunz, Henle, & Ninham, 2004). Early members (on the left) of the series increase the solvent surface tension, hence decrease the solubility of protein and polysaccharide molecules in a phenomenon known as "salting out". In contrast, later salts in the series, e.g. guanidinium, increase the solubility of macromolecules ("salting in"), hence decrease "the order" of water molecules in solution (Zhou, Wang, Shi, Chang, Yang & Cui, 2014).

Besides the classification of ions according to the lyotropic series, literature argues that salts have an effect on polysaccharides even when these do not carry major ionic groups (Jay-lin, & Ames, 1993). In the case of starch, small entities, with a molecular weight of up to about 1000g/mol, can freely penetrate the granule when they are placed in water. When inside the granule, salt affects the plasticising and solvent properties of the liquid phase, which impact on the phase and/or state transitions undergone by starch in relation to thermal treatment (Moreau, Bindzus, & Hill, 2011a).

Thermomechanical analysis, in particular, has proved to be a valuable method for the identification of structural and functional properties of starch and starch containing foodstuffs. These relate to the molecular mechanisms of gelatinisation, retrogradation, caramelisation, creation of amylose-lipid complexes, etc. (Li, Li, Wang, Özkan, & Mao, 2010; Lim, Chang, & Chung, 2001). The chain length and number of branches as well as the density and regularity of packing of the polysaccharide chains all influence these processes and have been researched extensively (Vandeputte, Vermeylen, Geeroms, & Declour, 2003). In high-solid preparations, the amount of moisture present has a significant influence on the vitrification behaviour of the starch matrix (Farahnaky, Majzoobi, & Shojaei, 2009).

However, there is scant information in the literature on the interplay between added counterions, spanning the length of the Hofmeister series, and commonly encountered glycosidic linkage in food biopolymers. Such research can address the relationship between added sodium or calcium ions, used widely in processed foods, and the energy-providing or dietary fibre prototypes of starch and cellulose with backbone defining  $\alpha$ -(1 $\rightarrow$ 4) or  $\beta$ -(1 $\rightarrow$ 4) glycosidic bonds. The work described in this Chapter aims to shed light on the aforementioned polymer/counterion matrix by initiating a study that addresses the effect of added sodium chloride on the structural properties of condensed potato starch preparations.

## **3.2 MATERIALS AND METHODS**

### *3.2.1 Materials*

#### *3.2.1.1 Potato starch*

The potato starch sample was a fine, white, free-flowing powder containing < 10mg/kg of sulphur dioxide and without known allergens. Typical nutritional analysis has shown a total carbohydrate content of 84%, 15% water, a protein content of 0.2% and 0.1% total fat (Penford Starch, Lane Cove, NSW, Australia).

#### *3.2.1.2 Sodium chloride*

The salt was purchased from Sigma Aldrich (Castle Hill, NSW, Australia) in a white powder form, with minimum purity by titration being 99.9%, and pH 6.8 for 1M in water at 20°C.

#### *3.2.1.3 Millipore water type 2*

The water was used by filtering with two stages of Millipore system Elix®.

### *3.2.1.4 Saturated salt solutions*

The salt solutions were used to achieve a series of moisture and relative humidity values for our starch/sodium chloride samples, i.e. lithium chloride (LiCl): moisture content 3.57% w/w, RH 11%; potassium acetate (CH<sub>3</sub>COOK): moisture content 8.01% w/w, RH 23%; magnesium chloride (MgCl<sub>2</sub>•6H<sub>2</sub>O): moisture content 11.63% w/w, RH 33%; sodium bromide (NaBr): moisture content 13.56% w/w, RH 58%; magnesium acetate [Mg(CH<sub>3</sub>COO)<sub>2</sub>•4H<sub>2</sub>O]: moisture content 15.66% w/w, RH 65%; sodium chloride (NaCl): moisture content 18.83% w/w, RH 75% (Sablani, Kasapis & Rahman, 2007). All salts were purchased from Sigma Aldrich (Castle Hill, NSW, Australia).

### *3.2.2 Sample preparation*

Potato starch powder was dry mixed with a wide range of added sodium chloride concentrations (0, 1.5, 3, 4.5 and 6%) and Millipore type 2 water was introduced piecemeal to achieve a total of 35% moisture content in all preparations prior to processing; all measurements were carried out carefully using a four decimal place analytical balance. The preparations were then mixed at ambient temperature with Rheomix (HAAKE, Newington, NH, USA) at a speed of 200rpm for 2min and transferred to a preheated hot press at 120°C for 7min pressurisation (about 59Bar). They were cooled to about 45°C, packaged and sealed separately with a moisture/gas impermeable plastic vacuum bag. Samples were cut into the desired shape and size (10mm x10mm x1 mm cubes) and stored in sealed desiccators for 4 weeks containing the aforementioned saturated salt solutions. Relative humidity to an equilibrium value in the starch/sodium chloride systems was checked periodically in two grams of the material with a water activity meter (Novasina aw set-1, Pfäffikon, Switzerland), and desired equilibrium levels were achieved within 4 weeks. The final moisture content after a 4-week desiccator storage was between 3.57% (RH 11%) and 18.83% w/w (RH 75%), as estimated for one gram of our materials by oven drying at 102°C overnight.

### 3.2.3 Instrumental protocol

#### 3.2.3.1 Dynamic mechanical analysis

Diamond DMA from Perkin-Elmer (Akron, Ohio, USA) with an external 60L liquid nitrogen Dewar was used for monitoring the tensile storage and loss modulus ( $E'$  and  $E''$ , respectively) of our materials. In doing so, the sample film was set on a twin grip clamp with the dimensions of 10mm width, 10mm length and 1mm thickness. Employing the tensile mode, cooling from ambient temperature to  $-100^{\circ}\text{C}$  was carried out followed by heating to  $150^{\circ}\text{C}$  at a scan rate of  $2^{\circ}\text{C}/\text{min}$ , and frequency of 1Hz. To minimise moisture loss during measurement, a thin layer of petroleum vacuum grease was used to coat the sample prior to loading onto the tensile grips. Isochronal routines were carried out in duplicate returning consistent results.

#### 3.2.3.2 Modulated differential scanning calorimetry

Thermal transfer analyser Q2000 (TA Instruments, New Castle, DE) was used. It was attached to a recirculated cooling system (RCS90), with ultra-pure nitrogen gas purging into the sample analysis chamber at a flow rate of  $50\text{mL}/\text{min}$ . About ten mg of the material was placed in a  $T_{zero}$  aluminium pan, hermetically sealed with an aluminium lid and analysed at modulated amplitude of  $\pm 0.53^{\circ}\text{C}$  for 40s. An extensive temperature range was accessed with successive cooling and heating routines from  $-80$  to  $180^{\circ}\text{C}$  at a scan rate of  $10^{\circ}\text{C}/\text{min}$ . All measurements were performed in triplicate to yield effectively overlapping thermograms.

#### 3.2.3.3 Fourier transform infrared spectroscopy

FTIR spectra were recorded on a Perkin Elmer Spectrum 100 using MIRacle TMZnSe single reflection ATR plate system (Perkin Elmer, Norwalk, CT). Starch/sodium chloride preparations were analysed at ambient temperature within a wavelength of  $600$  to  $4500\text{cm}^{-1}$  and a resolution of  $4\text{cm}^{-1}$ . Spectra are presented in absorbance mode based on eight average scans. Final results were obtained

following removal of the background signal at ambient temperature and have been repeated three times for each measurement.

#### *3.2.3.4 Scanning electron microscopy*

FEI Quanta 200 SEM (Hillsboro, OR, USA) was used to provide the microimage of our materials. In doing so, low vacuum conditions were operative, the high voltage electron beam was at 30kV, the spot size was 5.0, and the working distance was between 6.8–7.7mm with a magnification of 1600X. Samples were cut with a clean, sanitised surgical scalpel into 10mmx10mm x1 mm cubes, equilibrated at desiccators as described earlier, and cross sections of the specimen were examined.

#### *3.2.3.5 Wide angle X-ray diffraction*

Bruker D<sub>4</sub> Endeavour (Karlsruhe, Germany) was used to examine the phase morphology of starch/sodium chloride preparations. Prior to analysis, samples were prepared at an appropriate size and equilibrated against saturated salt solutions for 4 weeks. Accelerating voltage of 40kV, current of 35mA and position sensitive detectors (PSD) were utilised to obtain diffractograms within 2 $\theta$  angle of 5-90° with intervals of 0.1°. Spectra were processed on DIFFRAC<sup>plus</sup> Evaluation (Eva), version 10.0, revision 1 and measurements were performed in triplicate.

### 3.3 RESULTS AND DISCUSSION

#### 3.3.1 Rheological behaviour of the starch/sodium chloride mixture

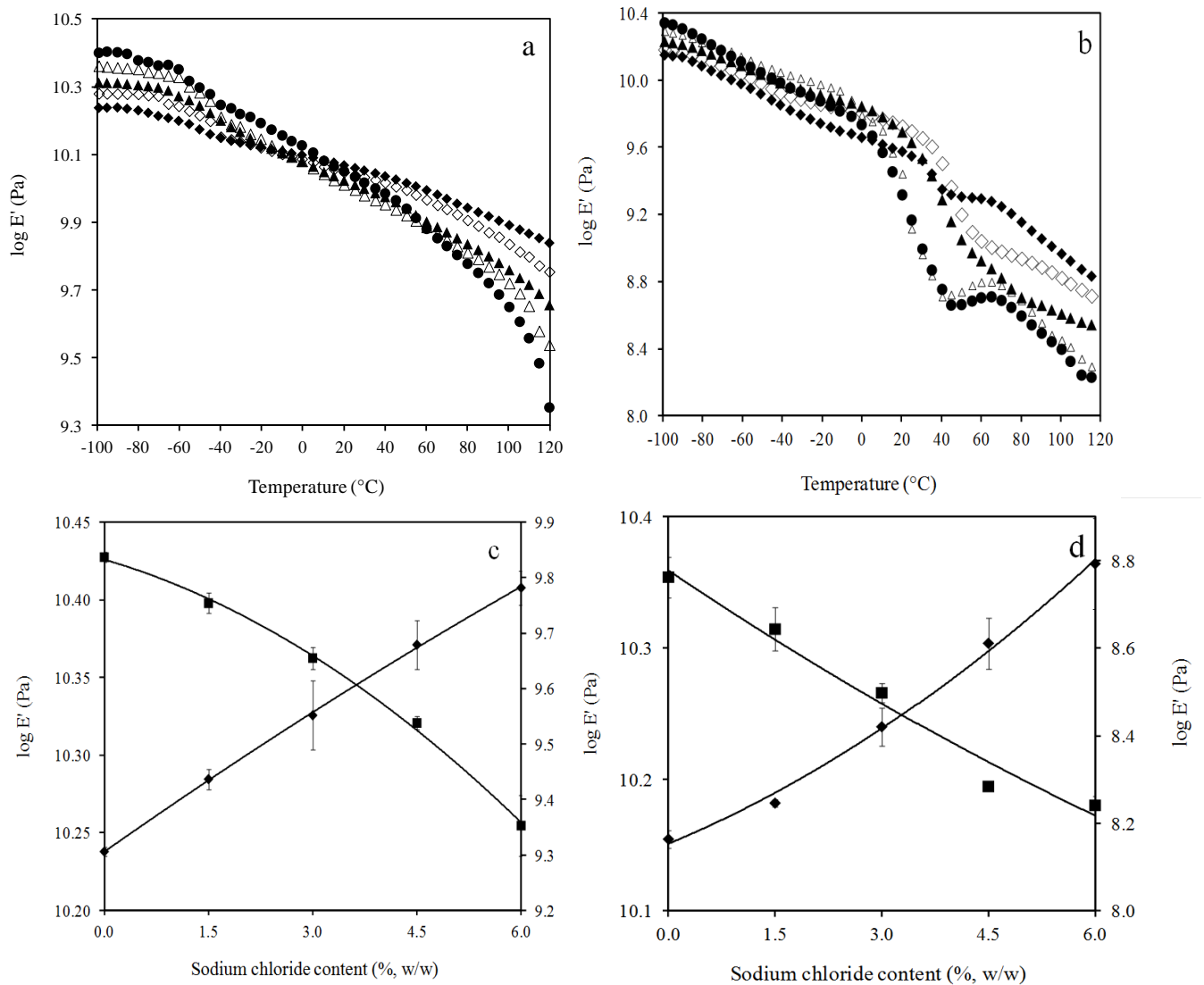
DMA was the method of choice in this work, since it is able to induce tensile vibrations on the composite film of potato starch with sodium chloride and analyse the material's response to the applied oscillatory force. Figure 3.1a illustrates overall heating profiles from -100 to 120°C of samples prepared at 3.6% w/w moisture content (RH 11%) in the presence of increasing levels of salt (0 to 6.0%). At the onset of the heating routine, all films have values of  $E'$  greater than  $10^{10}$  Pa. Matrices are within the glassy state where macromolecular motions are “frozen in” with a non-symmetrical arrangement (Biliaderis, 2009; Kasapis, 2009; Menard, 2008). Controlled heating at 2°C/min sees a reduction in the elasticity of the system, with values approaching  $10^{9.3}$  Pa at 120°C.

Figure 3.1b illustrates mechanical profiles for the opposite conditions of high moisture content (18.8% w/w) and relative humidity (RH 75%) in the starch/sodium chloride blend. Qualitatively, there is also a drop in the values of tensile modulus with heating from values in excess of  $10^{10}$  Pa at -100°C. This decrease in mechanical behaviour is quite extensive being about two orders of magnitude at the high end of the thermal routine, as compared to one order of magnitude for the corresponding temperature range in Figure 3.1a. Clearly, higher amounts of water result in considerable rearrangements in the matrix of the sample, as shown in the bimodal heating profiles in Figure 3.1b, due to alpha-relaxation of the polymer backbone and beta-relaxation of the side chains in the glassy matrix. This is sufficiently plasticised with increasing temperature to exhibit a malleable structure of reduced strength.

Figures 3.1c and 3.1d summarise the rheological results discussed thus far for the conditions of low and high moisture content/relative humidity, respectively. In both cases, starch films without sodium chloride exhibit lower values of tensile modulus at -100°C than the corresponding counterparts in the presence of salt. The trend is



highly reproducible and approaches maximum values in the presence of 6% sodium chloride in formulations.



**Figure 3.1** Heating profiles of tensile storage modulus for potato starch films (a) at a moisture content of 3.6% w/w (RH 11%) and (b) at a moisture content of 18.8% (RH 75%) in the presence of 0.0% ( $\blacklozenge$ ), 1.5% ( $\diamond$ ), 3.0% ( $\blacktriangle$ ), 4.5% ( $\triangle$ ), 6.0% ( $\bullet$ ) sodium chloride, and variation of tensile storage modulus for potato starch films with different levels of sodium chloride at  $-100^{\circ}\text{C}$  ( $\blacklozenge$ ; left y axis) and  $120^{\circ}\text{C}$  ( $\blacksquare$ ; right y axis) at a moisture content of 3.6% w/w (c) and 18.8% (d) scanned at the rate of  $2^{\circ}\text{C}/\text{min}$ , frequency of 1Hz and strain of 0.1% (error bars denote one standard deviation).

Strikingly, patterns of structure development reverse themselves at 120°C where, for both levels of moisture, increasing additions of sodium chloride yield softer networks. This result is consistent and develops as a tensile modulus drop of half an order of magnitude throughout the experimental range of salt addition.

Observations in Figures 3.1(a-d) suggest that the near neutral salt solutions of this investigation affect the morphology of potato starch. Gelatinisation has taken place during pressurisation at 120°C for 7min in the presence of increasing amounts of sodium chloride. It appears that molecular processes are not controlled solely by the simple concept of starch plasticisation in the presence of salt. It is known that addition of small molecule co-solutes increases the free volume of the polymeric matrix (Farahnaky, Farhat, Mitchell, & Hill, 2009).

In addition, sodium ions ( $\text{Na}^+$ ) attract starch  $-\text{OH}$  groups and interact electrostatically with phosphate groups that possess high charge density (Jay-lin, & Ames, 1993; Day, Fayet, & Homer, 2013). At the temperature regime of this investigation, the polysaccharide/cation interaction is capable of destabilising the starch granule leading to extensive gelatinisation and partial depolymerisation at high concentrations of added salt (Moreau, Bindzus, & Hill, 2011a; 2011b). Creation of a higher distribution of small molecular weight species, in the presence of sodium chloride, will increase molecular mobility with rising temperature that is unable to support efficiently three dimensional structures, hence leading to reduced tensile modulus values at 120°C as observed in these results. In contrast, smaller starch-like molecules are able to pack tightly within a high density matrix at subzero temperatures leading to reinforced networks and higher values of storage modulus following cooling to -100°C.

### *3.3.2 Calorimetric evidence on the glass transition of starch/sodium chloride mixtures*

Once the macromolecular aspects of structure development in these systems had been investigated, attention was focused on micromolecular behaviour and, in particular, the estimation of the  $T_g$ . Differential scanning calorimetry is suited for this type of analysis, which provides additional insights on the effect of salt in condensed starch preparations. Figure 3.2a depicts changes in heat flow as a function of thermal treatment for preparations with moisture content of 3.6% w/w (RH 11%). Increasing additions of sodium chloride produce a displacement in the heat capacity traces to higher temperatures. Overall, thermograms exhibit a sigmoidal pattern between 150 and 180°C, which is characteristic of the glass transition region.

Qualitatively, the same type of non-equilibrium behaviour is recorded in Figure 3.2b, where systems were made at the highest experimental moisture content of 18.8% w/w (RH 75%). Due to the lower level of solids in these systems, the calorimetric mechanism of devitrification is recorded within the temperature range of 120 to 150°C. Traditionally, this type of thermogram is used to pinpoint the onset and endset of the glass transition region, with the midpoint being considered as the empirical  $T_g$  (Moreau, Bindzus, & Hill, 2011b) and this approach is followed here with the results presented in Table 3.1.

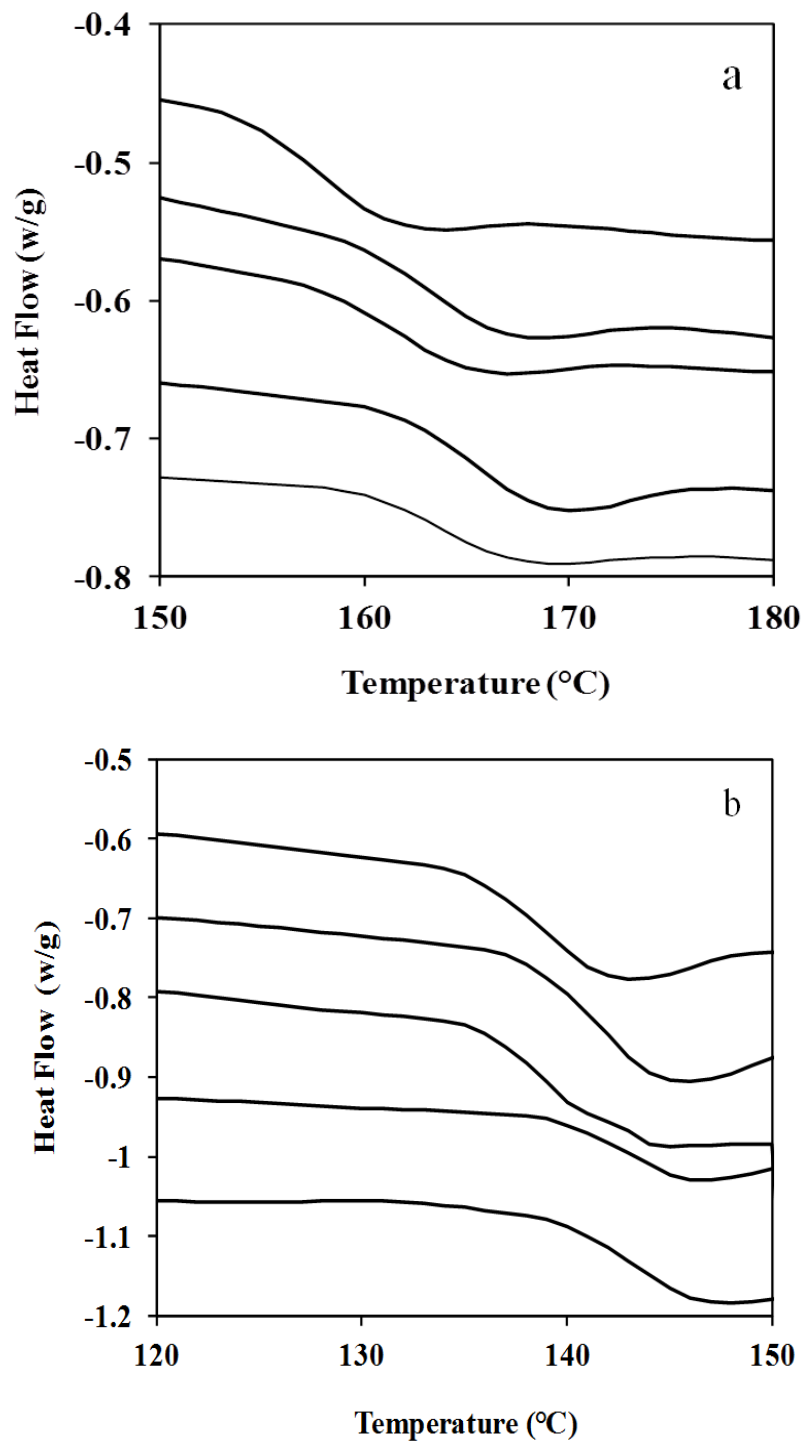


**Figure 3.2** DSC thermograms for potato starch in the presence of sodium chloride at 0.0%, 1.5%, 3.0%, 4.5%, 6.0% with (a) moisture content of 3.6% w/w (RH 11%) and (b) with moisture content of 18.8% w/w (RH 75%) arranged successfully downwards

**Table 3.1** Calorimetric markers of the glass transition recorded for potato starch/sodium chloride composites at different levels of relative humidity

Sodium chloride content (%)	RH 11%			RH 23%			RH 33%		
	Onset (°C)	Endset (°C)	$T_g$ (°C)	Onset (°C)	Endset (°C)	$T_g$ (°C)	Onset (°C)	Endset (°C)	$T_g$ (°C)
0.0	154.4	161.1	158.5	146.1	151.4	151.6	139.7	147.3	144.9
1.5	160.2	166.2	163.7	149.3	155.5	153.5	139.4	150.0	143.4
3.0	158.8	164.2	162.2	152.6	158.6	156.7	145.6	149.8	147.5
4.5	158.2	166.8	162.1	155.6	157.9	159.0	152.7	153.0	150.3
6.0	157.6	162.4	161.3	154.1	159.9	158.3	150.7	156.3	153.6
Sodium chloride content (%)	RH 58%			RH 65%			RH 75%		
	Onset (°C)	Endset (°C)	$T_g$ (°C)	Onset (°C)	Endset (°C)	$T_g$ (°C)	Onset (°C)	Endset (°C)	$T_g$ (°C)
0.0	139.5	145.0	144.5	138.1	143.2	141.3	134.9	141.2	139.0
1.5	138.0	144.1	144.2	129.1	135.6	132.6	135.8	143.9	142.2
3.0	139.1	145.2	144.3	137.1	145.3	143.0	125.1	134.7	133.7
4.5	145.5	149.1	146.5	136.8	144.0	141.8	137.3	145.8	143.8
6.0	145.9	150.6	148.1	137.4	145.5	143.5	139.8	145.7	146.1

**Note:** For all combinations of relative humidity and salt content in samples, onset, endset and  $T_g$  fall within  $\pm 0.4$  of the quoted values.

Clearly, variation in both moisture content/relative humidity and sodium chloride addition affects considerably the  $T_g$  of potato starch. In the case of 3% salt, for example, a RH increase from 11 to 75% is accompanied by a reduction in  $T_g$  values from 162.2 to 133.7°C, and similar reductions are recorded for the onset and endset temperatures of the thermograms. For the same amount of salt, increase in moisture content acts as plasticiser to enhance molecular mobility in samples. Within each category of relative humidity, the opposite trend in glassy consistency is observed with incorporation of salt in the starch matrix. In the case of RH 33%, for example, adding sodium chloride from 0 to 6% raises the  $T_g$  from 144.9 to 153.6°C, and likewise with the onset and endset temperatures of the thermal events. It appears, therefore, that the interactions of sodium ions with the phosphorylated (mainly amylopectin) molecules of starch and its hydroxyl groups produce dense structures in the glassy state (Figures 3.1c and 3.1d), which need to overcome a higher barrier of activation energy for molecular motions to ensue.

### 3.3.3 Infrared spectroscopy for the elucidation of molecular forces in the starch/salt system

Further identification of the structural fingerprints was pursued by examining using FTIR spectroscopy, the molecular forces responsible for the structural behaviour of our samples. Figure 3.3a shows the corresponding spectra for composites with moisture content of 3.6% w/w (RH 11%) over the range 1800 to 700  $\text{cm}^{-1}$ . These are dominated by the vibrations of glucose molecules and, in particular, three main modes of the IR spectrum have been highlighted at 946, 1000-1082 and 1158 $\text{cm}^{-1}$ .

The infrared absorption at 946 $\text{cm}^{-1}$  can be attributed to the C-O-C skeletal mode of  $\alpha$ -glycosidic linkage in starch. The overlapping bands between 1000 and 1082 $\text{cm}^{-1}$  are assigned progressively to C-O-H bending and C-O, C-C and O-H stretching. The absorbance band at 1158 $\text{cm}^{-1}$  is associated with C-O-C asymmetric stretching of glycosidic bonds (Deeyai, Suphantharika, Wongsagonsup, Dangtip, 2013). This technique has been used to identify the structural morphology of starch, with bands around 1022 $\text{cm}^{-1}$  being related to amorphous domains (Capron, Robert, Colonna, Brogly, & Planchot, 2007; Sevenou, Hill, Farhat & Mitchell, 2002). These are reflected well in the spectra of the present material although the relative ratio of amylose to amylopectin in samples can influence results.

The literature suggests that sodium ions can form coordination complexes with C-O-H and C-O-C groups of carbohydrates *via* electrostatic binding to hydroxyl groups or involvement of lone electron pair orbitals of oxygen atoms (Ma, Yu, He, & Wan, 2007). The effect of sodium chloride and its interactions with starch and water molecules could be observed within the region of 946 and 1158 $\text{cm}^{-1}$  in Figure 3.3a. There is an increase in peak intensity as a function of salt addition, which supports the concept of increasing interactions between salt and the hydrated polymeric matrix. Similar results have been recorded in Figure 3.3b for samples with moisture content of 18.8% w/w (RH 75%) but trends have been further intensified. The narrowing of peaks, mostly at about 1000 $\text{cm}^{-1}$ , with increasing levels of salt and, in particular, for samples with higher water content, strongly

supports the concept of modification in inter-double-helical links of starch, which is reflected in earlier evidence from rheology and calorimetry.

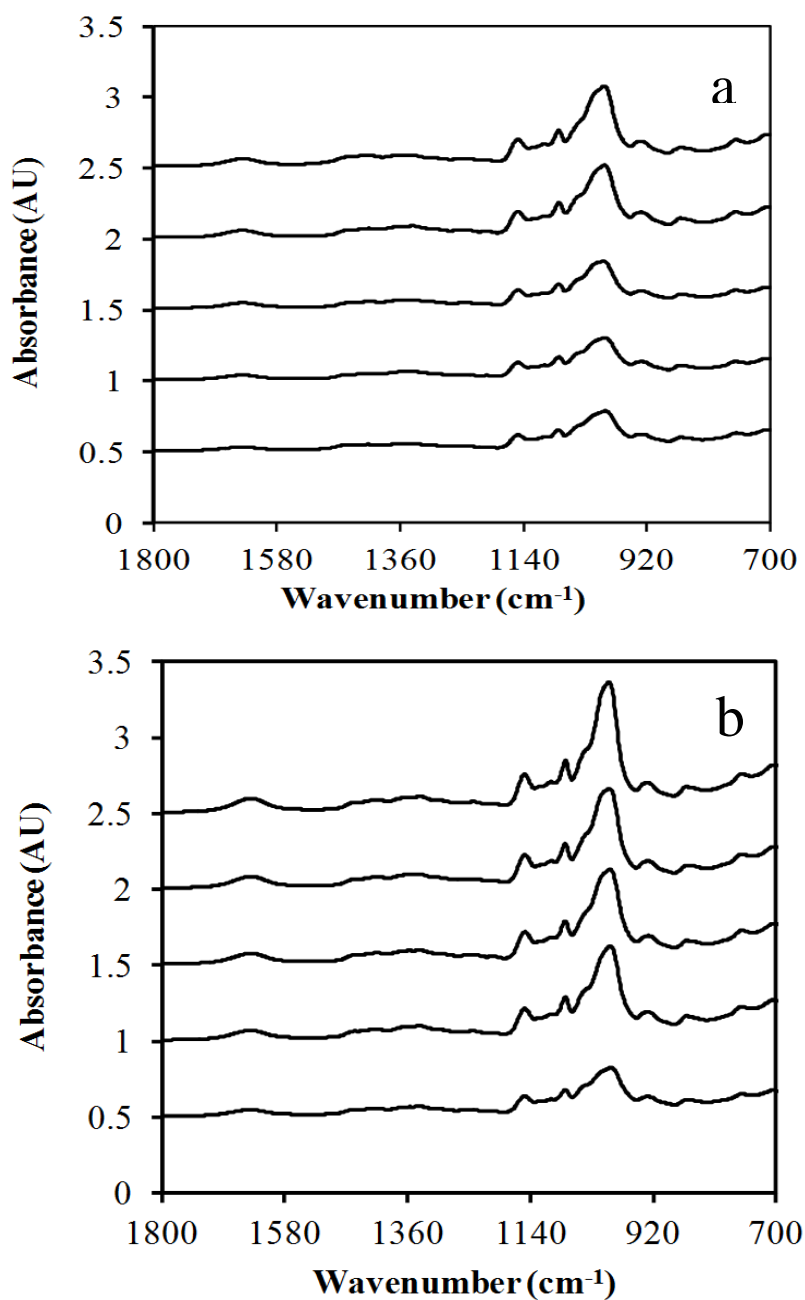


**Figure 3.3** FTIR spectra of potato starch in the presence of sodium chloride at 0.0%, 1.5%, 3.0%, 4.5%, 6.0% arranged upwards with moisture content of a) 3.6% w/w (RH 11%) and b) 18.8% w/w (RH 75%)

Finally, the relatively broad infrared band at  $1630\text{cm}^{-1}$  is associated with the vibrations of tightly bound water molecules absorbed in the amorphous regions of starch (Kizil, Irudayaraj, & Seetharaman, 2002; Deeyai, Suphantharika, Wongsagonsup, & Dangtip, 2013). This molecular event is evident in Figures 3.3a and 3.3b, and its intensity increases with both salt and water content in these preparations; the non-crystalline state of starch is, of course, in accordance with results of this investigation. The tertiary complex of starch, water and salt determines structural functionality, as is visually evident following hot pressurisation, with the starch films producing dense light-red or puffy white matrices with or without sodium chloride.

#### *3.3.4 X-ray diffraction analysis*

The phase morphology of the preparations was studied using wide angle X-ray diffraction. To start with, crystallinity in the systems is relatively low, since potato starch crystals were destroyed during heat processing at  $120^{\circ}\text{C}$  for 7min and only a slow re-crystallisation process is expected afterwards (Frost, Kaminski, Kirwan, Lascaris, Shanks, 2009; Mizuno, Mitsuiki, & Motoki, 1998). Figure 3.4 compares the diffraction patterns of samples with moisture content of 18.8% w/w (RH 75%) when subjected to a monochromatic radiation source. It was noted that addition of sodium chloride induces a subtle but reproducible change in the shape of the diffractogram at an angle of 10 to 12 degrees ( $2\theta$ ). At 17 degrees ( $2\theta$ ), there is a visible sharpening of the peak observed especially at 3.0, 4.5 and 6.0% sodium chloride. Further on, the appearance of a molecular event at 20 degrees ( $2\theta$ ) for starch samples with 4.5 and 6.0% salt is recorded. Finally, the peak at 23 degrees ( $2\theta$ ) has become broader at the highest level of sodium chloride used presently. In conclusion, the multiple changes in shape and intensity of the diffractograms within 10 and 28 degrees ( $2\theta$ ) relates to the formation of new and polydisperse species due to a plethora of interactions between sodium chloride and the hydrated starch network.



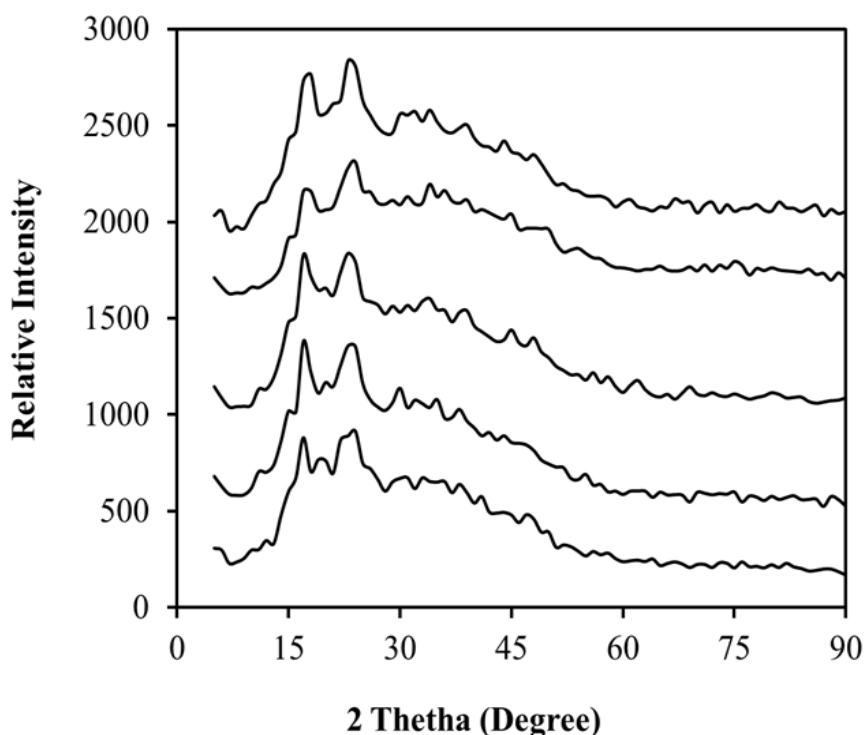


**Figure 3.4** X-ray diffractograms for potato starch with sodium chloride at 0.0%, 1.5%, 3.0%, 4.5%, 6% arranged successfully downwards at moisture content of 18.8% w/w (RH 75%)

### 3.3.5 Microscopic examination of the topology in starch/salt composites

SEM was employed to provide tangible evidence of the network topology in these potato starch/sodium chloride samples. Micrographs were obtained from carefully cut cross sections of the gel. Figures 3.5a and 3.5b show images of samples with a moisture content of 3.6% w/w (RH 11%), and Figures 3.5c and 3.5d are the corresponding images for a moisture content of 18.8% w/w (RH 75%). In both cases, the systems were prepared homogeneously ensuring thorough mixing of sodium chloride at levels of 0 and 6.0%, respectively. The absence of visible NaCl crystals further argues for molecular mixing of all ingredients in the composite. Following hot pressing at 120°C, it was noted that the higher the moisture content, the softer and more viscous-like were the samples. Featureless backgrounds were observed for the relatively dehydrated starch matrices in the presence or absence of

salt. In contrast, higher levels of moisture appear to allow extensive interactions between starch and added salt, with the outcome, in both cases, being an assembly of fibrillar-like structures. These appear to be dense and highly aggregated in the presence of 6.0% of the counterion.

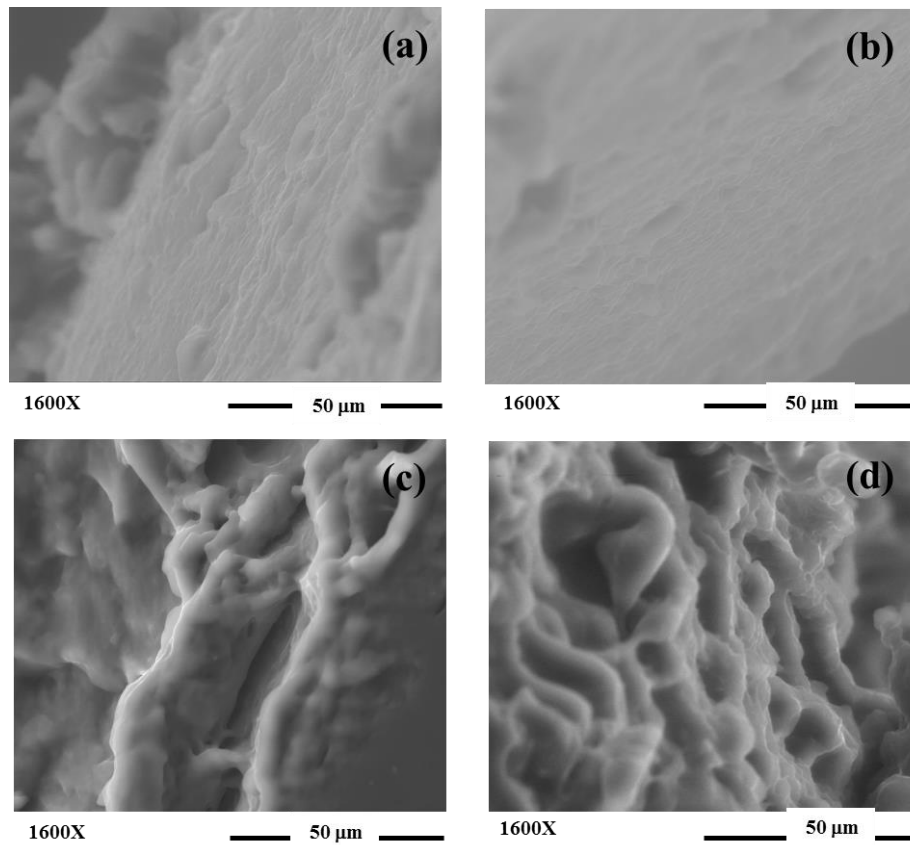


**Figure 3.5** SEM micrographs for potato starch with moisture content of 3.6% w/w (RH 11%) in the presence of sodium chloride (a) 0.0% and (b) 6.0%, and for moisture content of 18.8% w/w (RH 75%) in the presence of sodium chloride (c) 0.0% and (d) 6.0%

### 3.4 CONCLUSIONS

Structural properties and textural consistency of potato starch-sodium chloride based systems find widespread commercial applications across the food industry in existing product concepts and the development of new formulations. This study has shown that potential sodium-ion interactions with starch hydroxyl and phosphate groups alter considerably the mechanical properties of amorphous high-solid preparations. These become softer than starch-water systems at conditions of elevated temperatures governed by molecular mobility. In contrast, salt addition creates hard matrices at conditions of low temperature, which are characteristic of the mechanical glassy state. In the absence of consequential starch crystallinity, preparations exhibit glassy consistency with thermal treatment. Densely packed salt-polysaccharide segments in the glassy state have a high energy requirement to molecular mobility that raises the  $T_g$  with increasing counterion content. It remains to be seen whether calcium chloride addition, i.e. a cation member towards the opposite end of the lyotropic series, would also alter the molecular dynamics of a glassy starch matrix, and this is examined in the following Chapter of this thesis.

### 3.5 REFERENCES

- Albarracín, W., Sánchez, I. G., Grau, R., & Barat, J. M. (2011). Salt in food processing; usage and reduction: a review. *International Journal of Food Science and Technology*, 46, 1329-1336.
- Alvani, K., Qi, X., & Tester, R. F. (2012). Gelatinisation properties of native and annealed potato starches. *Starch/Stärke*, 64, 297-303.
- Biliaderis, C. G. (2009). Structure transitions and related physical properties of starch. In J. BeMiller & R. Whistler (Eds.), *Starch, chemistry and technology* (3rd ed.) (pp. 293-372). New York, Academic Press.
- Capron, I., Robert, P., Colonna, P., Brogly, M., & Planchot, V. (2007). Starch in rubbery and glassy states by FTIR spectroscopy. *Carbohydrate Polymers*, 68, 249-259.
- Considine, T., Noisuwan, A., Hemar, Y., Wilkinson, B., Bronlund, J., & Kasapis, S. (2011). Rheological investigations of the interactions between starch and milk proteins in model dairy systems: A review. *Food Hydrocolloids*, 25, 2008-2017.
- Copeland, L., Blazek, J., Salman, H., & Tang, M. C. (2009). Form and functionality of starch. *Food Hydrocolloids*, 23, 1527-1534.
- Day, L., Fayet, C., & Homer, S. (2013). Effect of NaCl on the thermal behaviour of wheat starch in excess and limited water. *Carbohydrate Polymers*, 94, 31-37.
- Deeyai, P., Suphantharika, M., Wongsagonsup, R., & Dangtip, S. (2013). Characterization of modified tapioca starch in atmospheric argon plasma under diverse humidity by FTIR spectroscopy. *Chinese physical society and IOP Publishing*, 30, Vol. 1, 018103-1 - 018103-4.
- Farahnaky, A., Farhat, I. A., Mitchell, J. R., & Hill, S. E. (2009). The effect of sodium chloride on the glass transition of potato and cassava starches at low moisture contents. *Food Hydrocolloids*, 23, 1483-1487.
- Farahnaky, A., Majzoobi, M., & Shojaei, Z. A. (2009). Effect of NaCl and water content on expansion and color of cassava and potato starches on baking. *Journal of Texture Studies*, 40, 676-691.

- Frost, K., Kaminski, D., Kirwan, G., Lascaris, E., & Shanks, R. (2009). Crystallinity and structure of starch using wide angle X-ray scattering. *Carbohydrate Polymers*, 78, 543-548.
- Hofmeister, F. (1888), Zur Lehre von der Wirkung der Salze. *Arch. Experimental Pathology and Pharmacology*, 24, 247-260.
- Jay-lin, J., & Ames, I. A. (1993). Mechanism of starch gelatinization in neutral salt solutions. *Starch/Stärke*, 5, 161-166.
- Kasapis, S. (2009). Glass transitions in foodstuffs and biomaterials: Theory and measurements. In M. S. Rahman (Ed.). *Food properties handbook*, (2nd ed) (pp. 207-245). Boca Raton, CRC Press/Taylor & Francis.
- Kizil, R., Irudayaraj, J., & Seetharaman, K. (2002). Characterisation of irradiated starches by using FT-Raman and FTIR spectroscopy. *Journal of Agricultural and Food Chemistry*, 50, 3912-2918.
- Kunz, W., Henle, J., & Ninham, B. W. (2004). 'Zur Lehre von der Wirkung der Salze' (about the science of the effect of salts): Franz Hofmeister's historical papers. *Current Opinion in Colloid and Interface Science*, 9, 19-37.
- Li, Q., Li, D., Wang, L.-J., Özkan, N., & Mao, Z.-H. (2010). Dynamic viscoelastic properties of sweet potato studied by dynamic mechanical analyzer. *Carbohydrate Polymers*, 79, 520-525.
- Lim, S.-T., Chang, E.-H., & Chung, H.-J. (2001). Thermal transition characteristics of heat-moisture treated corn and potato starches. *Carbohydrate Polymers*, 46, 107-115.
- Ma, X., Yu, J., He, K., & Wan, N. (2007). The effects of different plasticizers on the properties of thermoplastic starch as solid polymer electrolytes. *Macromolecular Materials and Engineering*, 292, 503-510
- Menard, K. P. (2008). Dynamic mechanical analysis: A practical introduction. (2nd ed.). Baton Rouge, CRC Press/Taylor & Francis.
- Mishra, S., & Rai, T. (2006). Morphology and functional properties of corn, potato and tapioca starches. *Food Hydrocolloids*, 20, 557-566.

- Mizuno, A., Mitsuiki, M., & Motoki, M. (1998). Effects of crystallinity on the glass transition temperature of starch. *Journal of Agricultural and Food Chemistry*, 46, 98-103.
- Moreau, L., Bindzus, W., & Hill, S. (2011a). Influence of salts on starch degradation: Part I- sodium chloride. *Starch/Stärke*, 63, 669-675.
- Moreau, L., Bindzus, W., & Hill, S. (2011b). Influence of salts on starch degradation: Part II- salt classification and caramelisation. *Starch/Stärke*, 63,676-682.
- Sablani, S. S., Kasapis, S., & Rahman, M. S. (2007). Evaluating water activity and glass transition concepts for food stability. *Journal of Food Engineering*, 78, 266-271.
- Sevenou, O., Hill, S. E., Farhat, I. A., & Mitchell, J. R. (2002). Organisation of the external region of the starch granule as determined by infrared spectroscopy. *International Journal of Biological Macromolecules*, 31, 79-85.
- Singh, N., Singh, J., Kaur, L., Sodhi, N. S., & Gill, B. S. (2003). Morphological, thermal and rheological properties of starches from different botanical sources. *Food Chemistry*, 81, 219-231.
- Vandeputte, G. E., Vermeulen, R., Geeroms, J., & Declour, J. A. (2003). Rice starches. I. Structural aspects provide insight into crystallinity characteristics and gelatinisation behaviour of granular starch. *Journal of Cereal Science*, 38, 43-52.
- Zhou, H., Wang, C., Shi, L., Chang, T., Yang, H., & Cui. M. (2014). Effects of salts on physicochemical, microstructural and thermal properties of potato starch. *Food Chemistry*, 156, 137-143.
- Zobel, H. F., & Stephen, A. M. (2006). Starches: structure, analysis, and applications. In A. M. Stephen, G. O. Phillips, & P. A. Williams (Eds.), *Food polysaccharides and their applications* (2nd ed.) (pp. 25-86). Florida, CRC Press/Taylor & Francis.

## CHAPTER 4

### CALCIUM CHLORIDE EFFECTS ON THE GLASS TRANSITION OF CONDENSED SYSTEMS OF POTATO STARCH

*Based on a Journal article published in Food Chemistry as:*

*“Calcium chloride effects on the glass transition of condensed systems of potato starch”*

#### ABSTRACT

The effect of calcium chloride on the structural properties of condensed potato starch undergoing a thermally induced glass transition has been studied using dynamic mechanical analysis and modulated differential scanning calorimetry. Extensive starch gelatinisation was obtained by hot pressing at 120°C for 7min producing materials that covered a range of moisture contents from 3.7% w/w (11% relative humidity) to 18.8% w/w (75% relative humidity). FTIR, ESEM and WAXD were also performed in order to elucidate the manner by which salt addition affects the molecular interactions and morphology of condensed starch. The experimental protocol ensured the development of amorphous matrices that exhibited thermally reversible glassy consistency. Both moisture content and addition of calcium chloride affected the mechanical strength and glass transition temperature ( $T_g$ ) of polymeric systems. Highly reactive calcium ions form a direct interaction with starch to alter considerably its structural properties *via* an anti-plasticizing effect, as compared to the polymer-water matrix.

**Keywords:** glass transition; calcium chloride; potato starch; high-solid systems; anti-plasticizing effect.

## 4.1 INTRODUCTION

The thermally induced glass transition is an important concept to rationalise the textural consistency and stability of condensed starchy products and starch-based films (Liu, Xie, Yu, Chen, & Li, 2009; Talja, Helén, Roos, & Jopuppila, 2007). Starch granules contain an amorphous phase, which is mainly composed of linear amylose and some of the partially crystalline branched amylopectin. During vitrification, that commonly follows starch gelatinisation, amorphous polymeric segments remain “frozen” in a random conformation resulting in slow molecular motions and effective immobilisation in the glassy state (Zeleznač & Hoseneý, 1987). Upon subsequent heating at a given scan rate, the glassy polymer converts into a rubbery system of high viscosity and increased configurational flexibility. This rubber-to-glass transformation is demarcated by the so-called  $T_g$ , which depends on the amylose/amylopectin content, surrounding relative humidity, molecular interactions between starch and low molecular weight co-solute, and the nature of the measuring protocol (Perdomo, Cova, Sandoval, Garía, Laredo, & Müller, 2009).

Starch based biomaterials and processed foods experience plasticising or anti-plasticising phenomena that alter considerably the glass-transition behaviour. Increase in the plasticizer content of water and polyols depresses the  $T_g$  and reduces the mechanical strength (Hulleman, Janssen, & Feil, 1998; Lourdin, Coignard, Bizot, & Colonna, 1997; Róz, Carvalho, Gandini, & Curvelo, 2006). Glycerol and xylitol, for example, form hydrogen bonds with the hydroxyl groups of starch leading to a reduction in intermolecular polymer associations and entanglements, and retention of backbone flexibility (Chaudhary, Adhikari, & Kasapis, 2011). Conversely, linoleic and oleic acids can act as anti-plasticizers aided by the steric accommodation of the fatty acid molecule within the hydrophobic cavity of amylose helices. This leads to an upward shift of  $T_g$  values in cassava starch matrices at a moisture content lower than 11% and in the presence of at least 2% added fatty acid (Luk, Sandoval, Cova, & Müller, 2013).



Various types of salt are regularly utilised in starch based formulations in order to enhance techno-functionality. Sodium chloride is a traditional preservative widely added in starch to act as a taste and/or flavour enhancer and a water-holding capacity or water activity modifier (Albarracin, Sánchez, Grau & Barat, 2011). The effect of sodium chloride on the glass transition of condensed starches (more than 80% solids in preparations) has been reported in the literature. Differential scanning calorimetry was used and the results were rationalised on the basis of non-dissociated (crystalline) salt molecules or dissociated (amorphous) ions depending on moisture levels (Farahnaky, Farhat, Mitchell & Hill, 2009).

Calcium chloride is another common food additive used in biomaterials and composites in order to improve, for example, the thermal engineering of starch-based biodegradable films (Jiang, Jiang, Gan, Zhang, Dai, & Zhang, 2012). Application of calcium chloride in the thermal processing of starch takes advantages of its high hygroscopic desiccating ability, better thermal and chemical stability than other salts, desirable thermal conductivity and non-toxicity (Tsoukpoe et al., 2015). Calcium counterion ( $\text{Ca}^{2+}$ ) is a stronger electrolyte than the sodium cation ( $\text{Na}^+$ ) because of the dense electric charge. In low-solid aqueous systems, calcium dissolves and forms complexes with ionic polysaccharides supporting the formation of salt bridges that have a firming effect on gels following heat treatment (Luna-Guzmán, & Barrett, 2000). It can also bind with the phosphoric acid residues of the amylophosphoric portions of native starch contributing strength and elasticity to the gel upon gelatinization (Noor, & Islam, 2006; Tomasik, & Schilling, 1998).

There is scant information in the literature on the effect of calcium chloride on the structural properties of high-solid starch preparations. This could take the form of plasticisation by increasing the free volume between adjacent polymer chains, hence depressing the values of  $T_g$ . Alternatively, it could interact directly with the chemical moieties of the polysaccharide chains, hence supporting polymeric interactions, reducing mobility and increasing the  $T_g$ . The aim of this investigation, therefore, is to employ a range of suitable physicochemical techniques in order to

provide fundamental understanding on the important role of calcium chloride in condensed starch based systems.

## **4.2 MATERIALS AND METHODS**

### *4.2.1 Materials*

#### *4.2.1.1 Potato starch*

A food-grade native potato starch was used, which was a white, fine free-flowing powder with a bland taste. It contains <10mg/kg of sulphur dioxide without known allergens. Typical nutritional value expressed as % per 100g of the material shows a total carbohydrate content of 84%, a water content of 15.08%, protein content of 0.2% and total fat content of 0.1% (Penford Starch, Lane Cove, NSW, Australia).

#### *4.2.1.2 Calcium chloride*

Calcium chloride, anhydrous in a white granule form ( $\leq 7.0\text{mm}$ ), with minimum purity by EDTA titration being 98.1%, was purchased from Sigma Aldrich (Castle Hill, NSW, Australia).

#### *4.2.1.3 Millipore water type 2*

Millipore system Elix® 10 water purification system was used to produce the Millipore type 2 analytical-grade water of this investigation (Merck KGaA, Germany).

#### *4.2.1.4 Saturated salt solutions*

Desiccating chambers were prepared to achieve a series of moisture and relative humidity values for our starch/calcium chloride samples, with the saturated salt solutions being purchased from Sigma Aldrich, i.e. lithium chloride (LiCl): moisture content 3.71% w/w, RH 11%; potassium acetate ( $\text{CH}_3\text{COOK}$ ): moisture

content 6.07% w/w, RH 23%; magnesium chloride ( $\text{MgCl}_2 \cdot 6\text{H}_2\text{O}$ ): moisture content 6.55% w/w, RH 33%; sodium bromide (NaBr): moisture content 11.49% w/w, RH 58%; magnesium acetate [ $\text{Mg}(\text{CH}_3\text{COO})_2 \cdot 4\text{H}_2\text{O}$ ]: moisture content 14.40% w/w, RH 65%; sodium chloride (NaCl): moisture content 18.83% w/w, RH 75% (Sablani, Kasapis & Rahman, 2007).

#### 4.2.2 *Sample preparation*

Potato starch powder, with a moisture content of 15.08% (w/w) that was taken into consideration for final sample preparation, was dry mixed with a wide range of added calcium chloride concentrations (0.0, 1.5, 3.0, 4.5 and 6.0% w/w) to achieve a total of 35.0% (w/w) moisture content. In doing so, Millipore type 2 water was introduced piecemeal prior to processing all preparations; weighing was carried out carefully using a four decimal place analytical balance. Then, twin screw Thermo Rheomix OS (HAAKE, Newington, NH, USA) were used to mix the mixture with a screw speed of 200rpm for 2min at ambient temperature. Mixture was placed on a stainless steel metal frame (130mm x 130mm x 2mm) sandwiched between two non-stick plastic sheets at the bottom and top of the frame. It was then transferred to a steam preheated hot press at 120°C for 7min achieving pressurisation of 59Bar.

Heated samples were cooled within the same press to about 45°C (to prevent air bubble formation on the starch film), packaged and sealed separately with a moisture/gas impermeable plastic vacuum bag, and stored at 4°C. To facilitate subsequent instrumental analysis, samples were cut into the desired shape and size (10mm x 10mm x 1mm) and stored in sealed relative-humidity desiccators for 4 weeks containing the aforementioned saturated salt solutions. Relative humidity to the required equilibrium value in the starch/calcium chloride systems was checked periodically with a water activity meter (Novasina aw set-1, Pfäffikon, Switzerland). The final moisture content of these preparations after a 4-week desiccator storage was between 3.71% w/w (RH 11%) and 18.83% w/w (RH 75%), as estimated by oven drying at 102°C overnight.

### *4.2.3 Instrumental protocol*

#### *4.2.3.1 Dynamic mechanical analysis*

Diamond DMA from Perkin-Elmer (Akron, Ohio, USA) with an external 60L liquid nitrogen Dewar was used for monitoring the tensile storage and loss modulus ( $E'$  and  $E''$ , respectively) of our materials. In doing so, the sample film was set on a twin grip clamp and tensile mode was employed. Cooling from ambient temperature to  $-100^{\circ}\text{C}$  was carried out followed by heating to  $150^{\circ}\text{C}$  at a scan rate of  $2^{\circ}\text{C}/\text{min}$ , and frequency of 1Hz. Strain employed was 0.1% throughout, which falls within the linear viscoelastic region (LVR) of the material. To minimise moisture loss during measurement, a thin layer of petroleum vacuum grease was used to coat the sample prior to loading onto the tensile grips. Isochronal routines were carried out in duplicate returning consistent results.

#### *4.2.3.2 Modulated differential scanning calorimetry*

Thermal transfer analyser Q2000 (TA Instruments, New Castle, DE) was used. It was attached to a recirculated cooling system (RCS90), with ultra-pure nitrogen gas purging into the sample analysis chamber at a flow rate of  $50\text{mL}/\text{min}$ . About ten mg of the material was placed in a Tzero aluminium pan, hermetically sealed with an aluminium lid and analysed at modulated amplitude of  $\pm 0.53^{\circ}\text{C}$  for 40s. An extensive temperature range was accessed with successive cooling and heating routines from  $-80$  to  $180^{\circ}\text{C}$  at a scan rate of  $10^{\circ}\text{C}/\text{min}$ . All measurements were performed in triplicate to yield effectively overlapping thermograms.

#### *4.2.3.3 Fourier transform infrared spectroscopy*

Data were recorded on a Perkin Elmer Spectrum 100 using MIRacle TMZnSe single reflection ATR plate system (Perkin Elmer, Norwalk, CT). Starch/calcium chloride preparations were analysed at ambient temperature within a wavelength of 650 to  $4500\text{nm}$  and a resolution of  $4\text{cm}^{-1}$ . Spectra are presented in absorbance mode

based on 32 average scans. Final results were obtained following removal of the background signal at ambient temperature and have been repeated three times for each measurement.

#### *4.2.3.4 Wide angle X-ray diffraction*

Bruker D4 Endeavour (Karlsruhe, Germany) was used to examine the phase morphology of starch/calcium chloride preparations. Accelerating voltage of 40kV, current of 35mA and position sensitive detectors (PSD) were utilised to obtain diffractograms within  $2\theta$  angle of 5-90° with intervals of 0.1°. Spectra were processed on DIFFRAC<sup>plus</sup> Evaluation (Eva), version 10.0, revision 1 and measurements were performed in triplicate.

#### *4.2.3.5 Scanning electron microscopy*

FEI Quanta 200 ESEM (Hillsboro, OR, USA) was used to provide the micro-images of our materials. In doing so, low vacuum conditions were operative, the high voltage electron beam was at 20kV, the spot size was 2.5, and the working distance was between 10.0 and 13.0mm with a magnification of 2400X. Samples were cut with a clean, sanitised surgical scalpel into 10 mm x 10 mm x 1 mm cubes, equilibrated at desiccators as described earlier, and cross sections of the specimen were examined.

#### *4.2.3.6 Energy dispersive X-ray spectroscopy (EDX)*

Philips XL30 SEM (Sussex, England) was used to recognise ionised atoms of starch films. The non-conductive specimens were attached to sample holders followed by carbon coating with a thickness of 5nm. The specimens were excited with an electron beam at 20kV and the emitted specific X-rays at different energy levels were recorded with an Oxford Instruments X-Max 20mm<sup>2</sup> detector (Oxford Instruments, Scott's valley, California, USA) with the assistance of Aztec software v3.1 (Oxford Instruments Nano analysis) to plot EDX spectra and analyse the element composition.

## 4.3 RESULTS AND DISCUSSION

### *4.3.1 Mechanical relaxations in starch/calcium chloride systems as a function of temperature*

DMA was used in this study, with the technique being able to induce tensile vibrations and measure the output response of the material by applying an oscillatory force, hence supplying information on the mechanical relaxations of the system. Figure 4.1a shows the variation in the values of storage modulus during heating from  $-100$  to  $120^{\circ}\text{C}$  for samples prepared at a moisture content of 3.7% (w/w) (RH 11%) in the presence of calcium chloride with increasing concentration from 0.0 to 6.0% (w/w). At the onset of the experimental routine, i.e.  $-100^{\circ}\text{C}$ , all films have  $E'$  values greater than  $10^{10}\text{Pa}$ , and mechanical properties fall within the glassy state where polymeric chains are immobile and only limited stretching and bending of chemical bonds is allowed (Biliaderis, 2009; Roudaut, Simatos, Champion, Contreras-Lopez, & Le Meste, 2004). Controlled heating at  $2^{\circ}\text{C}/\text{min}$  results in considerable reduction in the elasticity of the system, with values approaching  $10^{9.6}\text{Pa}$  at  $120^{\circ}\text{C}$ , thus entering the glass transition region of the viscoelastic master curve (Kasapis, 2009; Menard, 2008).

Figure 4.1b depicts dynamic oscillatory profiles for high moisture content (18.7% w/w; RH 75%) preparations of starch with calcium chloride. Qualitatively, there is also a drop in tensile storage modulus with controlled heating from values in excess of  $10^{10}\text{Pa}$  at  $-100^{\circ}\text{C}$ . Softening of the polymeric matrix is quite extensive, with  $E'$  values dropping almost two orders of magnitude to about  $10^{8.2}\text{Pa}$  at  $120^{\circ}\text{C}$ . It appears that increasing the level of moisture from 3.7 to 18.7% (w/w) encourages macromolecular relaxation, and the starch is sufficiently plasticized with raising temperature to exhibit a malleable structure of reduced mechanical strength.

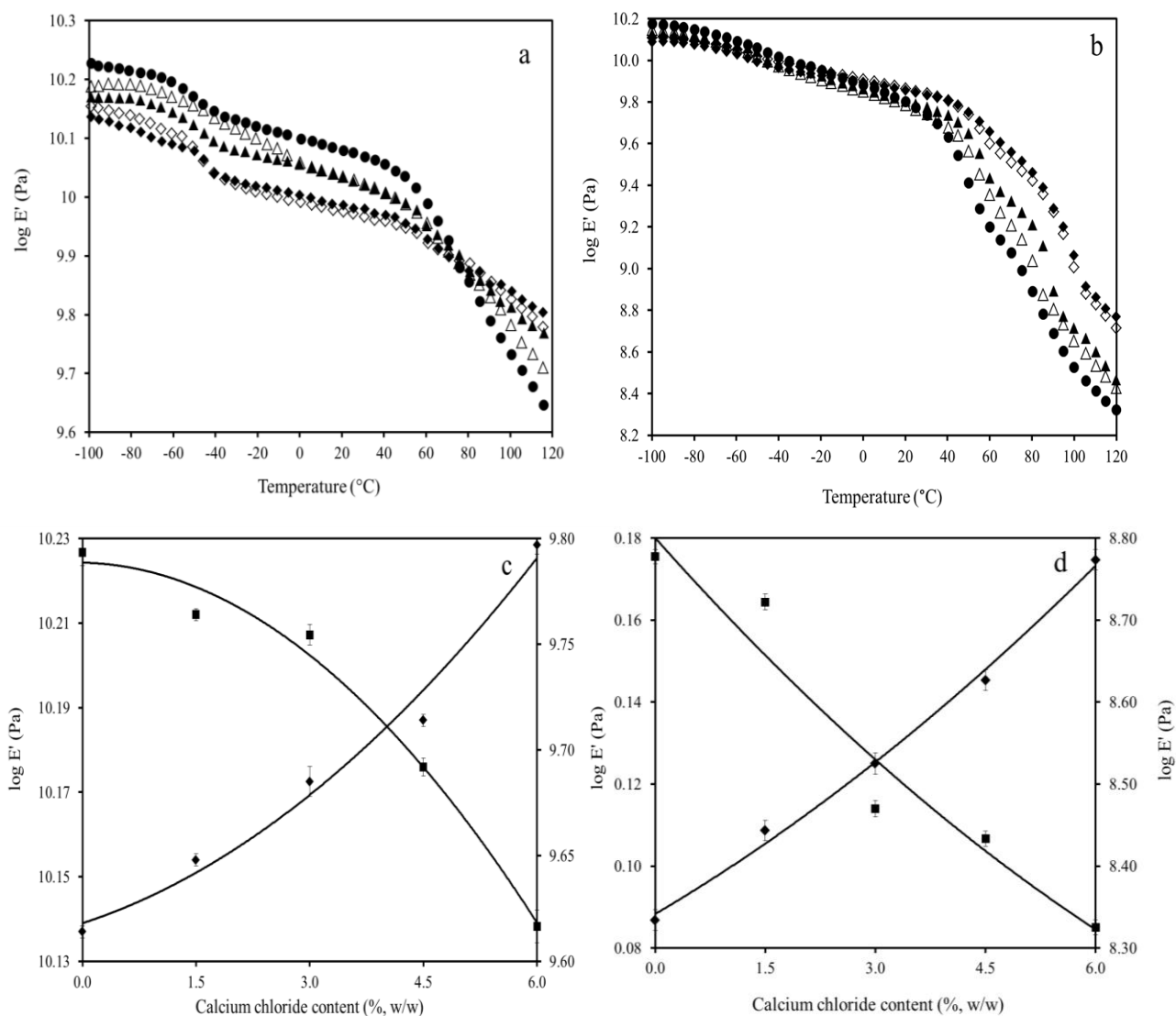


**Figure 4.1** Heating profiles of tensile storage modulus for potato starch films at a moisture content of (a) 3.7% w/w (RH 11%) and (b) 18.8% w/w (RH 75%) in the presence of 0.0 ( $\blacklozenge$ ), 1.5 ( $\diamond$ ), 3.0 ( $\blacktriangle$ ), 4.5 ( $\triangle$ ), 6.0% ( $\bullet$ ) w/w calcium chloride, and variation of tensile storage modulus for potato starch films with different levels of calcium chloride at  $-100^{\circ}\text{C}$  ( $\blacklozenge$ , left y axis) and  $120^{\circ}\text{C}$  ( $\blacksquare$ , right y axis) at a moisture content of (c) 3.7 and (d) 18.8% scanned at the rate of  $2^{\circ}\text{C}/\text{min}$ , frequency of 1Hz and strain of 0.1%.

Figures 4.1a and 4.1b suggest that the near neutral calcium chloride solutions of this investigation affect the morphology of potato starch. Pressurisation at 120°C for 7min induces starch gelatinisation, and the heating profile of all samples shows a significant mechanical relaxation between 30 and 120°C. The results are summarised in Figures 4.1c and 4.1d for the conditions of low and high moisture content, respectively. In both cases, starch without added counterion exhibits the lowest values of tensile shear modulus at -100°C. These rise almost monotonically in subsequent experimentation, with the effect being highly reproducible to reach maximum values at 6% (w/w) calcium chloride in formulations. Strikingly, patterns of structure development reverse themselves at 120°C where, for both levels of moisture, increasing additions of calcium chloride yield softer networks, with results at 120°C being consistent as before but inversed.

Results in Figures 4.1(a-d) argue that molecular processes are not controlled solely by the simple concept of starch plasticisation in the presence of calcium chloride. It is known that addition of sodium chloride to extruded starch products increases the free volume of the polymeric matrix (Farahnaky, Farhat, Mitchell, & Hill, 2009). In the case, however, calcium ions are capable of forming direct electrostatic interactions with the hydroxyl and phosphate groups of potato starch (Jay-lin, & Ames, 1993; Day, Fayet, & Homer, 2013). Aided by the thermal regime of this investigation, i.e. 120°C for 7min, the starch granules undergo extensive gelatinisation that can lead to partial depolymerisation at high levels of calcium chloride addition (Moreau, Bindzus, & Hill, 2011). Low molecular-weight polymeric species are not efficient network formers in the enhanced molecular-mobility environment at 120°C leading to a drop in the values of  $E'$  with increasing counterion addition. They are able, however, to pack effectively within the high density matrix of the glassy state at -100°C producing a stronger structure with larger amounts of calcium chloride.



#### 4.3.2 Calorimetric evidence on the vitrification of high-solid starch/calcium chloride systems

Once the macromolecular aspects of structure development in these systems had been investigated, the focus was on the micromolecular behaviour and, in particular, the estimation of the  $T_g$ . Differential scanning calorimetry is suited for this type of analysis, and provides additional insights on the effect of calcium chloride in condensed starch preparations. Figure 4.2a illustrates changes in heat flow as a function of thermal treatment for preparations with moisture content of 3.7% w/w (RH 11%). Increasing additions of calcium chloride produce a displacement in the heat capacity traces to higher temperatures. Overall, thermograms exhibit a sigmoidal pattern between 155 and 175°C, which is characteristic of the glass transition region.

Qualitatively, the same type of thermal behaviour is recorded in Figure 4.2b, where systems were made at the highest experimental moisture content of 18.8% w/w (RH 75%). Due to the lower level of solids in these systems, the calorimetric mechanism of devitrification is recorded within the temperature range of 135 to 155°C. Traditionally, this type of thermogram is used to pinpoint the onset and endset of the glass transition region, with the midpoint being considered as the empirical  $T_g$  (Moreau, Bindzus, & Hill, 2011) and this approach is followed here with the outcomes for the starch/calcium chloride system presented in Table 4.1.

Clearly, variation in both moisture content/relative humidity and calcium chloride addition affects considerably the  $T_g$  of potato starch. In the case of 6.0% w/w salt, for example, RH increase from 11 to 75% is accompanied with by a reduction in  $T_g$  values from about 165.8 to 146.7°C. For the same amount of the counterion ( $\text{Ca}^{2+}$ ), therefore, increase in moisture content acts as plasticiser to enhance molecular mobility in samples. Within each category of relative humidity, the opposite trend in glassy consistency is observed with incorporation of calcium chloride in the starch matrix. In the case of 11.5% (w/w) moisture content (RH 58%), for example, adding calcium chloride from 0 to 6% w/w raises the  $T_g$  from about 146.2 to

151.6°C. It appears that the interactions of calcium ions with the phosphorylated (mainly amylopectin) molecules of starch and its hydroxyl groups produce dense structures in the glassy state, as also argued from the mechanical data in Figures 4.1a and 4.1b, which need to overcome a higher barrier of activation energy for molecular motions to ensue.

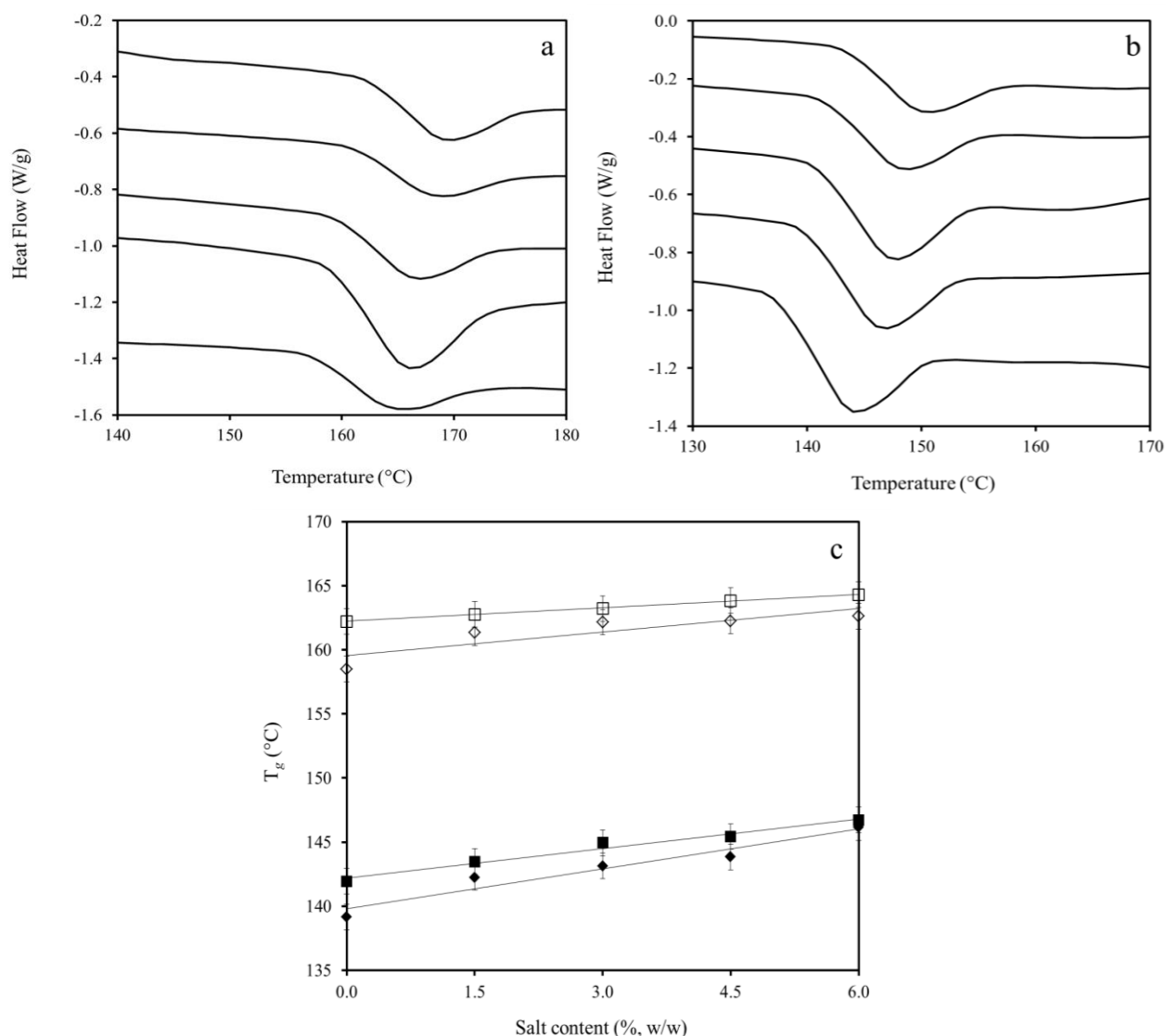


**Figure 4.2** Thermograms of potato starch films with a moisture content of (a) 3.7% w/w (RH 11%) and (b) 18.8% w/w (RH 75%) and calcium chloride content arranged successively upwards: 0.0, 1.5, 3.0, 4.5, 6.0% w/w, and T<sub>g</sub> values of these samples with moisture content of (c) 3.7% (open symbols) and 18.8% (filled symbols) for sodium chloride (diamonds) and calcium chloride (squares) as a function of salt content (scan rate of 10°C/min).

**Table 4.1**  $T_g$  values at moisture contents from 3.7% w/w (RH 11%) to 18.8% w/w (RH 75%) for potato starch with calcium chloride contents between 0 and 6.0% (w/w)

Calcium chloride content (%)	RH 11%			RH 23%			RH 33%		
	Onset (°C)	Endset (°C)	$T_g$ (°C)	Onset (°C)	Endset (°C)	$T_g$ (°C)	Onset (°C)	Endset (°C)	$T_g$ (°C)
0.0	157.43	162.48	161.72	158.60	161.96	160.81	148.73	158.24	156.99
1.5	157.94	163.28	161.80	160.21	162.57	161.24	156.67	159.67	158.58
3.0	158.36	164.96	162.14	161.48	162.47	162.02	157.12	160.68	159.58
4.5	159.00	165.14	162.61	162.51	163.89	162.65	158.67	162.53	161.24
6.0	161.10	167.88	165.75	163.46	164.94	163.52	161.75	163.58	162.55
Calcium chloride content (%)	RH 58%			RH 65%			RH 75%		
	Onset (°C)	Endset (°C)	$T_g$ (°C)	Onset (°C)	Endset (°C)	$T_g$ (°C)	Onset (°C)	Endset (°C)	$T_g$ (°C)
0.0	141.13	147.76	146.20	139.57	144.07	141.77	137.37	141.93	141.91
1.5	143.87	148.32	147.51	140.37	144.66	143.73	139.67	144.28	143.46
3.0	145.26	149.77	149.31	141.07	145.42	145.20	140.56	145.08	144.93
4.5	147.22	151.62	150.73	142.71	146.91	146.84	142.50	146.02	145.43
6.0	148.21	152.66	151.55	144.30	148.70	148.22	144.28	147.23	146.71

**Note:** For all combinations of relative humidity and calcium chloride content in samples, onset, endset and glass transition temperatures fall within  $\pm 0.3$  of the quoted values

The results of the present investigation using calcium chloride can be contrasted with corresponding work on potato starch films with sodium chloride (Chuang, Panyoyai, Shanks, & Kasapis, 2015). In both cases, calorimetric evidence indicates that increasing moisture content from 3.7 to 18.8% (w/w) results in a 20°C drop in the values of  $T_g$  due to the plasticizing effect of water molecules on the potato starch matrix (Figure 4.2c). Within a given moisture content, i.e. either 3.7 or 18.8% (w/w), endothermic events exhibit a reproducible increase in the  $T_g$  values of starch/calcium chloride samples, as compared to the sodium chloride counterparts, for each level of salt addition.

This outcome further emphasises the importance of the relative intensity of specific electrostatic interactions between hydrophilic parts of the starch molecule and positively charged counterions, which belong to the opposite ends of “salting out” (sodium cation) and “salting in” (calcium cation) of the Hofmeister series (Hofmeister, 1988; Kunz, Henle, & Ninham, 2004). The stronger antiplasticising effect of calcium ions, as densely charged carriers, in comparison to that of sodium ions, indicates that the focus of the discussion to interpret results in these systems should be on the added cations as opposed to the chlorine anions.

#### *4.3.3 Infrared spectroscopy for the elucidation of molecular forces in the starch/calcium chloride system*

FTIR spectroscopy was used to investigate the nature of the molecular forces involved in the structure of the potato starch/calcium chloride preparations. Figure 4.3a shows the corresponding spectra for a moisture content of 3.7% w/w (RH 11%) over the range 4000 to 700 $\text{cm}^{-1}$ . These are dominated by the vibrations of glucose molecules highlighted at 945, 1000-1080, 1155, 1675 and 2944 $\text{cm}^{-1}$ , as well as the formation of hydrogen bonds at the range of 3300-3400  $\text{cm}^{-1}$ .

The infrared absorption at 945 $\text{cm}^{-1}$  can be attributed to the C-O-C skeletal mode vibrations of  $\alpha$ -glycosidic linkage in starch. The overlapping bands between 1000 and 1080 $\text{cm}^{-1}$  are characteristic of C-O-H bending, and C-O, C-C and O-H stretching. The absorbance band at 1155 $\text{cm}^{-1}$  is associated with C-O and C-C asymmetric stretching of glycosidic bonds (Deeyai, Suphantharika, Wongsagonsup, Dangtip, 2013; Kizil, Irudayaraj, & Seetharaman, 2002). In addition, the absorption spectra in the region of 3300 to 3400 $\text{cm}^{-1}$  correspond to the highly polar hydroxyl groups in starch that form a plethora of intermolecular and intramolecular hydrogen bonds (Li, Zeng, Gao, & Li, 2011).

It was well established that calcium ions have a higher sorption capacity and electrical charge than sodium ions (Tomasik, & Schilling, 1998), hence the former are able to create strong coordination complexes with C-O-C groups presented in

the starch molecule (Jiang, Jiang, Gan, Zhang, Dai, & Zhang, 2012). The effect of calcium chloride, and its interactions with starch and water molecules, is seen within the range of 945 to 1155 $\text{cm}^{-1}$  in Figure 4.3a.

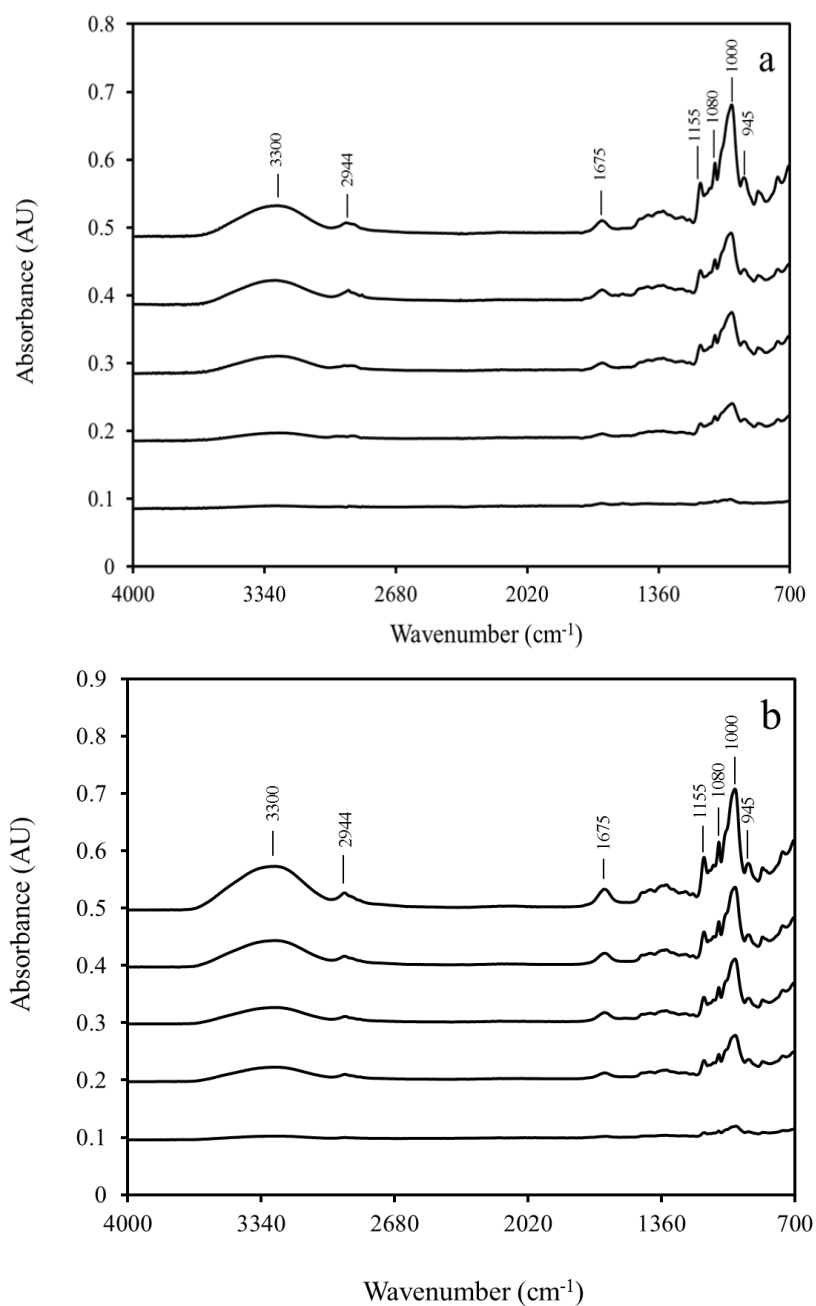


**Figure 4.3** FTIR spectra showing the absorbance of potato starch in the presence of calcium chloride content of 0.0, 1.5, 3.0, 4.5, 6.0% w/w arranged successfully upwards with moisture content of (a) 3.7% w/w (RH 11%) and (b) 18.8% w/w (RH 75%)

There was an increase in peak intensity as a function of counterion addition, which could be explained by increasing interactions in the sample. Similar results have been recorded in Figure 4.3b for materials with a moisture content of 18.8% w/w (RH 75%) but the trends have been further intensified.

The narrowing of peaks, mostly at about  $1000\text{cm}^{-1}$ , with increasing levels of counterion and, in particular, for samples with higher water content in Figure 4.3b, supports the concept of modifications in the inter-double-helical links of starch. These effects are reflected in macromolecular characteristics of the polymeric network discussed earlier from thermomechanical evidence. Furthermore, identification of water absorbed in the amorphous regions of starch can be seen as a broad band with maximum intensity at  $1675\text{cm}^{-1}$  (Capron, Robert, Colonna, Brogly, & Planchot, 2007; Sevenou, Hill, Farhat & Mitchell, 2002).

The C-H stretch at  $2944\text{cm}^{-1}$  is assigned to the  $\text{CH}_2$  deformation of the amylose molecules in potato starch (Kizil, Irudayaraj, & Seetharaman, 2002), and can be clearly observed in the spectra of our samples with the highest amount of calcium chloride (Figures 4.3a and 4.3b). The relatively broad infrared band at  $3300\text{cm}^{-1}$  is associated with hydrogen bonds between starch and small molecule solvent or co-solute. It is understood that high charge-density counterions can weaken the normal intramolecular and intermolecular associations of starch by replacing them with stronger interactions between polymer and solvent or co-solute (Ma & Yu, 2004). The increasing intensity of this FTIR band with calcium chloride addition argues for cohesive interactions between ionised calcium and oxygen atoms of the starch molecule that facilitate the formation of coordinated complexes among the three main components of the condensed matrix, i.e. starch, water and counterions.

#### *4.3.4 X-ray diffraction analysis in high-solid starch/calcium chloride preparations*

The molecular morphology of our systems was further examined using wide angle X-ray diffraction. In general, any crystallinity or regular order should be relatively small, since the architecture of potato starch was largely destroyed during heat

processing at 120°C for 7min, and the kinetics of re-crystallisation, if any, should be very low in this high-solid matrix (Frost, Kaminski, Kirwan, Lascaris, Shanks, 2009; Mizuno, Mitsuiki, & Motoki, 1998).

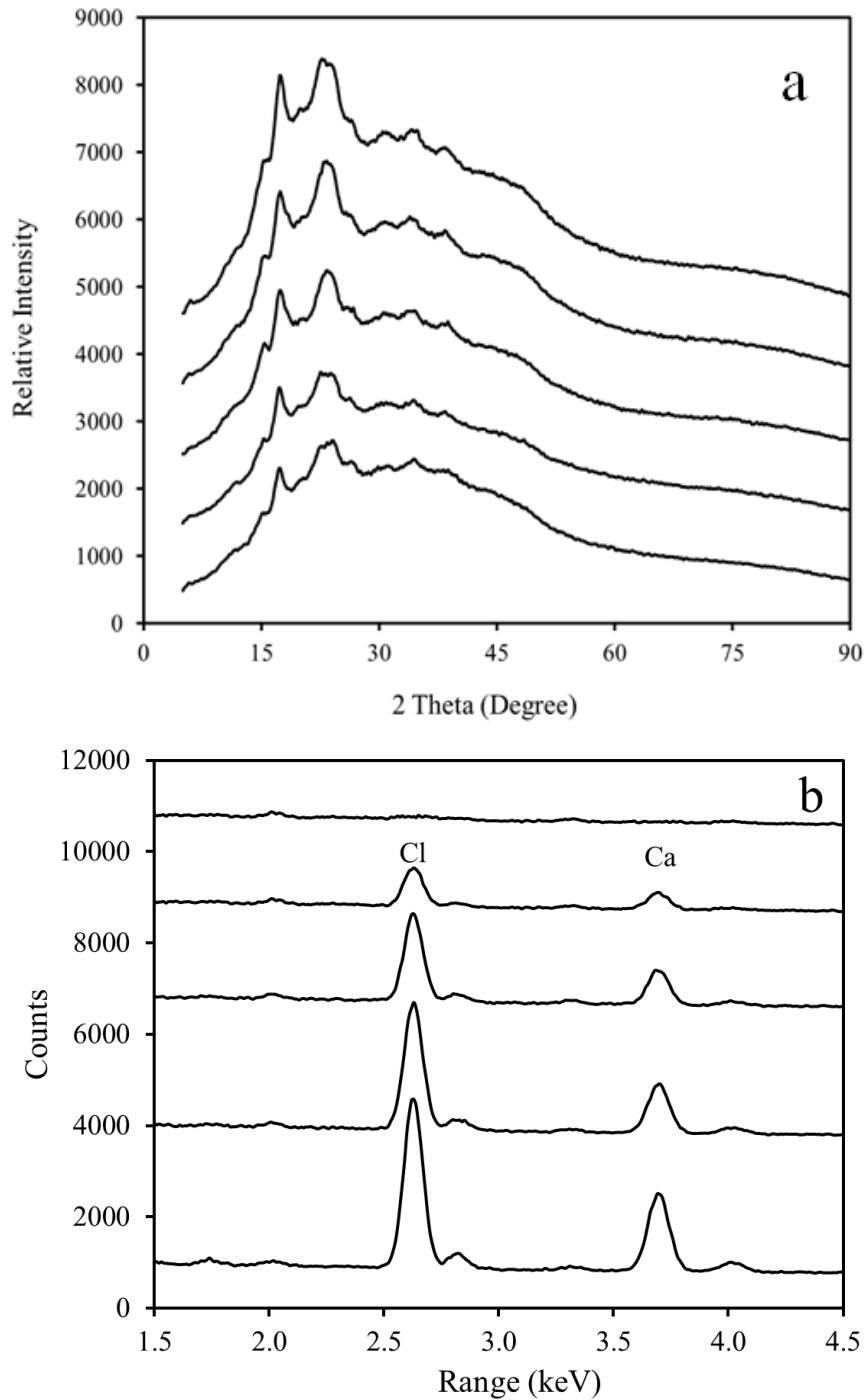


**Figure 4.4** X-ray diffractograms (a) and EDX spectra (b) for potato starch at a moisture content of 18.8% w/w (RH 75%) in the presence of calcium chloride content of 0.0, 1.5, 3.0, 4.5, 6.0% w/w arranged successfully downwards

X-ray diffraction patterns of preparations with a moisture content of 18.8% w/w (RH 75%) subjected to a monochromatic radiation source are shown in Figure 4.4a. The presence of salt induces a subtle but reproducible change in the shape of the diffractogram from 14 to 15 degrees ( $2\theta$ ). At 17 degrees ( $2\theta$ ), there is a sharp peak observed especially in the high-solid materials without counterion, and its intensity is reduced thereafter with increasing addition of calcium chloride. Finally, the peak at 22 degrees ( $2\theta$ ) becomes gradually broader and smaller in intensity as a function of added salt.

Certainly, there is no evidence from the X-ray diffractograms, i.e. sharp and narrow diffraction peaks, that the calcium chloride is present in crystalline form in the materials. This is an agreement with the EDX observations in Figure 4.4b where illustrating relatively peak events of increased intensity are recorded with increasing addition of the counterion to the condensed starch matrix. It supports the mechanism of ionised calcium atoms that interact directly with polar parts of the starch molecule to alter its molecular characteristics and glass transition phenomena.

#### *4.3.5 Microscopic examination of the starch/calcium chloride network*

SEM was employed to provide tangible evidence of the network topology in the potato starch/calcium chloride samples following hot pressing at 120°C for 7min. Micrographs are shown in Figure 4.5 for two distinct moisture contents and three levels of the counterion. Fibrillar structures of larger strand thickness, with increasing moisture content, are observed in starch assemblies without added calcium chloride (Figures 4.5a and 4.5d). The absence of visible calcium chloride grains in the remaining micrographs indicates thorough mixing, and the preparation of macroscopically homogenous systems with molecular solvation of the counterion at 3.0 and 6.0% (w/w) levels of addition.



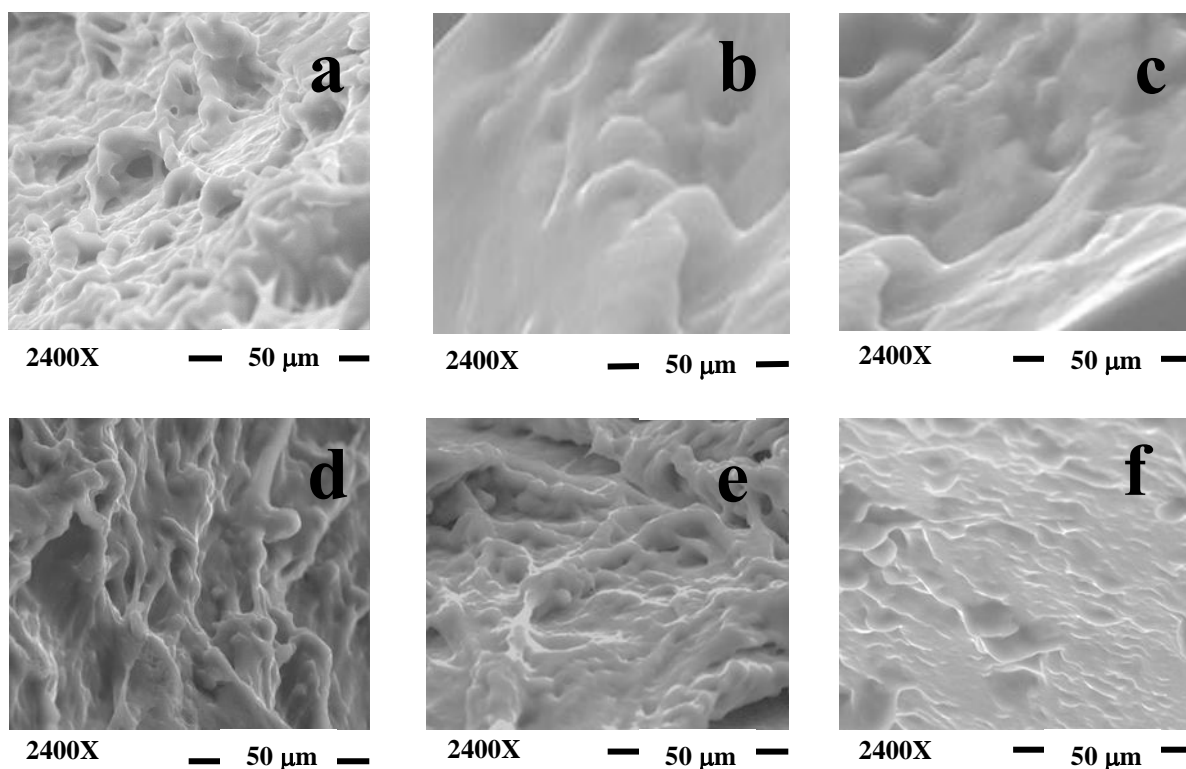


**Figure 4.5** SEM micrographs of potato starch with moisture and calcium chloride contents of (a) 3.7 and 0.0%, (b) 3.7 and 3.0%, (c) 3.7 and 6.0%, (d) 18.8 and 0.0%, (e) 18.8 and 3.0%, (f) 18.8 and 6.0% w/w, respectively

Featureless backgrounds were observed in Figures 4.5b and 4.5c for the relatively dehydrated starch matrices in the presence of  $\text{CaCl}_2$ . In contrast, moisture incorporation at 18.8% (w/w) supports the retention of some fibrillar-like structure at the two levels of calcium chloride addition (Figures 4.5e and 4.5f), which, however, is less well defined than for the starch/water counterparts. Visual observations further lend support to the concept of calcium ions controlling the macromolecular behaviour of gelatinised potato starch at solid levels that allow thermally induced vitrification.

## 4.4 CONCLUSIONS

Examination of condensed model systems of potato starch with calcium chloride can assist in the rationalisation of the functional properties of cereal based food products and biodegradable food packaging. This study gelatinised the starch granule turning it into a polymeric material, which upon subsequent cooling exhibited classical mechanical behaviour of glassy consistency, as documented in the master curve of viscoelasticity (Kasapis, 2008). A series of physical probes was then utilised to provide good evidence for the development of macroscopically homogeneous mixtures where calcium chloride molecules dissociate to their ions. Dissolved calcium atoms then form specific electrostatic interactions with the polar and negatively charged (amylopectin is partially phosphorylated) sequences of the potato starch molecule. The outcome of this interaction is thermally stable structures leading to higher values of the  $T_g$  for starch with increasing salt addition at a given moisture level. It appears that under the thermal conditions employed in this investigation, i.e. steam preheated hot press, and sample composition, amorphous calcium ions, as opposed to crystallised calcium chloride molecules, have an antiplasticising effect on potato starch that stabilises the polymeric matrix in the glassy state.

## 4.5 REFERENCES

- Albarracin, W., Sánchez, I. G., Grau, R., & Barat, J. M. (2011). Salt in food processing; usage and reduction: a review. *International Journal of Food Science and Technology*, 46, 1329-1336.
- Biliaderis, C. G. (2009). Structure transitions and related physical properties of starch. In J. BeMiller & R. Whistler (Eds.), *Starch, chemistry and technology* (3rd ed.) (pp. 293-372). New York, Academic Press.
- Capron, I., Robert, P., Colonna, P., Brogly, M. & Planchot, V. (2007). Starch in rubbery and glassy states by FTIR Spectroscopy, *Carbohydrate Polymers*, 68, 249-259.
- Chaudhary, D. S., Adhikari, B. P., & Kasapis, S. (2011). Glass-transition behaviour of plasticized starch biopolymer systems-A modified Gordon-Taylor approach. *Food Hydrocolloids*, 25, 114-121.
- Chuang, L., Panyoyai, N., Shanks, R. & Kasapis, S. (2015). Effect of sodium chloride on the glass transition of condensed starch systems. *Food Chemistry*, 184, 65-71.
- Day, L., Fayet, C. & Homer, S. (2013). Effect of NaCl on the thermal behaviour of wheat starch in excess and limited water. *Carbohydrate Polymers*, 94, 31-37.
- Deeyai, P., Supphantharika, M., Wongsagonsup, R., Dangtip, S. (2013). Characterization of modified tapioca starch in atmospheric argon plasma under diverse humidity by FTIR spectroscopy. *Chinese physical society and IOP Publishing*, 30, 018103-1 - 018103-4.
- Farahnaky, A., Farhat, I. A., Mitchell, J. R., & Hill, S. E. (2009). The effect of sodium chloride on the glass transition of potato and cassava starches at low moisture contents. *Food Hydrocolloids*, 23, 1483-1487.
- Frost, K., Kaminski, D., Kirwan, G., Lascaris, E. & Shanks, R. (2009). Crystallinity and structure of starch using wide angle X-ray scattering. *Carbohydrate Polymers*, 78, 543-548.
- Hofmeister, F. (1988). Zur Lehre von der Wirkung der Salze. *Archiv für experimentelle Pathologie und Pharmakologie*, 24, 247-260.

- Hulleman, S. H. D., Janssen, F. H. P., & Feil, H. (1998). The role of water during plasticization of native starches. *Polymers*, 39, 2043-2048.
- Jay-lin, J. & Ames, I. A. (1993). Mechanism of starch gelatinization in neutral salt solutions. *Starch/Stärke*, 5, 161-166.
- Jiang, X., Jiang, T., Gan, L., Zhang, X., Dai, H., & Zhang, X. (2012). The plasticizing mechanism and effect of calcium chloride on starch/poly(vinyl alcohol) films. *Carbohydrate Polymers*, 90, 1677-1684.
- Kasapis, S. (2008). Recent advances and future challenges in the explanation and exploitation of the network glass transition of high sugar/biopolymer mixtures. *Critical Reviews in Food Science and Nutrition*, 48, 185-203.
- Kasapis, S. (2009). Glass transitions in foodstuffs and biomaterials: Theory and measurements. In M. S. Rahman (Ed.), *Food properties handbook*, (2nd ed) (pp. 207-245). Boca Raton, CRC Press/Taylor & Francis.
- Kizil, R., Irudayaraj, J., & Seetharaman, K. (2002). Characterization of irradiated starches by using FT-Raman and FTIR Spectroscopy. *Journal of Agriculture and Food Chemistry*, 50, 3912-3918.
- Kunz, W. Henle, J., & Ninham, B. W. (2004). 'Zur Lehre von der Salze' (about the science of the effect of salts): Franz Hofmeister's historical papers. *Current Opinion in Colloid and Interface Science*. 9, 19-37.
- Li, G., Zeng, J., Gao, H. & Li, X. (2011). Characterization of phosphate monoester resistance starch. *International Journal of food Properties*, 14, 978-987.
- Liu, H., Xie, F., Yu, L., Chen, L., & Li, L. (2009). Thermal processing of starch-based polymers. *Progress in Polymer Science*. 34, 1348-1368.
- Lourdin, D., Coignard, L., Bizot, H., & Colonna, P. (1997). Influence of equilibrium relative humidity and plasticizer concentration on the water content and glass transition of starch materials. *Polymers*, 38, 5401-5406.
- Luk, E., Sandoval, A. J., Cova, A., & Müller, A. J. (2013). Anti-plasticization of cassava starch by complexing fatty acids. *Carbohydrate Polymers*, 98, 659-664.

- Luna-Guzmán, I. & Barrett, D. M. (2000). Comparison of calcium chloride and calcium lactate effectiveness in maintaining shelf stability and quality of fresh-cut cantaloupes. *Postharvest Biology and Technology*, 19, 61-72.
- Ma, X. F., & Yu, J. G. (2004). Formamide as the plasticizer for thermoplastic starch. *Journal of Applied Polymer Science*, 93, 1769-1773.
- Menard, K. P. (2008). *Dynamic mechanical analysis: A practical introduction*. (2nd ed.). Baton Rouge, CRC Press/Taylor & Francis.
- Mizuno, A., Mitsuiki, M., & Motoki, M. (1998). Effects of crystallinity on the glass transition temperature of starch. *Journal of Agricultural and Food Chemistry*, 46, 98-103.
- Moreau, L., Bindzus, W. & Hill, S. (2011). Influence of salt on starch degradation: Part II- salt classification and caramelisation. *Starch/Stärke*, 63, 676-682.
- Noor, M. A. M., & Islam, M. N. (2006). Effect of modification on the functional properties of rice starch. In J. F. Kenedy, G. O. Phillips and P. A. Williams. (Eds.), *Recent advances in environmentally compatible biopolymers* (pp. 79-90). Cambridge, Woodhead Publishing.
- Tsoukpoe, N., Rammelberg, K. E., Lele, H. U., Korhammer, A. F., Watts, K., Schmidt, B. A. T., & Ruck, W. K. L. (2015). A review on the use of calcium chloride in applied thermal engineering. *Applied Thermal Engineering*, 751, 513-531.
- Perdomo, J., Cova, A., Sandoval, A. J., Garía, L., Laredo, E., & Müller, A. J. (2009). Glass transition temperatures and water sorption isotherms of cassava starch. *Carbohydrate Polymers*, 76, 305-3013.
- Roudaut, G., Simatos, D., Champion, D., Contreras-Lopez, E., & Le Meste, M. (2004). Molecular mobility around the glass transition temperature: a mini review. *Innovative Food Science and Emerging Technologies*, 5, 127-134.
- Róz, A. L. D., Carvalho, A. J. F., Gandini, A. & Curvelo, A. A. S. (2006). The effect of plasticizers on thermoplastic starch compositions obtained by melt processing. *Carbohydrate Polymers*, 63, 417-424.

- Sablani, S.S., Kasapis, S. & Rahman, M.S. (2007). Evaluating water activity and glass transition concepts for food stability. *Journal of Food Engineering*, 78, 266-271.
- Sevenou, O., Hill, S. E., Farhat, I. A., & Mitchell, J. R. (2002). Organisation of the external region of the starch granule as determined by infrared spectroscopy. *International Journal of Biological Macromolecules*, 31, 79-85.
- Talja, R. A., Helén, H., Roos, Y. H., & Jopuppila, K. J. (2007). Effect of various polyols and polyols contents on physical and mechanical properties of potato starch-based films. *Carbohydrate Polymers*, 67, 288-295.
- Tomasik, P., & Schilling, C. H. (1998). Complexes of starch with inorganic guests. *Advances in Carbohydrate Chemistry and Biochemistry*. 53, 263-343.
- Zeleznak, K. J., & Hosney, R. C. (1987). The glass transition in starch. *Cereal Chemistry*. 64, 121-124.

## CHAPTER 5

### EFFECT OF SALT ON THE GLASS TRANSITION OF CONDENSED TAPIOCA STARCH SYSTEMS

#### ABSTRACT

There is a growing interest in tapioca starch's application to food and plastics due to its economic value of production. The influence of salt inclusion (NaCl and CaCl<sub>2</sub>), up to 6% w/w, on the physicochemical properties of condensed tapioca starch system was investigated in this work. The samples were prepared by hot pressing at 120°C for 7 min producing condensed systems that covered a range of moisture contents from 7.34% w/w (23% relative humidity) to 19.52% w/w (75% relative humidity). Experimental work was performed using dynamic mechanical analysis, modulated differential scanning calorimetry, Fourier transform infrared spectroscopy, wide angle X-ray diffraction and scanning electron microscopy. Increasing the salt level enhances the mechanical strength of the starch system and shifts the glass transition temperature to a higher value, as monitored calorimetrically. The antiplasticising effects of both NaCl and CaCl<sub>2</sub> are the same since they arise from non-specific interactions between the added counterions and the hydroxyl groups of the polysaccharide.

**Keywords:** glass transition, sodium chloride, calcium chloride, tapioca starch, high-solid systems

## 5.1 INTRODUCTION

Tapioca, also known as cassava, is one of the most important crops in tropical countries, rating third after rice and maize. It is estimated that the global production of cassava is around 260 million tonnes a year (FAO, 2013). As the most economical source of energy, tapioca yields a carbohydrate content that is 40% and 25% higher than rice and maize, respectively (Tonukari, 2004). The crop is also well-known for the ease of plantation and low input requirement (Breuninger, Piyachomkwan, & Sriroth, 2009). It has good resistance to drought; hence, it can grow in areas with low rainfall or infertile soil. As a result, there is a notable increase in the processing of cassava roots in the last few decades in order to harvest tapioca starch.

There is promising growth for the tapioca starch industry as consumers shift towards lower-fat foods, reduced dependence on chemical modifications, and some avoidance of cereal starches. Tapioca starch has been widely utilised in numerous food products, for instance, baby foods (Smalligan, Kelly, & Estela, 1977), noodles (Ishigaki, Saito, & Fujita, 1994), snacks and biscuits (Plata-Oviedo & Camargo, 1998). Its low residuals and bland flavour contribute to the food industry's preference of using tapioca starch compared to cereal counterparts. Further, it has been a starch of choice in textile and paper industries due to its economic value. Demand for cassava starch as a raw material for the production of bioethanol is also growing rapidly (Matthews, 2013).

Similar to all other starches, tapioca starch primarily consists of two major molecular entities, amylose and amylopectin. The content of the former, which is essentially a linear helical molecule, typically ranges from 17 to 20%. The latter, which is a highly branched fraction, is generally a larger molecule with molecular weight of  $10^7$ - $10^9$ Da, compared to amylose with molecular size of  $10^5$ - $10^6$ Da (Perez, Baldwin, & Gallant, 2009). The polymer has low levels of fat, protein, and ash, and a lower amylose content than other amylose-containing starches, and high



molecular weight amylose and amylopectin (Swinkels, 1985). The functionality of the starch is markedly influenced by moisture content, starch source, and environmental conditions such as temperature, pressure, mechanical damage, physical modifications, chemical modifications, hydrophilic hydrocolloids, and presence of small molecular solutes such as salt (Biliaderis, 2009).

Salts are commonly incorporated in starch-based products to enhance flavour and techno-functionality, with sodium chloride and calcium chloride being the most widely used salts (Albarracin, Sanchez, Grau, & Barat, 2011). Inclusion of sodium chloride has been known to increase the gelatinisation temperature of tapioca starch and delay the retrogradation of the starch gels (Chatakanonda, Wongprayoon, & Sriroth, 2007). Muhrbeck and Eliasson (1987) investigated the effect of various salts on potato starch gels and found that the counterions interfered with the gel formation. They suggested that the ions neutralised the electric charge of the starch molecule, thus preventing the formation of crosslinks between the phosphate groups of the polymeric chains.

Current diet trends emphasise the importance of salt reduction in processed foods due to the health issues associated with high salt intake. However, salt reduction does not only affect the organoleptic profile of food products but also influences their texture and stability. Therefore, it is imperative to understand the role of salt on the phase behaviour of starch based systems. The aim of this work is to probe the influence of two widely used salts, sodium chloride and calcium chloride, on the structural properties of condensed tapioca starch systems, conditioned at different relative humidity values.

## 5.2 MATERIALS AND METHODS

### 5.2.1 *Materials*

#### 5.2.1.1 *Tapioca starch*

A food-grade native tapioca starch was used, which was a light grey, fine free-flowing powder with a bland taste. It contains 7ppm of sulphur dioxide without known allergens. According to Brabender analysis, it has a gelling temperature from 66 to 77°C with a temperature peak at 77°C; this was analysed with 6% dry basis of the material. Typical nutritional values (%w/w) show a starch content of 87.0%, moisture content of 12.4%, ash content of 0.1%, pH of 6, and bacteriological characteristics of mold and yeast of about 75 CFU/g (Scalzo Food Industries, West Melbourne, VIC, Australia).

#### 5.2.1.2 *Sodium chloride and calcium chloride*

Sodium chloride and calcium chloride were purchased from Sigma Aldrich (Castle Hill, NSW, Australia). Sodium chloride is a white powder, with minimum purity by titration being 99.9%, and pH 6.8 for 1M in water at 20°C. Anhydrous calcium chloride is a white granular form ( $\leq 7.0$  mm), with minimum purity by EDTA titration being 98.1%.

#### 5.2.1.3 *Millipore water type 2*

Millipore system Elix® 10 water purification system was used to produce the Millipore type 2 analytical-grade water of this investigation (Merck KGaA, Germany).

#### 5.2.1.4 *Saturated salt solutions*

Desiccating chambers were prepared to achieve a series of moisture and relative humidity values for our starch/sodium chloride and starch/calcium chloride samples, with the saturated salt solutions being purchased from Sigma Aldrich, i.e.

potassium acetate ( $\text{CH}_3\text{COOK}$ ): moisture content 7.34% w/w, RH 23%; sodium bromide ( $\text{NaBr}$ ): moisture content 10.44% w/w, RH 58%; sodium chloride ( $\text{NaCl}$ ): moisture content 19.52% w/w, RH 75% (Sablani, Kasapis & Rahman, 2007).

### 5.2.2 *Sample preparation*

Tapioca starch powder, with a moisture content of 14.0% (w/w) that was taken into consideration for final sample preparation, was dry mixed with a wide range of added salt (sodium chloride or calcium chloride) concentrations (0.0, 1.5, 3.0, 4.5 and 6.0% w/w) to achieve a total of 35.0% (w/w) moisture content. In doing so, Millipore type 2 water was introduced piecemeal prior to processing all preparations; weighing was carried out carefully using a four decimal place analytical balance.

A twin screw Thermo Rheomix OS (HAAKE, Newington, NH, USA) blender was then used to mix the sample with a screw speed of 200rpm for 2min at ambient temperature. The mixture was then placed on a stainless steel metal frame (130mm x 130mm x 2mm) sandwiched between two non-stick plastic sheets at the bottom and top of the frame. It was then transferred to a steam preheated hot press at 120°C for 7min and pressurised at 59Bar.

Heated samples were cooled within the same press to about 45°C (to prevent air bubble formation on the starch film), packaged and sealed separately in a moisture/gas impermeable plastic vacuum bag, and stored at 4°C. To facilitate subsequent instrumental analysis, samples were cut into the desired shape and size (10mm x 10mm x 1 mm) and stored in sealed relative-humidity desiccators for 8 weeks containing the aforementioned saturated salt solutions.

Relative humidity to the required equilibrium value in the starch/salt systems was checked periodically with a water activity meter (Novasina aw set-1, Pfäffikon, Switzerland). The final moisture content of these preparations after an 8-week

desiccator storage was from 7.34% w/w (RH 23%), and 10.44% w/w (RH 58%) to 19.52% w/w (RH 75%), as estimated by oven drying at 102°C overnight.

### 5.2.3 *Methods*

#### 5.2.3.1 *Dynamic mechanical analysis*

Diamond DMA from Perkin-Elmer (Akron, Ohio, USA) with an external 60L liquid nitrogen Dewar was used for monitoring the tensile storage and loss modulus ( $E'$  and  $E''$ , respectively) of our materials. In doing so, the sample film was set on a twin grip clamp and tensile mode was employed. Cooling from ambient temperature to -110°C was carried out followed by heating to 180°C at a scan rate of 2°C/min, and frequency of 1 Hz. To minimise moisture loss during measurement, a thin layer of petroleum vacuum grease was used to coat the sample prior to loading onto the tensile grips. Isochronal routines were carried out in duplicate returning consistent results.

#### 5.2.3.2 *Modulated differential scanning calorimetry*

Thermal transfer analyser Q2000 (TA Instruments, New Castle, DE) was used. It was attached to a recirculated cooling system (RCS90), with ultra-pure nitrogen gas purging into the sample analysis chamber at a flow rate of 50mL/min. About ten mg of the material was placed in a Tzero aluminium pan, hermetically sealed by a crimper with an aluminium lid on top of the pan and analysed at modulated amplitude of  $\pm 0.53^\circ\text{C}$  for 40s. An extensive temperature range was accessed with successive cooling and heating routines from -90 to 200°C at a scan rate of 10°C/min. All measurements were performed in triplicate to yield effectively overlapping thermograms from this work.

#### 5.2.3.3 *Fourier transform infrared spectroscopy*

Data were recorded on a Perkin Elmer Spectrum 100 using MIRacle TMZnSe single reflection ATR plate system (Perkin Elmer, Norwalk, CT). Starch/salt

preparations were analysed at ambient temperature within a wavelength of 650 to 4500 $\text{cm}^{-1}$  and a resolution of 4 $\text{cm}^{-1}$ . Spectra are presented in absorbance mode based on 32 average scans. Final results were obtained following removal of the background signal at ambient temperature and have been repeated three times for each measurement.

#### *5.2.3.4 Wide angle X-ray diffraction*

Bruker D4 Endeavour (Karlsruhe, Germany) was used to examine the phase morphology of starch/salt preparations. Accelerating voltage of 40kV, current of 35 mA and position sensitive detectors (PSD) were utilised to obtain diffractograms within  $2\theta$  angle of 5-90° with intervals of 0.1°. Spectra were processed on DIFFRACplus Evaluation (Eva), version 10.0, revision 1 and measurements were performed in triplicate.

#### *5.2.3.5 Scanning electron microscopy*

FEI Quanta 200 (Hillsboro, OR, USA) was used to provide the micro-images of our materials. In doing so, low vacuum conditions were operative, the high voltage electron beam was at 20kV, the spot size was 5, and the working distance was between 8.9 and 11.4mm with a magnification of 2400X. Samples were cut with a clean, sanitised surgical scalpel into 10mm x 10mm x 1 mm cubes, equilibrated at desiccators as described earlier, and cross sections of the specimen were examined.

## 5.3 RESULTS AND DISCUSSION

### 5.3.1 Mechanical properties of condensed tapioca starch/salt systems

This section of the study aims to elucidate the macromolecular aspects of structure development in condensed tapioca starch systems. In order to understand the mechanical characteristics of the starch/salt mixtures, which are the focus of this investigation, the materials were cooled from ambient temperature to  $-100^{\circ}\text{C}$  followed by heating to  $100^{\circ}\text{C}$  at a fixed scan rate of  $2^{\circ}\text{C}/\text{min}$ , and a constant modulation frequency of 1 Hz. Figure 5.1a portrays the overall heating profiles of samples prepared at 7.34% moisture content (RH 23%) in the presence of increasing levels of calcium chloride ( $\text{CaCl}_2$ ), i.e. 0 to 6.0%, w/w.

At the beginning of the heating routine, i.e.  $-100^{\circ}\text{C}$ , the values of  $E'$  for all films are greater than  $10^{10.2}$  Pa. There is a gradual decrease in the elasticity of the films during heating, with the values of  $E'$  approaching  $10^{9.5}$  Pa at the end of the heating regime ( $100^{\circ}\text{C}$ ). A similar pattern is observed in samples prepared with sodium chloride (NaCl) at moisture content of 7.34% (RH 23%), with  $E'$  declining during heating from values in excess of  $10^{10.2}$  Pa at  $-100^{\circ}\text{C}$  to about  $10^{9.2}$  Pa at  $100^{\circ}\text{C}$  (Figure 5.1b). This behaviour indicates an alteration in the physical state of the samples from the glassy state, where large-scale molecular motions are absent and the polymer chains are in a non-symmetrical arrangement, to a more mobile and highly viscous state as the temperature increase (Biliaderis, 2009).

Figures 5.1c and 5.1d illustrate the mechanical profiles for the high moisture condition of 19.52% (RH 75%) in starch/ $\text{CaCl}_2$  and starch/NaCl blends, respectively. Both blends display a similar reduction in tensile storage modulus from values in excess of  $10^{10.1}$  Pa at  $-100^{\circ}\text{C}$  during thermal treatment. The controlled heating softens considerably the polymeric matrix of the starch/ $\text{CaCl}_2$  and starch/NaCl blends, with  $E'$  values plunging almost two orders of magnitude to about  $10^{8.6}$  and  $10^{8.4}$  Pa at  $100^{\circ}\text{C}$ , respectively. It appears that the increase in moisture content from 7.34 to 19.52% exerts a plasticising effect on the starch

systems, thereby reducing the mechanical strength of the films. The moisture induces macromolecular relaxation, mainly alpha-relaxation of the polymer backbone and beta-relaxation of the side chains in the glassy matrix (Averous & Boquillon, 2004).

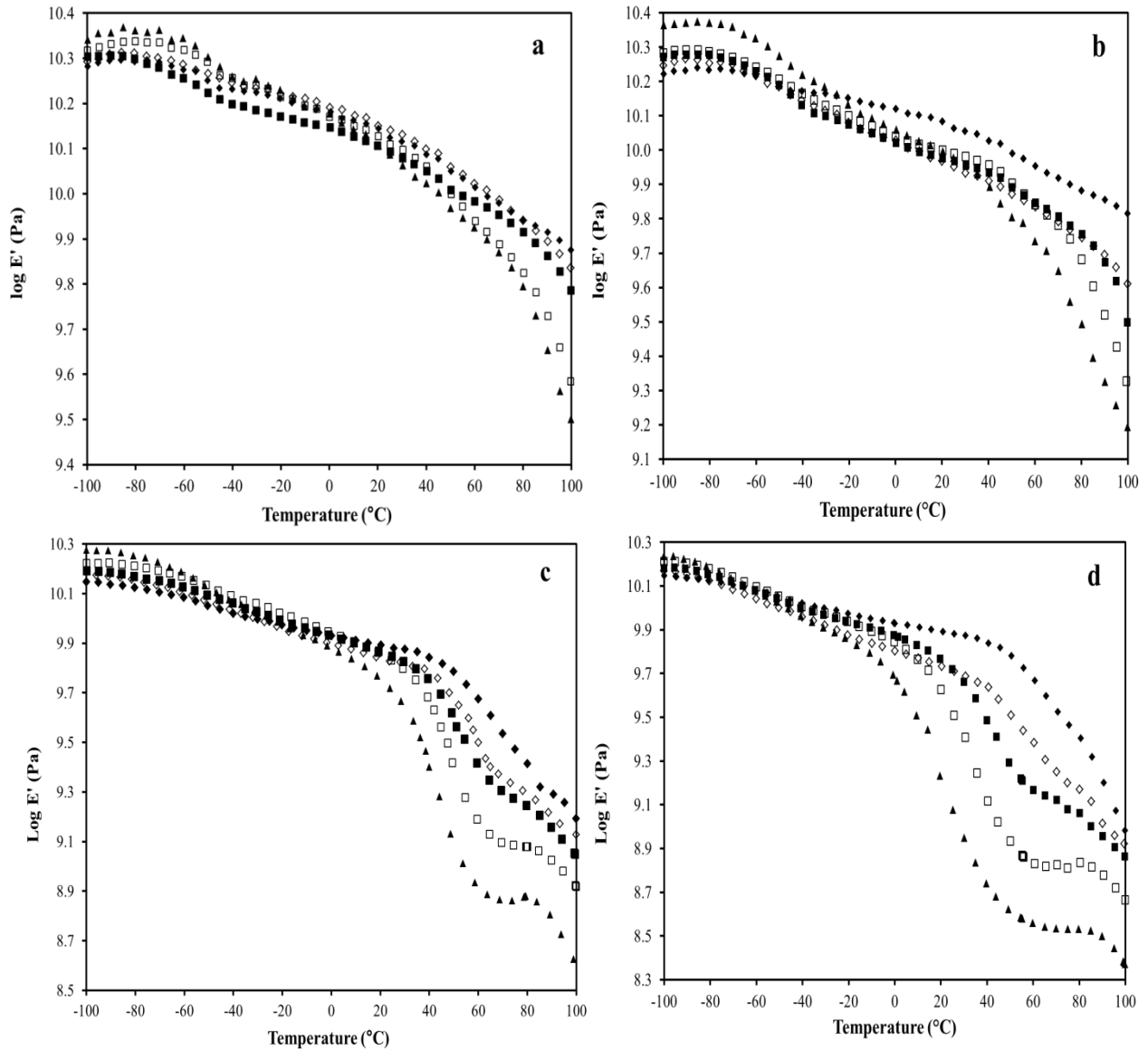


**Figure 5.1** Heating profiles of tensile storage modulus for tapioca starch films in the presence of salt at 0.0% ( $\blacklozenge$ ), 1.5% ( $\diamond$ ), 3.0% ( $\blacksquare$ ), 4.5% ( $\square$ ), 6.0% ( $\blacktriangle$ ) at a moisture content of 7.34% w/w (RH 23%) with (a) calcium chloride and (b) sodium chloride, and at a moisture content of 19.52% (RH 75%) with (c) calcium chloride and (d) sodium chloride.

Summary of the rheological findings discussed so far for the conditions of low and high moisture content/relative humidity is presented in Figures 5.2a-b and 5.2c-d, respectively.

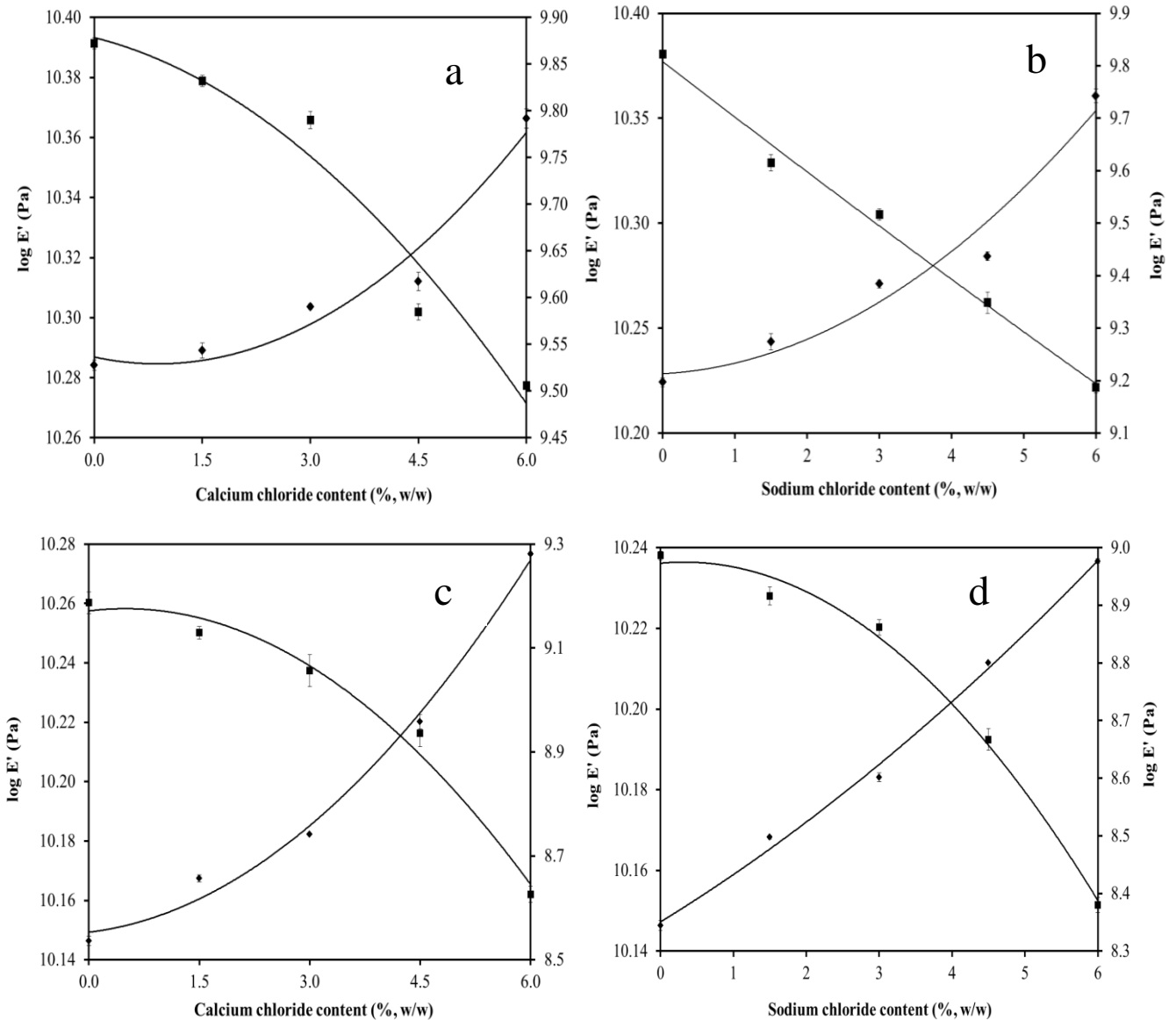


**Figure 5.2** Variation of tensile storage modulus for tapioca starch films with different levels of salt at  $-100^\circ\text{C}$  (◆; left y axis) and  $100^\circ\text{C}$  (■; right y axis) at a moisture content of 7.34% w/w (RH 23%) with (a) calcium chloride (b) sodium chloride, and at a moisture content of 19.52% w/w (RH 75%) with (c) calcium chloride (d) sodium chloride (scan rate is  $2^\circ\text{C}/\text{min}$ , frequency is 1 Hz, and error bars denote one standard deviation).



We observed reduction in  $E'$  values at 100°C with increasing counterion ( $\text{Na}^+$  and  $\text{Ca}^{2+}$ ) addition, for both levels of moisture. For instance, inclusion of  $\text{CaCl}_2$  from 0 to 6% w/w in samples with moisture content of 7.34% (RH 23%) decreases the tensile storage modulus at low temperature from  $10^{9.87}$  to  $10^{9.51}$  Pa (Figure 5.2a). At the high temperature end of this investigation, the polysaccharide/cation interactions are capable of destabilising the starch granule leading to partial depolymerisation at high concentrations of added salt.

The generation of small molecular-weight species becomes unable to support efficiently a three-dimensional network due to the enhanced molecular-mobility environment of 100°C. In contrast, the smaller-starch molecules are able to pack tightly within the high density matrix at subzero condition, i.e. -100°C. Further, there is a reinforcing effect in the network, at subzero temperatures, with the addition of counterion being able to form direct electrostatic interaction with the -OH groups of starch (Day, Fayet & Homer, 2013).

### 5.3.2 *Calorimetric evidence on the vitrification of condensed starch/salt systems*

Modulated differential scanning calorimetry (MDSC) was used to investigate the phase transitions of our single tapioca starch systems and starch/salt preparations. The heating profiles of our samples display glass transition phenomena obtained from MDSC at the controlled scan rate of 10°C/min (Figures 3a-d). The onset and endset of the heat capacity change region in thermograms are generally understood as the glass transition region. The central point of this region is considered as the calorimetrically derived glass transition temperature ( $T_g$ ). The approach is adopted in this study to produce the  $T_g$  values of the starch/salt systems seen in Table 1.

Traces of heat flow of starch/ $\text{NaCl}$  and starch/ $\text{CaCl}_2$  mixtures at moisture content of 7.34% (RH 23%) as a function of temperature are given in Figures 5.3a and 5.3b respectively. In general, the thermograms of both starch/ $\text{NaCl}$  and starch/ $\text{CaCl}_2$  systems demonstrate a sigmoidal pattern between 140 and 180°C. We note a shift in the heat capacity traces to higher temperature as the levels of salt, i.e.  $\text{NaCl}$  and  $\text{CaCl}_2$ , are raised from 0 to 6% w/w. For example, in the case of RH 23%, adding

sodium chloride from 0 to 6% w/w increases the glass transition temperature from 151.36 to 163.05°C (Table 1).

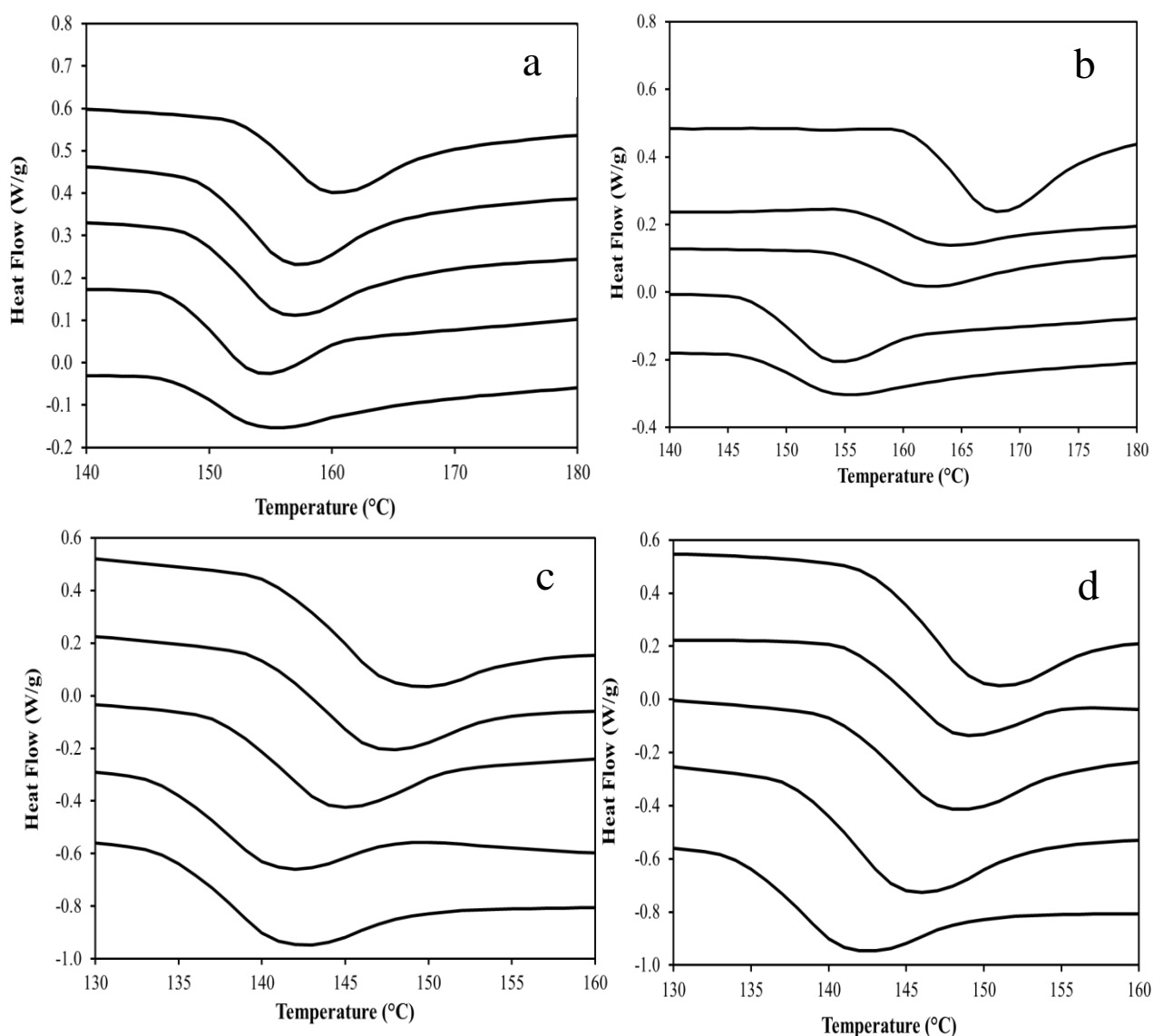


**Figure 5.3** DSC thermograms of tapioca starch films in the presence of salt at 0.0%, 1.5%, 3.0%, 4.5%, and 6.0% arranged successfully upwards at a moisture content of 7.34% w/w (RH 23%) with (a) calcium chloride and (b) sodium chloride, and at a moisture content of 19.52% (RH 75%) with (c) calcium chloride and (d) sodium chloride.

Similar thermal behaviour is observed in Figures 5.3c and 5.3d, where systems were prepared at the highest experimental moisture content of 19.52% w/w (RH 75%).

However, the calorimetric mechanism of devitrification is recorded within the lower temperature range of 130 to 160°C owing to the presence of a higher amount of moisture in these systems. For instance, in the case of 3% CaCl<sub>2</sub>, increase in RH from 23% to 75% leads to a reduction in  $T_g$  values from 153.58 to 142.07°C, and similar reductions are recorded for the onset and endset temperatures of the thermograms (Table 5.1). An increase in moisture content acts as a plasticiser to enhance the molecular mobility of the amorphous regions in starch matrices, therefore, reducing the glass transition temperature (Kasapis, 2005; Slade & Levine, 1994).

**Table 5.1**  $T_g$  values determined from DSC for tapioca starch with sodium chloride and calcium chloride content up to 6% w/w at different relative humidity values.

<b>Sodium chloride content (%)</b>	<b>RH 23%</b>			<b>RH 58%</b>			<b>RH 75%</b>		
	<b>Onset (°C)</b>	<b>Endset (°C)</b>	<b><math>T_g</math> (°C)</b>	<b>Onset (°C)</b>	<b>Endset (°C)</b>	<b><math>T_g</math> (°C)</b>	<b>Onset (°C)</b>	<b>Endset (°C)</b>	<b><math>T_g</math> (°C)</b>
0.0	147.36	151.40	151.36	139.50	144.46	144.22	134.68	138.83	138.76
1.5	147.41	151.89	151.45	143.13	148.36	147.42	135.13	143.20	142.30
3.0	154.67	158.86	157.10	144.02	148.86	148.01	140.67	145.93	145.04
4.5	158.34	160.52	159.39	146.13	149.51	149.42	141.56	146.68	146.10
6.0	161.39	165.03	163.05	146.16	151.01	150.01	142.81	147.30	147.26
<b>Calcium chloride content (%)</b>	<b>RH 23%</b>			<b>RH 58%</b>			<b>RH 75%</b>		
	<b>Onset (°C)</b>	<b>Endset (°C)</b>	<b><math>T_g</math> (°C)</b>	<b>Onset (°C)</b>	<b>Endset (°C)</b>	<b><math>T_g</math> (°C)</b>	<b>Onset (°C)</b>	<b>Endset (°C)</b>	<b><math>T_g</math> (°C)</b>
0.0	147.36	151.40	151.36	139.50	144.46	144.22	134.68	138.83	138.76
1.5	147.41	151.70	151.43	140.79	144.76	144.64	134.97	140.10	138.86
3.0	149.10	153.64	153.58	142.28	147.04	146.78	137.53	142.26	142.07
4.5	149.78	154.33	154.04	145.47	150.76	149.66	139.85	144.76	144.56
6.0	152.75	158.10	157.36	146.05	151.15	150.22	140.96	146.21	145.44

**Note:** For all combinations of relative humidity and sodium chloride and calcium chloride content in samples, onset, endset and glass transition temperatures fall within  $\pm 0.3$  of the quoted values. The moisture contents for RH 23%, 58% and 75% are 7.34%, 10.44% and 19.52%, w/w

It is evident that the presence of counterions ( $\text{Na}^+$  and  $\text{Ca}^{2+}$ ) contributes to an anti-plasticising effect on the tapioca starch matrix as shown in Figures 5.3(a-d). Similar behaviour is reported on the corresponding work with potato starch (Chuang, Panyoyai, Katopo, Shanks, & Kasapis, 2016; Chuang, Panyoyai, Shanks, & Kasapis, 2015) and wheat starch systems (Kweon, Slade, & Levine, 2008). We postulate that the counterions are capable of forming electrostatic interactions with the  $-\text{OH}$  groups of tapioca starch, which lead to a reduction in free volume and the creation of cohesive matrices.

Calcium ions, as dense charge carriers, have been shown to demonstrate a stronger antiplasticising pattern in potato starch-salt systems in comparison to that of the monovalent sodium ions (Chuang et al, 2016; 2015). The dissolved calcium forms complexes with the polar and negatively charged sequences (amylopectin is phosphorylated) of the potato starch molecule (Day, Fayet & Homer, 2013; Jay-lin & Ames, 1993). It appears, however, that there is no significant variation in the glass transition temperature values of tapioca starch-salt systems upon inclusion, at the same level, of either  $\text{NaCl}$  or  $\text{CaCl}_2$  for a given moisture level (Table 5.1). Such a result is attributed to the absence of phosphate groups in tapioca starch molecules.

### 5.3.3 FTIR analysis

FTIR spectroscopy is a powerful technique, which was employed to elucidate the molecular structure of starch/salt preparations, creating a molecular fingerprint of the samples. The corresponding spectra of starch/salt blends are presented in Figures 5.4a-b for moisture content of 7.34% w/w (RH23%), and Figures 5.4c-d for moisture content of 19.52% w/w (RH75%) respectively.

Spectra of starch/ $\text{CaCl}_2$  and starch/ $\text{NaCl}$  blends at moisture content of 7.34% (RH 23%) over the range  $4000\text{-}650\text{cm}^{-1}$  are shown in Figures 5.4a and 5.4b respectively. The vibrations of glucose molecules dominate the spectra of both blends below the region  $1320\text{cm}^{-1}$ . These vibrations originate from the C-O-C of  $\alpha$ -1,4 glycosidic linkages that can be observed as a strong infrared band around  $1000\text{ cm}^{-1}$  (Kizil,

Irudayaraj, & Seetharaman, 2002). The infrared absorptions around between 1156 and  $1080\text{cm}^{-1}$  can be attributed to the vibrations of C-O and C-O-H groups in starch. The broad band around  $3300\text{cm}^{-1}$  has been assigned as the stretching mode of O-H groups of starch and the peak at  $2950\text{cm}^{-1}$  corresponds to C-H stretching vibrations (Lazano-Vazquez, et al., 2015; Xia et al., 2015).

The narrowing of peaks, predominantly at about  $1000\text{cm}^{-1}$ , with increasing levels of counterion, in particular, for samples with a higher moisture content (Figures 5.4c-d), supports the concept of modification in the inter-helical links of starch. Moreover, the peak around  $1660\text{cm}^{-1}$  corresponds to the deformation vibration of the hydroxyl groups in bound water (Xia et al, 2015). The strong peak intensity around  $3300\text{cm}^{-1}$  in samples with higher moisture content (Figures 5.4c-d) indicate the interaction between hydroxyl groups of tapioca starch and water (Bergo, Freitas, & do Amaral Sorbral, 2012).

Literature has recorded that calcium and sodium ions form complexes with C-O-H and C-O-C groups of the starch molecule, with the former being able to produce stronger complexes due to higher sorption capacity and electrical charge (Jiang, Jiang, Gan, Zhang, Dai, & Zhang, 2012; Tomasik, & Schilling, 1998). The interaction between counterion and starch molecule is recorded within the wavelength of 1080 and  $1000\text{cm}^{-1}$  (Figures 5.4a-d). There is an increasing trend in peak intensity as a function of counterion addition, for both of them, which supports the concept of strengthening interactions in condensed salt/starch materials.

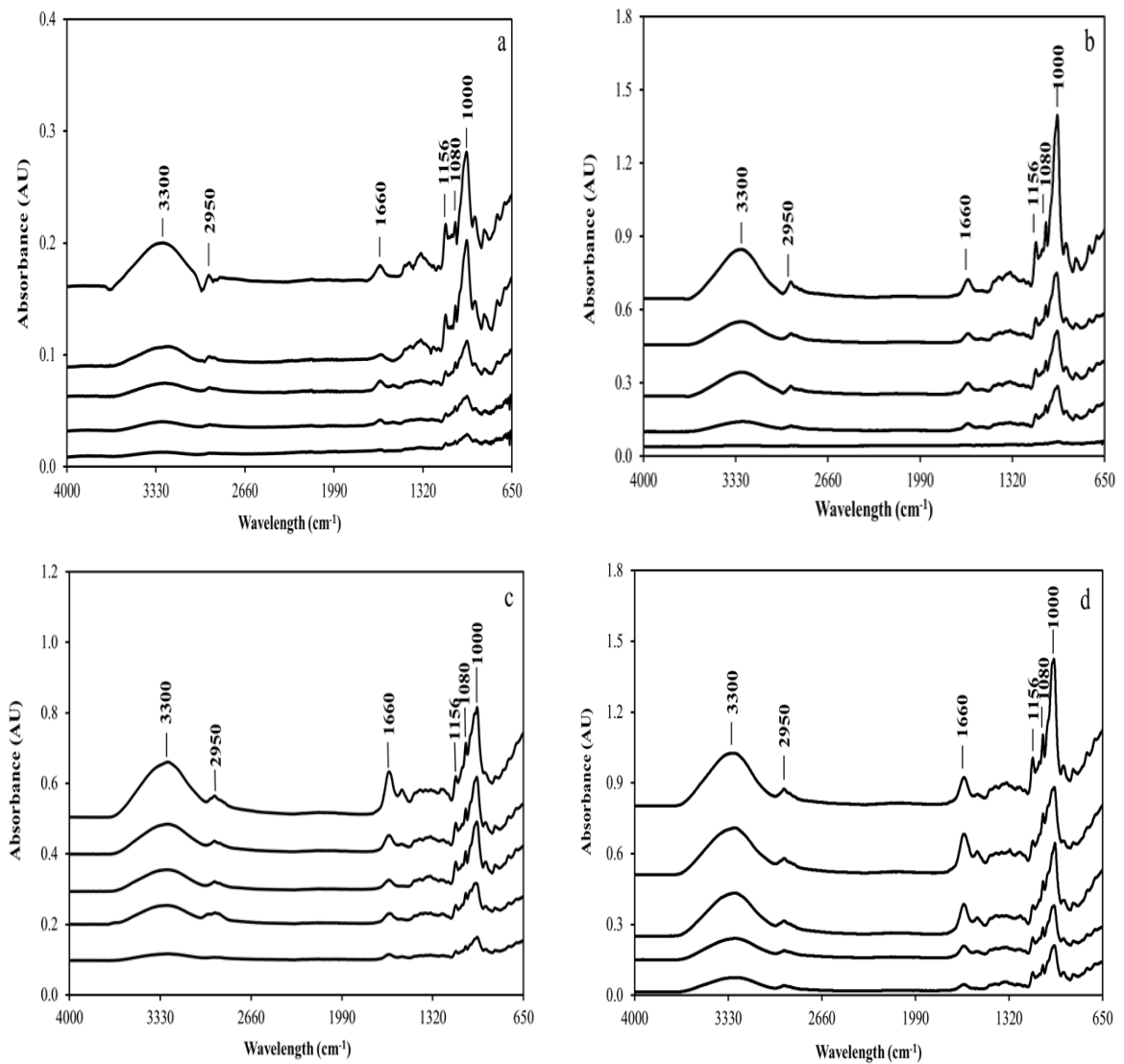


**Figure 5.4** FTIR spectra of tapioca starch films in the presence of salt at 0.0%, 1.5%, 3.0%, 4.5%, and 6.0% arranged successfully upwards at a moisture content of 7.34% w/w (RH 23%) with (a) calcium chloride and (b) sodium chloride, and at a moisture content of 19.52% (RH 75%) with (c) calcium chloride and (d) sodium chloride.

#### 5.3.4 X-Ray analysis

The semi-crystalline structure of the tapioca starch films with salt addition was examined using wide angle X-ray diffraction. It was found that the films were mainly composed of amorphous regions due to extensive heat treatment, with small crystalline fractions, if any, being developed during storage (Famá, Goyanes, & Gerschenson, 2007; Famá, Rojas, Goyanes, & Gerschenson, 2005). Possible crystallisation of single-helical structures of amylose typically occurs within a short amount of time after thermal treatment (van Soest & Vliegenthart, 1997).

Figures 5.5a and 5.5b depict the diffraction patterns of films with a moisture content of 7.34% w/w (RH 23%) following CaCl<sub>2</sub> and NaCl addition, respectively. It is observed that pure starch films show a V-type crystal structure as indicated by the presence of peaks at around 15, 17 and 22°(2θ) (Mitrus, 2009; van Soest & Vliegenthart, 1997). Addition of salt causes subtle changes in the shape and intensity of diffraction patterns in films mainly at around 17 and 22°(2θ).

The relative signal intensity decreases as a function of increasing salt concentration due to the interaction between salt and the hydrated starch network. Similar patterns are noted in Figures 5.5c and 5.5d for hydrated starch systems with a moisture content of 19.52% w/w (RH 75%), an outcome which further adds credit to the argument of interactions between counterions and starch molecules leading at high temperatures to granule gelatinisation and partial depolymerisation of the chemical sequences.

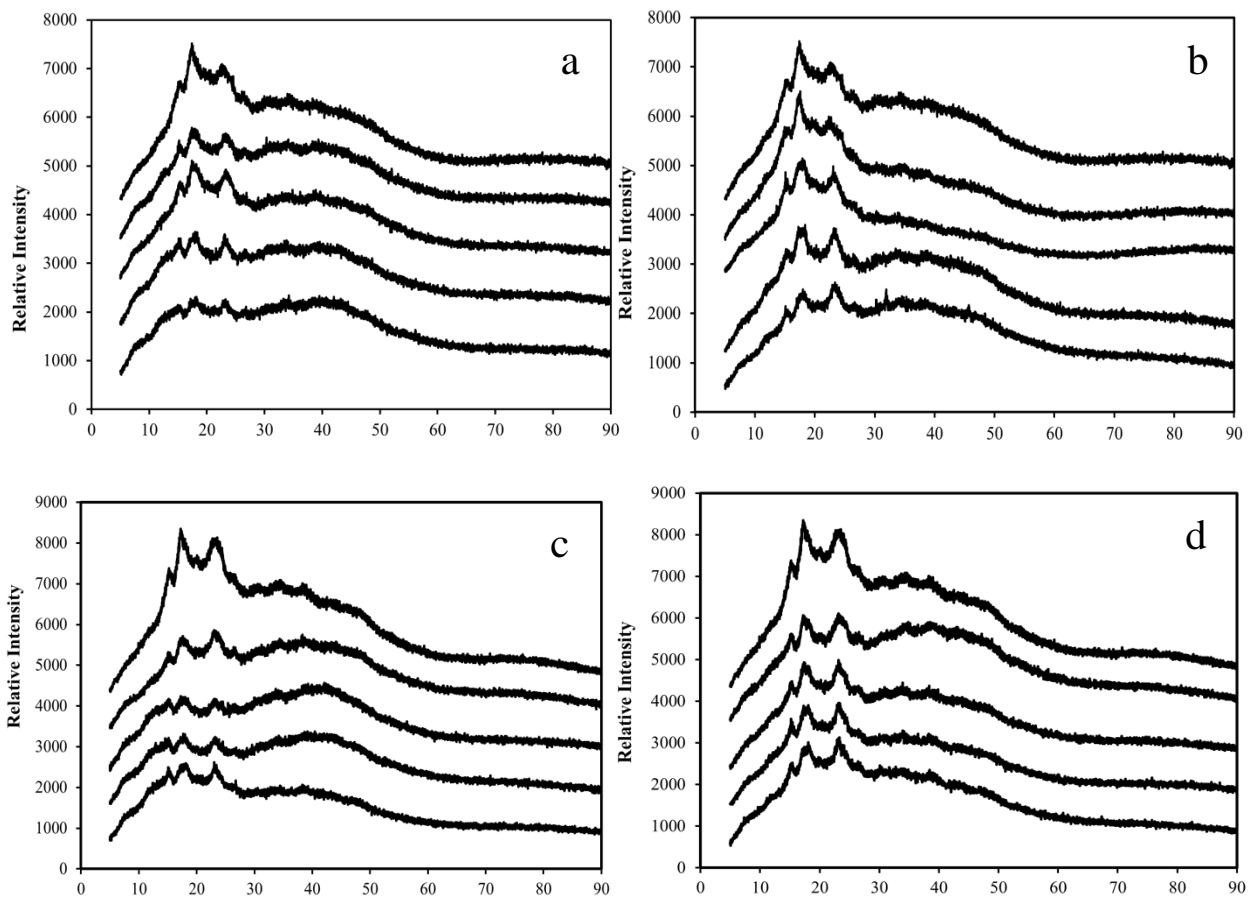


**Figure 5.5** X-ray diffractograms of tapioca starch films in the presence of salt at 0.0% 1.5%, 3.0%, 4.5%, and 6.0% arranged successfully downwards at a moisture content of 7.34% w/w (RH 23%) with (a) calcium chloride and (b) sodium chloride, and at a moisture content of 19.52% (RH 75%) with (c) calcium chloride and (d) sodium chloride.

### 5.3.5 Morphology of starch/salt systems

Cross sections of tapioca starch/salt samples were subjected to scanning electron microscopy (SEM) examination to provide concrete evidence of the three-dimensional structure topology. Figures 5.6(a-f) present micrographs of the samples at 2400X magnification with a moisture content of 7.34% w/w (RH 23%) and 19.52% w/w (RH 75%); top and bottom depictions, respectively. Besides the two distinct moisture contents, the micrographs cover pure starch materials and two



types of salt/starch mixtures, i.e. sodium chloride and calcium chloride at 6% levels of addition.

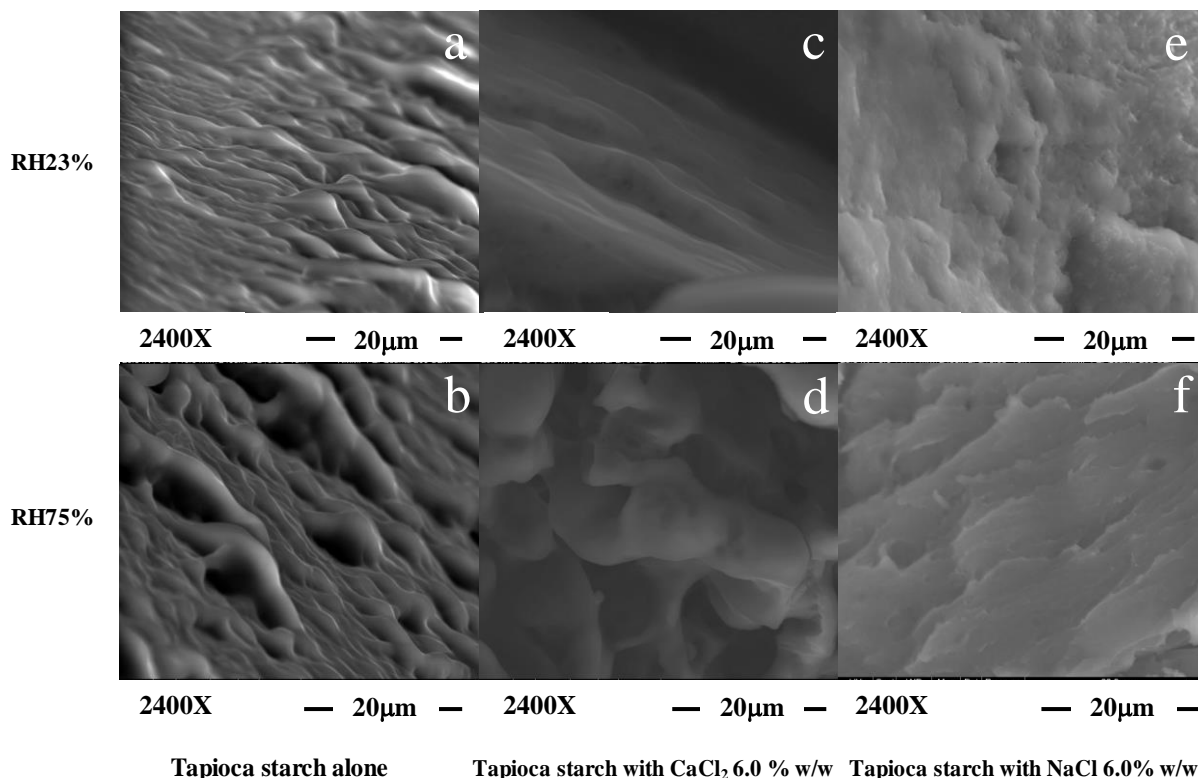


**Figure 5.6** SEM micrographs for tapioca starch systems with moisture content of 7.34% (RH 23%) in the presence of (a) 0% salt, (c) 6.0% CaCl<sub>2</sub>, (e) 6.0% NaCl, and for moisture content of 19.52% w/w (RH 75%) in the presence of (a) 0% salt, (d) 6.0% CaCl<sub>2</sub> and (f) 6.0% NaCl

Starch systems without the addition of salt show fibrillar-like structures with a relatively homogenous surface as observed in Figures 5.6a and 5.6b at low and high moisture contents, respectively. Visual observations of starch matrices in the presence of salt display dense and highly aggregated structures due to the extensive interaction between counterion and gelatinised starch network (Figures 5.6c-5.f). The absence of visible NaCl and CaCl<sub>2</sub> crystals in these starch systems further suggests that thorough mixing and molecular solvation of the counterions has been achieved in the film preparation. The changing nature of starch morphology further supports the concept of added cation/polymeric matrix interactions in these preparations.

## 5.4 CONCLUSIONS

Tapioca starch-based films are inherently brittle and lack the intrinsic thermomechanical integrity required for food and bio-plastics applications. This study found that tapioca starch's techno-functionality could be enhanced by introducing counterions in the condensed carbohydrate matrix. It was found that cations ( $\text{Na}^+$  and  $\text{Ca}^{2+}$ ) provided from chloride salts are capable of forming electrostatic interactions with the starch's hydroxyl groups, an outcome which induces an antiplasticising effects on the polymeric matrix. Such interaction leads to a higher glass transition temperature for the gelatinised starch molecule with increasing salt addition at a given moisture level. Possible variations in the counterion effects are indistinguishable in the non-phosphorylated amylopectin sequences of cassava starch, as opposed to that of potato starch with some phosphate groups, which allows for the stronger effects of calcium addition (earlier chapter in this thesis). In particular, calorimetric evidence argues for statistical similarity in the values of glass transition temperature of tapioca starch upon inclusion of similar percentage amounts of monovalent sodium or divalent calcium ions at the same level of total solid material.

## 5.5 REFERENCES

- Albarracin, W., Sanchez, I., Grau, R., & Barat, J. M. (2011). Salt in food processing: usage and reduction - A review. *International Journal of Food Science and Technology*, 46, 1329-1336.
- Averous, L. & Boquillon, N. (2004). Biocomposites based on plasticized starch: thermal and mechanical behaviours. *Carbohydrate Polymers*, 56, 111-122.
- Bergo, P., Freitas, I. C., & do Amaral Sobral, P. J. (2012). Effects of moisture content on structure and dielectric properties cassava starch films. *Starch-stärke*, 64, 835-839.
- Biliaderis, C. G. (2009). Structural transitions and related physical properties of starch. In J. BeMiller & R. Whistler (Eds.), *Starch: Chemistry and Technology* (3rd ed.). San Diego, CA: Academic Press.
- Breuninger, W. F., Piyachomkwan, K., & Sriroth, K. (2009). Tapioca/cassava starch: production and use. In J. BeMiller & R. Whistler (Eds.), *Starch: Chemistry and Technology* (3rd ed.). San Diego, CA: Academic Press.
- Chatakanonda, P., Wongprayoon, S., & Sriroth, K. (2007). Gelatinization characteristics and kinetics of cassava starch in the presence of sodium chloride and sucrose. In P. Tomasik, V. P. Yuryev & E. Bertoft (Eds.), *Starch: Progress in Basic and Applied Science* (pp. 289-295). Malopolska, Poland: Polish Society of Food Technologists.
- Chuang, L., Panyoyai, N., Katopo, L., Shanks, R., & Kasapis, S. (2016). Effect of calcium chloride on the glass transition of condensed starch systems. *in press*.
- Chuang, L., Panyoyai, N., Shanks, R., & Kasapis, S. (2015). Effect of sodium chloride on the glass transition of condensed starch systems. *Food Chemistry*, 184, 65-71.
- Day, L., Fayet, C. & Homer, S. (2013). Effect of NaCl on the thermal behaviour of wheat starch in excess and limited water. *Carbohydrate Polymers*, 94, 31-37.
- Famá, L., Goyanes, S., & Gerschenson, L. (2007). Influence of storage time at room temperature on the physicochemical properties of cassava starch films. *Carbohydrate Polymers*, 70, 265-273.

- Famá, L., Rojas, A. M., Goyanes, S., & Gerschenson, L. (2005). Mechanical properties of tapioca-starch edible films containing sorbates. *LWT*, 38, 631-639.
- FAO. (2013). *FAOSTAT*. Rome: Retrieved from [faostat.fao.org/default.aspx](http://faostat.fao.org/default.aspx).
- Ishigaki, T., Saito, H., & Fujita, A., (1994). U.S. Patent No. 5332592.
- Jay-lin, J. & Ames, I. A. (1993). Mechanism of starch gelatinization in neutral salt solutions. Jiang, X., Jiang, T., Gan, L., Zhang, X., Dai, H., & Zhang, X. (2012). The plasticizing mechanism and effect of calcium chloride on starch/poly(vinyl alcohol) films. *Carbohydrate Polymers*, 90, 1677-1684. *Starch/Stärke*, 5, 161-166.
- Kasapis, S. (2005). Glass transition phenomena in dehydrated model systems and foods: a review. *Drying technology*, 23, 731-757.
- Kizil, R., Irudayaraj, J., & Seetharaman, K. (2002). Characterisation of irradiated starches by using FT-Raman and FTIR spectroscopy. *Journal of Agricultural and Food Chemistry*, 50, 3912-2918.
- Kweon, M., Slade, L., & Levine, H. (2008). Effect of sodium chloride on glassy and crystalline melting transitions of wheat starch treated with high hydrostatic pressure: prediction of solute-induced barostability from nonmonotonic solute-induced thermostability. *Starch-Stärke*, 60, 127-133.
- Lozano-Vazquez, G., Lobato-Calleros, C., Escalona- Buendia, H., Charez, G., Alvarez-Ramirez, J., & Vernon-Carter, E. J. (2015). Effect of the weight ratio of alginate-modified tapioca starch on the physicochemical properties and release kinetics of chlorogenic acid containing beads. *Food Hydrocolloids*, 48, 301-311.
- Matthews, C. (2013). *Cassava's huge potential as 21st Century crop*. Rome: FAO.
- Mitrus, M. (2009). TPS and Its Nature. In L. P. B. M. Janssen & L. Moscicki (Eds.), *Thermoplastic Starch*. Weinheim, Germany: Wiley-VCH Verlag GmbH & Co.
- Muhrbeck, P., & Eliasson, A. C. (1987). Influence of pH and ionic strength on the viscoelastic properties of starch gels - A comparison of potato and cassava starches. *Carbohydrate Polymers*, 7(4), 291-300.

- Perez, S., Baldwin, P. M., & Gallant, D. J. (2009). Structural features of starch granules I. In J. BeMiller & R. Whistler (Eds.), *Starch: Chemistry and Technology* (3rd ed.). San Diego, CA: Academic Press.
- Plata-Oviedo, M. & Camargo, C. (1998). Effects of acid treatments and drying processes on physico-chemical and functional properties of cassava starch. *Journal of the Science of Food and Agriculture*, 77, 103-108.
- Sablani, S. S., Kasapis, S., & Rahman, M. S. (2007). Evaluating water activity and glass transition concepts for food stability. *Journal of Food Engineering*, 78, 266-271.
- Slade, L., & Levine, H. (1994). Water and glass transition - dependence of the glass transition on composition and chemical structure: special implications for flour functionality in cookie baking. *Journal of Food Engineering*, 22, 143-188.
- Smalligan, W. J., Kelly, V. J., & Estela, E. G. (1977). U.S. Patent No. 4013799.
- Swinkels, J. J. M. (1985). Composition and properties of commercial native starches. *Starch - Stärke*, 37, 1-5.
- Tomasik, P., & Schilling, C. H. (1998). Complexes of starch with inorganic guests. *Advances in Carbohydrate Chemistry and Biochemistry*. 53, 263-343.
- Tonukari, N. J. (2004). Cassava and the future of starch. *Electronic Journal Of Biotechnology*, 7, 5-8.
- van Soest, J. J. G., & Vliegenthart, J. F. G. (1997). Crystallinity in starch plastics: consequences for material properties. *Trends in Biotechnology*, 15, 208-213.
- Xia, W., Wang, F., Li, J., Wei, X., Fu, T., Cui, L., Li, T., & Liu, Y. (2015). Effect of high speed jet on the physical properties of tapioca starch. *Food Hydrocolloids*, 49, 35-41.

## CHAPTER 6

### EFFECT OF MICROCRYSTALLINE CELLULOSE ON THE STRUCTURAL PROPERTIES OF CONDENSED POTATO STARCH SYSTEMS

#### ABSTRACT

The present study aims to investigate the effect of addition of microcrystalline cellulose (MCC), up to 6.0% w/w, on the physicochemical properties of potato starch based films. The samples were prepared by hot pressing at 120°C for 7 min producing condensed systems that covered a range of moisture contents from 4.2% (11% relative humidity) to 17.5% (75% relative humidity). Experimental work was performed utilising dynamic mechanical analysis, modulated differential scanning calorimetry, Fourier transform infrared spectroscopy, wide angle X-ray diffraction and scanning electron microscopy. Rheological tests reveal that the inclusion of microcrystalline cellulose improves the mechanical strength of the starch films. Both moisture content and the presence of fibre have plasticising effect on the composites producing a reduction in the glass transition temperatures, as mentioned calorimetrically. Results from the remaining techniques suggest that there is no specific and non-trivial interaction between starch and MCC, an outcome which indicates that the cellulose fibres acts as inert filler in the polymeric composite.

**Keywords:** glass transition, microcrystalline cellulose, potato starch, high-solid systems

## 6.1 INTRODUCTION

Edible and biodegradable composites with enhanced properties and versatility are of great interest to food packaging industries, since they do not contribute to environmental pollution. Starch based composites possess good film-forming properties that provide efficient barriers against oils and lipids (Averous & Boquillon, 2004). However, their moisture barriers are poor due to their hydrophilic nature. Moreover, biodegradable composites with high level of starch are brittle in nature; therefore, they are often processed in blend system with natural plasticisers and commercial fibres in order to improve their mechanical and barrier properties (Vieira, da Silva, dos Santos, & Beppu, 2011).

Numerous chemical and physical reactions, such as water diffusion, granule expansion, gelatinisation, decomposition, melting and crystallisation, occur during thermal processing of starch based composites. Gelatinisation, which aims to destruct the crystalline structure of starch granules, is particularly crucial in film formation process because it is the basis of the conversion of starch to a thermoplastic. The majority of films are prepared by “hot compounding” techniques, which include calendaring, extrusion, injection and compression molding (Liu, Xie, Yu, Chen, & Li, 2009). Such techniques combine the formulated ingredients under heat and shearing forces followed by molten plastic formation, cooling, and then development of the film’s strength and integrity (Vieira, da Silva, dos Santos, & Beppu, 2011).

Incorporation of natural plant fibres in polymer composites is gaining much interest because they are non-toxic, biodegradable and recyclable (Spolijaric, Genovese, & Shanks, 2009). Several studies have investigated the incorporation of cellulose based fibres attained from cotton, flax, hemp, jute, sisal, kenaf and coir, in polymer composites (Acha, Reboredo, & Marcovich, 2007; Eichhorn et al., 2001; Koh & Kasapis, 2011; Mutjé et al., 2006; Panaitescu et al., 2007; Wong, Shanks, & Hodzic, 2002; Zampaloni et al., 2007). Such fibres are less susceptible to fracture during

processing due to their flexibility (Bledzki & Gassan, 1999; Kalaitzidou & Fukushima, 2007; Ljungberg, Cavaillé, & Heux, 2006).

Microcrystalline cellulose (MCC) is a natural fibre being widely exploited in pharmaceutical, food, paper and composite manufacturing industries (Edge, Steele, Chen, Tobbyn, & Stainforth, 2000; Kasapis, 1999; Nawan, Hassn, Ali, Kassem, & Mohamed, 2010; Samir, Alloin, & Dufresne, 2005; Sxchuh, Allard, Herrmann, Gibis, Kohlus, & Weiss, 2013). The alpha cellulose is partially depolymerised by treating wood pulp with mineral acid solution followed by rinsing and spray drying. The acid treatment cleaves the  $\beta$ -1,4 linkage between glucopyranose units of cellulose in the amorphous regions of cellulose particles (Sun, 2008).

MCC can be classified as a partially amorphous polymer in the presence of microcrystalline regions, with the amorphous part being sensitive to moisture addition (Stubberud, Arwidsson, Larsson, & Graffner, 1996). The degree of crystallinity of commercial MCC determined by X-ray diffraction and infrared measurement is about 60–80% (Sun, 2008). Water can plasticise the polymer and increase the molecular mobility because of the disruption of hydrogen bonds between cellulose molecules (Dawoodbhai & Rhodes, 1989). This leads to a decrease in glass transition temperature of the amorphous parts,  $T_g$ , which implies the transformation from a hard, rigid, and glassy state to a soft, flexible, and rubbery state (Oksanen & Zografi, 1990; Slade & Levine, 1991).

The fibre is a hygroscopic material due to the presence of abundant hydroxyl groups on cellulose chains and the relatively large surface to volume ratio of microfibrils as a result of their small size (Guy, 2009; Iijima & Takeo, 2000; Sun, 2008). At 25°C and in a 50% relative humidity environment, its equilibrium moisture content is approximately 5% (Thoorens, Krier, Leclercq, Carlin, & Evrard, 2011). A number of studies have suggested that the microcrystalline cellulose is thermally stable at high temperature, i.e. up to 300°C (Kiziltas, Gardner, Han, & Yang, 2011; Trache, Donnot, Khimeche, Benelmir, & Brosse, 2014), which is higher than the melting temperatures of synthetic polymers, such as polystyrene (242°C) and polyvinyl



acetate (65°C) (Lemstra, Kooistra, & Challa, 1972; Fragiadakis, & Runt, 2010). This unique characteristic makes MCC-filled polymer composite suitable for use in high-temperature processing applications.

Inclusion of microcrystalline cellulose as a filler in starch based composites is known to alter their mechanical properties (Ma, Chang, & Yu, 2008). However, the effect of systematically changing water content on the physicochemical properties of these MCC-reinforced starch composites has not been undertaken. This study aims to provide insights into the thermo-mechanical behaviour and morphology of condensed starch/MCC composites subjected to conditioning over a wide range of relative humidity values.

## **6.2 MATERIALS AND METHODS**

### *6.2.1 Materials*

#### *6.2.1.1 Potato starch*

Potato starch was supplied by Penford Starch (Lane Cove, NSW, Australia). The material is a white free-flowing powder containing <10 mg/kg of sulphur dioxide and no known allergens. Typical nutritional analysis (% w/w) shows a total carbohydrate content of 84%, water content of 15%, protein content of 0.2% and fat content of 0.1%.

#### *6.2.1.2 Microcrystalline cellulose*

MCC (Avicel® PH-101) was purchased from Sigma Aldrich (Castle Hill, NSW, Australia). The material has a particle size of approximately 50µm, degree of polymerisation of 210, moisture content of 4.1% and pH value of 6.4.

### *6.2.1.3 Millipore water*

Millipore system Elix<sup>®</sup> 10 water filtration system was utilised to obtain the Millipore type 2 analytical-grade water of this investigation (Merck KGaA, Germany).

### *6.2.1.4 Saturated salt solutions*

Saturated salt solutions were used to achieve a series of moisture and relative humidity values for our starch/MCC samples, i.e. lithium chloride (LiCl): moisture content 4.15% w/w, RH 11%; potassium acetate (CH<sub>3</sub>COOK): moisture content 6.51% w/w, RH 23%; magnesium chloride (MgCl<sub>2</sub>•6H<sub>2</sub>O): moisture content 8.22% w/w, RH 33%; sodium bromide (NaBr): moisture content 14.26% w/w, RH 58%; magnesium acetate [Mg(CH<sub>3</sub>COO)<sub>2</sub>•4H<sub>2</sub>O]: moisture content 15.80% w/w, RH 65%; sodium chloride (NaCl): moisture content 17.48% w/w, RH 75% (Sablani, Kasapis & Rahman, 2007). All salts were purchased from Sigma Aldrich (Castle Hill, NSW, Australia).

### *6.2.2 Sample preparation*

Potato starch powder, with a moisture content of 15% (w/w) that was taken into consideration for final sample preparation, was dry mixed with a wide range of added cellulose concentrations (0.0, 1.5, 3.0, 4.5 and 6.0% w/w) to achieve a total of 35.0% (w/w) moisture content. In doing so, Millipore type 2 water was incorporated piecemeal prior to processing all preparations; weighing was carried out carefully using a four decimal place analytical balance. Then, the mixture was mixed at ambient temperature using twin screw Thermo Rheomix OS (HAAKE, Newington, NH, USA) at a screw speed of 200rpm for 2min. Mixture was placed on a stainless steel metal frame (130mm x 130mm x 2mm) sandwiched between two non-stick plastic sheets at the bottom and top of the frame. Afterwards, it was transferred to a steam preheated hot press at 120°C for 7min pressurisation at 59 Bar.

The same press was employed to cool the heated samples to about 45°C in order to prevent air bubble formation on the starch film. Following cooling, the samples were packaged and sealed separately with a moisture/gas impermeable plastic vacuum bag. To facilitate subsequent instrumental analysis, samples were cut into the desired shape and size (10mm x 10mm x 1 mm) and stored in sealed relative-humidity desiccators for 4 weeks containing the aforementioned saturated salt solutions. Relative humidity to the required equilibrium value in the starch/cellulose films was checked periodically with a water activity meter (Novasina aw set-1, Pfäffikon, Switzerland). The final moisture content of these preparations after a 4-week desiccator storage was between 4.15% w/w (RH 11%) and 17.48% w/w (RH 75%), as estimated by oven drying at 102°C overnight.

### *6.2.3 Instrumental protocol*

#### *6.2.3.1. Dynamic mechanical analysis*

Diamond DMA from Perkin-Elmer (Akron, Ohio, USA) with an external 60L liquid nitrogen Dewar was used for monitoring the tensile storage and loss modulus ( $E'$  and  $E''$ , respectively) of our materials. In doing so, the sample film was set on a twin grip clamp with the dimensions of 10mm width, 10mm length and 1mm thickness. Employing the tensile mode, cooling from ambient temperature to -110°C was carried out followed by heating to 180°C at a scan rate of 2°C/min, and frequency of 1Hz. To minimise moisture loss during experimentation, a thin layer of petroleum vacuum grease was used to coat the sample prior to loading onto the tensile grips. Isochronal routines were carried out in duplicate returning consistent results.

#### *6.2.3.2 Modulated differential scanning calorimetry*

MDSC Q2000 (TA Instruments, New Castle, DE) was used to analyse the thermal transitions of our materials. About ten milligram of the sample was placed in a  $T_{\text{zero}}$  aluminium pan, hermetically sealed with an aluminium lid by using a sample cell

crimper and analysed at modulated amplitude of  $\pm 0.53^{\circ}\text{C}$  for 40 s. An extensive temperature range was accessed with successive cooling and heating routines from -90 to  $220^{\circ}\text{C}$  at a scan rate of  $10^{\circ}\text{C}/\text{min}$ . All measurements were performed in triplicate to yield effectively overlapping thermograms.

#### *6.2.3.3 Fourier transform infrared spectroscopy*

Perkin Elmer Spectrum 100 with MIRacle TMZnSe single reflection ATR plate system (Perkin Elmer, Norwalk, CT) was utilised to produce FTIR spectra. Starch/cellulose preparations were analysed at ambient temperature within a wavelength of  $650$  to  $4000\text{cm}^{-1}$  and a resolution of  $4\text{ cm}^{-1}$ . Spectra are presented in absorbance mode based on 32 average scans. Final results were obtained following removal of the background signal at ambient temperature.

#### *6.2.3.4 Wide angle X-ray diffraction*

Bruker D<sub>4</sub> Endeavour (Karlsruhe, Germany) was used to examine the phase morphology of starch/cellulose preparations. Prior to analysis, samples were prepared at an appropriate size and equilibrated against saturated salt solutions for 4 weeks. Accelerating voltage of  $40\text{kV}$ , current of  $35\text{mA}$  and position sensitive detectors (PSD) were utilised to obtain diffractograms within  $2\theta$  angle of  $5$ - $90^{\circ}$  with intervals of  $0.1^{\circ}$ . Spectra were processed on DIFFRAC<sup>plus</sup> Evaluation (Eva), version 10.0, revision 1 and measurements were performed in triplicate.

#### *6.2.3.5 Scanning electron microscopy*

FEI Quanta 200 (Hillsboro, OR, USA) was used to provide the microstructure of our materials. Dried specimens were cut with a clean, sanitised surgical scalpel into  $10\times 10\times 1$  mm cubes, equilibrated at desiccators as described earlier, and cross sections of the specimen were examined. Observing the microstructure of these materials requires exposure to a low vacuum condition at an accelerating voltage of  $20\text{kV}$  and pressure of  $0.5\text{Torr}$ .

## 6.3 RESULTS AND DISCUSSION

### 6.3.1 Mechanical properties of starch/MCC films

Figure 6.1a illustrates the variation of storage modulus ( $E'$ ) of samples prepared at 4.2% w/w moisture content (RH 11%) during heating from -100 to 60°C in the presence of increasing levels of MCC, i.e. 0 to 6.0% w/w. At the beginning of the heating routine, i.e. -100°C, the values of  $E'$  for all films are greater than  $10^{10.2}$ Pa. There is a gradual decrease in the elasticity of the films during heating, with the values of  $E'$  approaching  $10^{9.9}$ Pa at the end of the heating regime (60°C). This event indicates a shift in the physical state of the samples from a glassy state, where large-scale molecular motions cease with the polymer chains are in non-symmetrical arrangement, to a more mobile and highly viscous state (Biliaderis, 2009).

This decreasing pattern in the tensile storage modulus is also apparent in Figure 6.1b for the high moisture content (17.5% w/w; RH 75%) of the starch/MCC films. A drop in  $E'$  values was observed during heating from values in excess of  $10^{10.1}$ Pa at -100°C to about  $10^{9.5}$ Pa at 60°C. The decrease in the mechanical property is quite considerable, being about an order of magnitude at the high end of the thermal regime, as compared to half an order of magnitude for the corresponding temperature range in Figure 6.1a. It appears that higher moisture content induces macromolecular relaxation, mainly alpha-relaxation of the polymer backbone (Averous & Boquillon, 2004; Avérous & Moro, 2001). This is sufficiently plasticised with increasing temperature to display a flexible structure of reduced strength.

A summary of the rheological findings discussed so far for the conditions of low and high moisture content/relative humidity is presented in Figures 6.1c and 6.1d, respectively. Clearly, starch films without MCC in both conditions produce lower  $E'$  values at -100°C compared to the corresponding counterparts with MCC inclusion. This trend is also observed for tensile modulus at +60°C and approaches maximum values in the presence of 6.0% MCC in formulations.

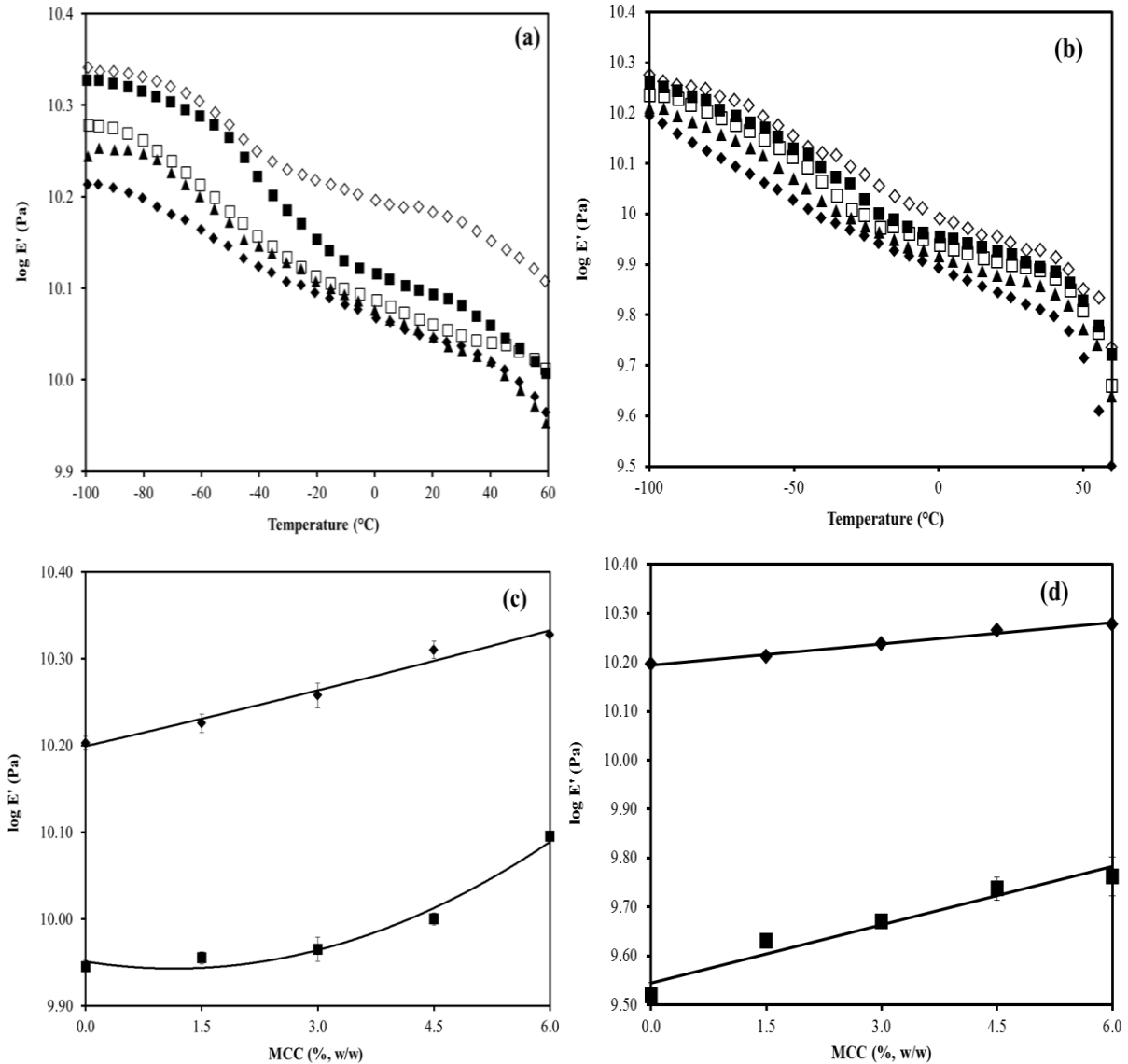


**Figure 6.1** Heating profiles of tensile storage modulus for potato starch films (a) at a moisture content of 4.2% w/w (RH 11%) and (b) at a moisture content of 17.5% (RH 75%) in the presence of 0.0% ( $\blacklozenge$ ), 1.5% ( $\blacktriangle$ ), 3.0% ( $\square$ ), 4.5% ( $\blacksquare$ ), 6.0% ( $\diamond$ ) MCC, and variation of tensile storage modulus for potato starch films with different levels of MCC at -100 $^{\circ}\text{C}$  ( $\blacklozenge$ ) and +60 $^{\circ}\text{C}$  ( $\blacksquare$ ) at a moisture content of 4.2% w/w (c) and 17.5% w/w (d) scanned at the rate of 2 $^{\circ}\text{C}/\text{min}$ , frequency of 1 Hz (error bars denote one standard deviation).

The findings in Figures 6.1a-d imply that inclusion of MCC has a positive effect on the tensile storage modulus of the composites, which increases with MCC content. This demonstrates the reinforcement capability of MCC, which is in agreement with

results reported by other researchers (Cataldi, Dorigato, Deflorian, Pegoretti, 2014; Kiziltas, Gardner, Han, & Yang, 2011; Mathew, Oksman, & Sain, 2005; Spolijaric, Genovese, & Shanks, 2009). It is believed that homogeneous dispersion of MCC, in the form of filler throughout the starch matrix, promote uniform transfer of stress tensors from the polymeric matrix of gelatinized starch to the fibre particles, hence preventing the development of localized stress defects. The macromolecular outcome is an improvement in the mechanical profile of the fibre-reinforced composite (Spolijaric, Genovese, & Shanks, 2009).

### 6.3.2 Thermal stability of starch/MCC films

Rheological analysis in the preceding paragraph elucidated the macromolecular aspects of structure development in these systems. The purpose of this section is to investigate the micromolecular aspects and, in particular, the estimation of the glass transition temperature,  $T_g$ . Modulated differential scanning calorimetry is a suitable technique for this type of analysis, which provides additional insights on the presence of MCC in condensed starch films.

Figure 6.2a portrays changes in heat flow during heating cycle for preparations with moisture content of 4.2% w/w (RH 11%). Thermograms show a sigmoidal pattern between 165 and 190°C, which is a characteristic of the glass transition region. Addition of MCC reveals a shift in the heat capacity traces to lower temperatures. The same pattern of thermal behaviour is recorded in Figure 6.2b, where films are prepared at the highest experimental moisture content of 17.5% w/w (RH 75%). The thermal mechanism of devitrification is observed within the temperature range of 130 to 160°C owing to lower level of solids in these composites.

The empirical  $T_g$  typically can be derived as the central point of the onset and endset of the glass transition region in thermogram. The approach is employed in this investigation to produce the  $T_g$  values of the starch/MCC composites seen in Table 6.1. It is evident that inclusion of MCC and variation in moisture content/relative humidity strongly affect the  $T_g$  of potato starch. For instance, in the case of RH

11%, adding MCC from 1.5% to 6% decreases the  $T_g$  from 181.1 to 172.2°C. Within each relative humidity, the level of starch is reduced in the presence of increased MCC concentration in order to maintain consistent moisture content. It appears, therefore, the decrease in  $T_g$  values is a result of the decrease in the level of starch in the systems since MCC acts as inert filler in the composites.

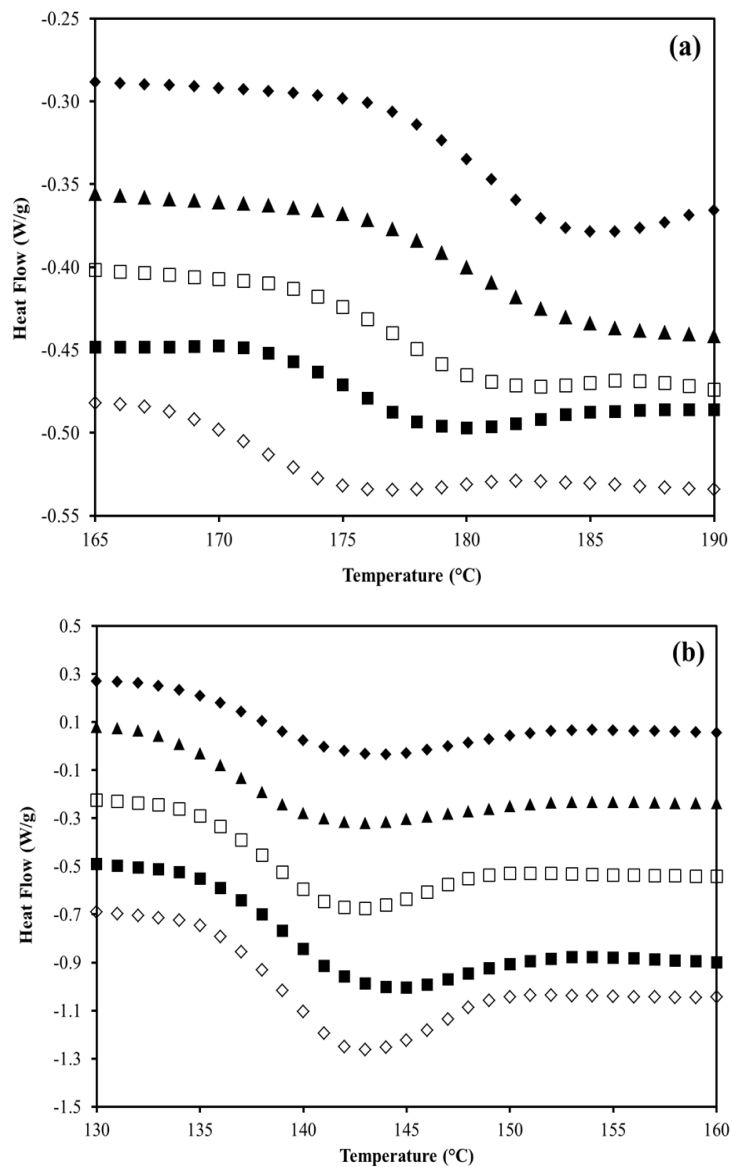


**Figure 6.2** DSC thermograms for potato starch in the presence of MCC at 0.0%, 1.5%, 3.0%, 4.5%, 6.0% with (a) moisture content of 4.2% w/w (RH 11%) and (b) with moisture content of 17.5% w/w (RH 75%) arranged successfully downwards.



**Table 6.1**  $T_g$  values determined from DSC for potato starch and MCC content up to 6% w/w at different relative humidity values

MCC content (%)	RH 11% (Moisture content 4.15%)			RH 23% (Moisture content 6.51%)			RH 33% (Moisture content 8.22%)		
	Onset (°C)	Endset (°C)	$T_g$ (°C)	Onset (°C)	Endset (°C)	$T_g$ (°C)	Onset (°C)	Endset (°C)	$T_g$ (°C)
0.0	154.8	161.3	160.5	150.3	154.8	154.4	143.7	147.0	145.7
1.5	176.4	182.7	181.1	146.2	150.6	149.9	144.9	146.0	144.2
3.0	176.4	182.3	177.7	145.3	148.8	148.7	143.6	144.9	143.8
4.5	175.3	182.1	175.5	143.3	146.6	145.5	142.8	144.5	143.6
6.0	169.3	178.0	172.2	141.2	145.0	144.6	142.1	144.2	143.3
MCC content (%)	RH 58% (Moisture content 14.26%)			RH 65% (Moisture content 15.80%)			RH 75% (Moisture content 17.48%)		
	Onset (°C)	Endset (°C)	$T_g$ (°C)	Onset (°C)	Endset (°C)	$T_g$ (°C)	Onset (°C)	Endset (°C)	$T_g$ (°C)
0.0	137.1	141.7	140.5	135.8	140.2	140.1	134.9	138.8	138.7
1.5	136.3	141.4	140.3	135.8	140.1	140.0	133.9	138.4	137.6
3.0	134.9	139.7	139.6	134.9	139.7	139.5	133.4	136.9	136.3
4.5	134.7	138.9	138.7	132.6	138.8	138.7	132.2	135.0	134.7
6.0	134.1	138.7	138.4	132.5	138.7	138.2	131.1	133.9	133.8

**Note:** For all combinations of relative humidity and MCC content in samples, onset, endset and glass transition temperatures fall within  $\pm 0.2$  of the quoted values

In the case of 6% MCC, for example, increase in RH from 11% to 75% leads to a drop in  $T_g$  values from 172.2 to 133.8°C, and similar reductions are recorded for the onset and endset temperatures of the thermograms. The outcome is in agreement with the findings from corresponding work on potato starch films with added counterions of sodium and calcium, and argues that the rise in moisture content acts as plasticiser to enhance molecular mobility in samples (Chuang, Panyoyai, Shanks, & Kasapis, 2015).

### 6. 3.3 Infrared spectroscopy analysis

FTIR spectroscopy was used to elucidate the chemical structure of the starch/MCC samples. The corresponding spectra for composites with moisture content of 4.2% w/w (RH 11%) and 17.5% w/w (RH 75%) over a wide wave range of 650 to 4000  $\text{cm}^{-1}$  are presented in Figures 6.3a and 6.3b respectively. The vibrations of glucose

molecules dominate the spectra of single starch preparations below the region  $1320\text{ cm}^{-1}$ . These vibrations originate from the C-O-C of  $\alpha$ -1,4 glycosidic linkages that can be observed as a strong infrared band around  $1000\text{ cm}^{-1}$  (Kizil, Irudayaraj, & Seetharaman, 2002). The spectra of single MCC preparations display distinct peaks between  $1000$  and  $1100\text{ cm}^{-1}$ , which are attributed to the C-C, C-OH, C-H ring and side group vibrations. The infrared absorption at  $3297$  and  $3361\text{ cm}^{-1}$  are associated with hydrogen bonds in cellulose I, which include two intramolecular H-bonds, (O(2)H---O(6) and O(3)H---O(5)), and one intermolecular H-bond (O(6)H---O(3) ) (Fan, Dai, & Huang, 2012).

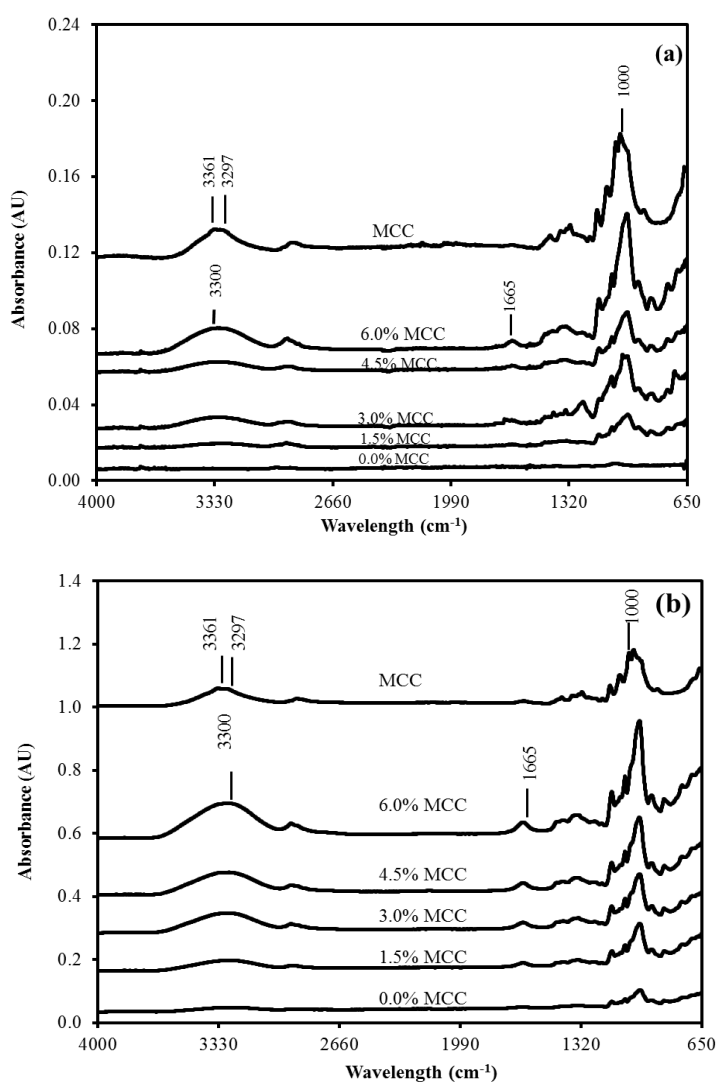


**Figure 6.3** FTIR spectra of potato starch in the presence of MCC at 0.0%, 1.5%, 3.0%, 4.5%, 6.0% and MCC alone arranged upwards with moisture content of (a) 4.2% w/w (RH 11%) and (b) 17.5% w/w (RH 75%).

Three main regions in the IR spectra of starch/MCC composites were observed: 1000-1100, 1665 and 3000-3600 $\text{cm}^{-1}$ . The overlapping bands between 1000 and 1100  $\text{cm}^{-1}$  are characteristics of C-O-H bending, and C-O, C-C and O-H stretching. The weak band observed at 1665 $\text{cm}^{-1}$  represents the vibrations of tightly bound water molecules absorbed in the amorphous regions. The broad peak between 3000 and 3600 $\text{cm}^{-1}$  corresponds to the O-H stretching mode of starches (Deeyai, Suphantharika, Wongsagonsup, & Dangtip, 2013; Kizil, Irudayaraj, & Seetharaman, 2002).

The presence of MCC contributes to the narrowing of peaks, predominantly at about 1000 $\text{cm}^{-1}$ , with increasing levels of fibre, in particular, for samples with higher moisture content in Figure 6.3b. There is an upward trend in the peak intensity as a function of fibre concentration, which could be explained by the increase of C-H vibration from the cellulosic fibre. Furthermore, the intensity of the peaks related to O-H stretching, i.e. 3300 and 1665 $\text{cm}^{-1}$ , is greater than the peaks in Figure 6.3a due to higher water content, i.e. 17.5%.

#### 6. 3.4 X-ray diffraction analysis

The degree of crystallinity of potato starch in the composites is expected to be relatively low due to the heat treatment at 120°C for 7min, which destroys the majority of the starch crystals. Typically, only a slow re-crystallisation process occurs following the heating process. Figures 6.4a and 6.4b display X-ray diffractograms of films with moisture content of 4.2% w/w (RH 11%) and 17.5% w/w (RH 75%) respectively. Pure potato starch films in both conditions show a V-type crystal structure with two peaks at around 16 and 22 degrees ( $2\theta$ ) (van Soest & Vliegthart, 1997). This type of crystal structure is formed as a result of recrystallization of single-helical structures of amylose during cooling after processing (Mitrus, 2009). On the other hand, the MCC systems exhibit two sharp peaks, at around 22 and 34 degrees ( $2\theta$ ), and one broad peak at around 15 degrees

( $2\theta$ ) which are characteristics of the cellulose I crystal structure (Klemm, Heublein, Fink & Bohn, 2005).

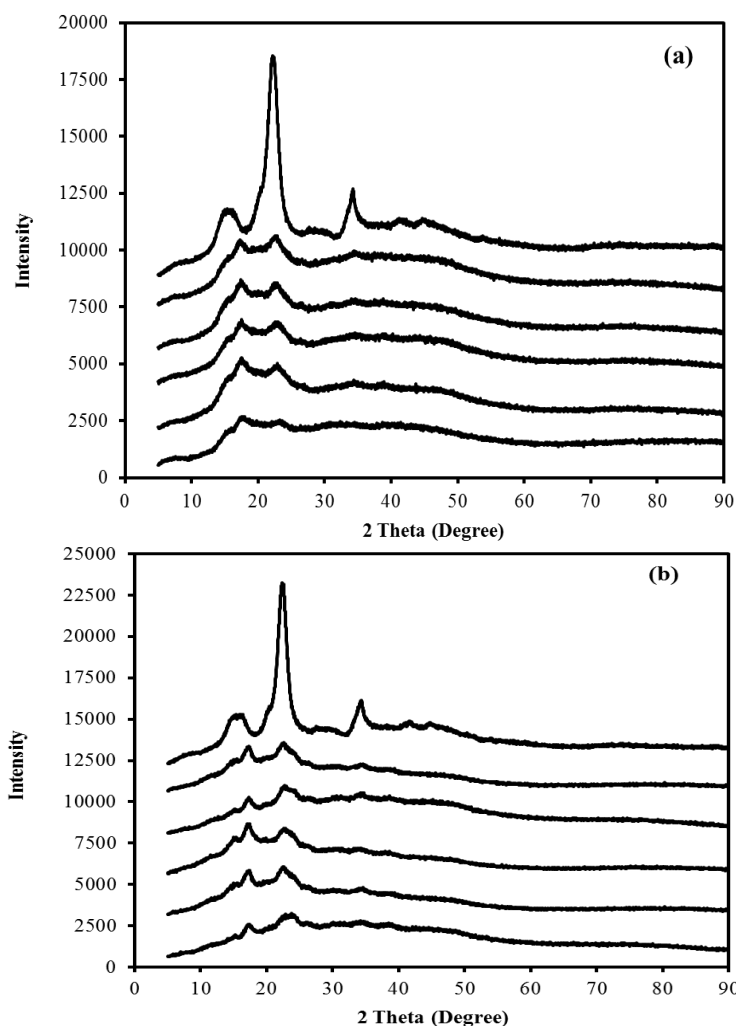


**Figure 6.4** X-ray diffractograms of potato starch with MCC at 0.0%, 1.5%, 3.0%, 4.5%, 6% and MCC only and arranged successfully upwards with moisture content of (a) 4.2 % w/w (RH 11%) and (b) 17.5% w/w (RH 75%).

The starch/MCC films demonstrate similar diffraction patterns to pure starch film as indicated by the presence of two peaks at around 16 and 22 degrees ( $2\theta$ ). These results support the finding from Müller, Laurindo, & Yamashita (2009) which also reported diffraction peaks at 16 and 23 degrees ( $2\theta$ ) in cassava starch/cellulose fibre films. It is observed that addition of MCC induces minor changes in the shape of the diffractograms at 10-25 degree angle ( $2\theta$ ). There is a visible sharpening of the peak

and increase in intensity at around 22 degrees ( $2\theta$ ) in the presence of increased MCC concentration.

### 6.3.5 Morphology of starch/MCC films

Cross section of potato starch/MCC films was subjected to SEM observation to provide tangible evidence of the network topology in single phase and composite materials. SEM micrographs at 3000x magnification of the films at moisture content 4.2% (RH 11%) and 17.5% (RH 75%) are shown in Figures 6.5a-b and 6.5c-d, respectively. Besides two distinct moisture contents, the micrographs display two levels of MCC, i.e. 0.0, and 6.0% w/w.

In general, all films portray a smooth and curvy surface, typical of homogenous materials with an amorphous nature. Fibrillar-like structures are observed in Figures 6.5a and 6.5c for the dehydrated starch matrices without the addition of cellulose particles. It appears that higher moisture content, i.e. 17.5%, contributes to the formation of strands with larger thickness, as seen in Figure 6.5c. The absence of visible cellulose fibres in the remaining micrographs (Figures 6.5b and 6.5d) indicates that these are well cemented in the continuous phase of starch matrix.

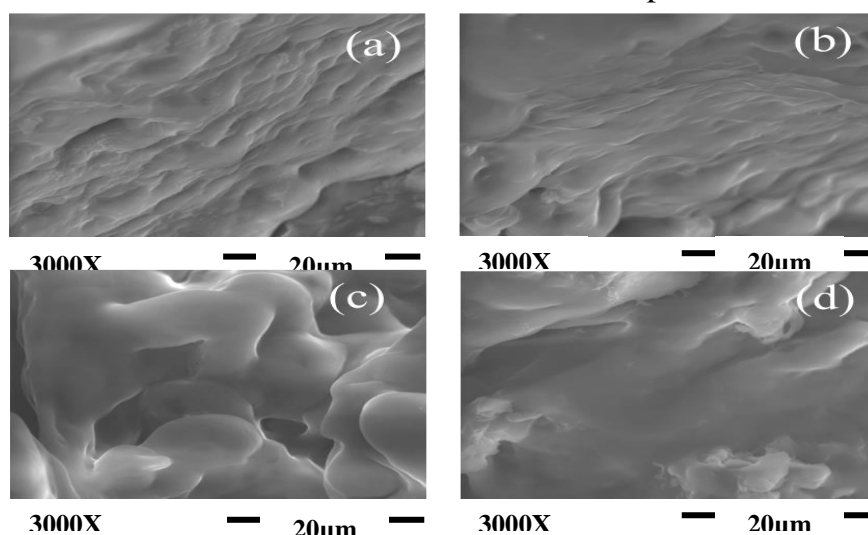


**Figure 6.5** SEM micrographs for potato starch with moisture content of 4.2% w/w (RH 11%) in the presence of MCC (a) 0.0% and (b) 6.0%, and for moisture content of 17.5% w/w (RH 75%) in the presence of MCC (c) 0.0% and (d) 6.0%.

## 6.4 CONCLUSIONS

Natural fibres, including microcrystalline cellulose, can assist in the development of bio-degradable food packaging materials with versatile properties. The results from this study reveal that introduction of microcrystalline cellulose alters considerably the mechanical properties of high-solid starch preparations that have been gelatinised to form largely amorphous three dimensional structures. The reinforcing effect can be attributed to an effective dispersion of microcrystalline cellulose particles throughout starch system in the form of an inert filler phase, as opposed to outcomes of a direct and specific interaction between the two polymeric materials. Further, under the thermal conditions of processing in this investigation, inclusion of microcrystalline cellulose lowers consistently the glass transition temperature of the composite with increasing fibre content. This result indicates that the measured values of glass transition temperature using differential scanning calorimetry reflect the reduction in starch content of the continuous matrix without contributions from the filler phase of the MCC particles.

## 6.5 REFERENCES

- Acha B, Reboredo M.M., Marcovich N. E. (2007). Creep and mechanic dynamical behaviour of PP-jute composites: effect of the interfacial adhesion. *Composites: Part A, Applied Science and Manufacturing*, 38, 1507-1516.
- Avérous, L. & Moro, C. F. L. (2001). Plasticized starch-cellulose interactions in polysaccharide composites. *Polymer*, 42, 6565-6572.
- Averous, L. & Boquillon, N. (2004). Biocomposites based on plasticized starch: thermal and mechanical behaviours. *Carbohydrate Polymers*, 56, 111-122.
- Biliaderis, C. G. (2009). Structure transitions and related physical properties of starch. In J. BeMiller & R. Whistler (Eds.), *Starch, chemistry and technology* (3rd ed.) (pp. 293-372). New York, Academic Press.
- Bledzki, A., & Gassan, J. (1999). Composites reinforced with cellulose based fibres. *Progress in Polymer Science*, 24, 221-274.
- Cataldi, A., Dorigato, A., Deflorian, F., & Pegoretti, A. (2014). Effect of the water sorption on the mechanical response of microcrystalline cellulose-based composites for art protection and restoration. *Journal of Applied Polymer Science*, 131, DOI: 10.1002/app.40741.
- Chuang, L., Panyoyai, N., Shanks, R., & Kasapis, S. (2015). Effect of sodium chloride on the glass transition of condensed starch systems. *Food Chemistry*, 184, 65-71.
- Dawoodbhai, S. & Rhodes, C.T. (1989). The effect of moisture on powder flow and on compaction and physical stability of tablets. *Drug Development and Industrial Pharmacy*, 15, 1577-1600.
- Deeyai, P., Suphantharika, M., Wongsagonsup, R., Dangtip, S. (2013). Characterization of modified tapioca starch in atmospheric argon plasma under diverse humidity by FTIR spectroscopy. *Chinese physical society and IOP Publishing*, 30, 018103-1 to 018103-4.
- Edge, S., Steele, D. F., Chen, A., Tobby, M. J., & Stainforth, J. N. (2000). The mechanical properties of compact of microcrystalline cellulose and silicified

microcrystalline cellulose, *International Journal of Pharmaceutics*, 200, 67-72.

- Eichhorn S, Baillie C.A., Zafeiropoulos N., Mwaikambo L.Y., Ansell M.P., Dufresne A., Entwistle, K. M., Herrera-Franco, P. J., Escamilla, G. C., Groom, L., Hughes, M., Hill, C., Rials, T. G., & Wild, P. M. (2001) Review: current international research into cellulosic fibres and composites. *Journal of Materials Science*, 36, 2107-2131.
- Fan, M., Dai, D. & Huang, B. (2012). Fourier transform infrared spectroscopy for natural fibers. In S. Salih (Ed.), *Fourier Transform - Materials Analysis* (Chapter 3, pp. 45-68). Available from:  
<http://www.intechopen.com/books/fourier-transform-materials-analysis/fourier-transform-infrared-spectroscopy-for-natural-fibres>
- Fragiadakis, D. & Runt, J. (2010). Microstructure and Dynamics of Semicrystalline Poly(ethyleneoxide)-Poly(vinyl acetate) Blends. *Macromolecules*, 43, 1028-1034.
- Guy, A. (2009). Cellulose, microcrystalline. In R. C. Rowe, P. J. Sheskey, M. E. Quinn (Eds.), *Handbook of Pharmaceutical Excipients* (pp. 129-133), American Pharmacists Association (USA), Pharmaceutical Press (UK).
- Iijima, H. & Takeo, K. (2000). Microcrystalline cellulose: an overview. In G. O. Phillips, P. A. Williams (Eds.), *Handbook of Hydrocolloids* (pp. 331-346), Cambridge, Woodhead Publishing Ltd.
- Kalaitzidou, K., Fukushima, H., & Drzal, L. T. (2007). Mechanical properties and morphological characterization of exfoliated graphite-polypropylene nanocomposites. *Composites: Part A, Applied Science and Manufacturing*, 38, 1675-1682.
- Kasapis, S. (1999). The elastic moduli of the microcrystalline cellulose-gelatin blends. *Food Hydrocolloids*, 13, 543-546.
- Kizil, R., Irudayaraj, J., & Seetharaman, K. (2002). Characterisation of irradiated starches by using FT-Raman and FTIR spectroscopy. *Journal of Agricultural and Food Chemistry*, 50, 3912-2918.



- Kiziltas, A., Gardner, D. J., Han, Y., & Yang, H. (2011). Dynamic mechanical behaviour and thermal properties of microcrystalline cellulose (MCC)-filled nylon 6 composites. *Thermochimica Acta*, 519, 38-43.
- Klemm, D., Heublein, B., Fink, H.-P., & Bohn, A. (2005). Cellulose: Fascinating biopolymer and sustainable raw material. *Angewandte Chemie - International Edition*, 44, 3358-3393.
- Koh, L.W. & Kasapis, S. (2011). Orientation of short microcrystalline cellulose fibers in a gelatin matrix. *Food Hydrocolloids*, 25, 1402-1405.
- Lemstra, P. J., Kooistra, T. & Challa, G. (1972). Melting behavior of isotactic polystyrene. *Journal of Polymer Science, Part A-2*, 10, 823-833.
- Liu, H., Xie, F., Yu, L., Chen, L. & Li, L. (2009). Thermal processing of starch-based polymers. *Progress in Polymer Science*, 34, 1348-1368.
- Ljungberg, N., Cavaillé, J. Y., Heux, L. (2006). Nanocomposites of isotactic polypropylene reinforced with rod-like cellulose whiskers. *Polymer*, 47, 6285-6292.
- Ma, X., Chang, P. R. & Yu, J. (2008). Properties of biodegradable thermoplastic pea starch/carboxymethyl cellulose and pea starch/microcrystalline cellulose composites. *Carbohydrate Polymers*, 72, 369-375.
- Mathew, A. P., Oksman, K. & Sain, M. (2005). Mechanical properties of biodegradable composites from poly lactic acid (PLA) and microcrystalline cellulose (MCC). *Journal of Applied Polymer Science*, 97, 2014-2025.
- Mitrus, M. (2009). TPS and Its Nature. In L. P. B. M. Janssen & L. Moscicki (Eds), *Thermoplastic Starch*, Wiley-VCH Verlag GmbH & Co., Weinheim, Germany.
- Müller, C. M. O., Laurindo, J. B. & Yamashita, F. (2009). Effect of cellulose fibers on the crystallinity and mechanical properties of starch-based films at different relative humidity values. *Carbohydrate Polymers*, 77, 293-299.
- Mutjé, P., Vallejos, M. E., Gironès, J., Vilaseca, F., López, A., López, J. P., (2006). Effect of maleated polypropylene as coupling agent for

- polypropylene composites reinforced with hemp strands. *Journal of Applied Polymer Science*, 102, 833-840.
- Nawan, G. A. M., Hassn, F. A. M., Ali, K. E., Kassem, J. M. & Mohamed, S. H. S. (2010). Utilization of microcrystalline cellulose prepared from rice straw in manufacture of yoghurt. *Journal of American Science*, 6, 226-231.
- Oksanen, C. A. & Zografi, G. (1990). The relationship between the glass transition temperature and water vapour absorption of polyvinylpyrrolidone. *Pharmaceutical Research*, 7, 654-657.
- Panaitescu, D., Donescu, D., Bercu, C., Vuluga, D. M., Iorga, M., & Ghiurea, M. (2007). Polymer composites with cellulose microfibrils. *Polymer Engineering & Science*, 47, 1228-1234.
- Sablani, S. S., Kasapis, S., & Rahman, M. S. (2007). Evaluating water activity and glass transition concepts for food Quality. *Journal of Food Engineering*, 78, 266-271.
- Samir, M. A. S. A., Alloin, F., & Dufresne, A. (2005). Review of recent research into cellulosic whiskers, their properties and their application in nanocomposite field. *Biomacromolecules*, 6, 612-626.
- Slade, L. & Levine, H. (1991). Beyond water activity: Recent advances based on an alternative approach to the assessment of food quality and safety. *Critical Review of Food Science and Nutrition*, 30, 115-360.
- Spolijaric, S., Genovese, A., & Shanks, R. A. (2009). Polypropylene-microcrystalline cellulose composites with enhanced compatibility and properties. *Composites: Part A, Applied Science and Manufacturing*, 40, 791-799.
- Stubberud, L., Arwidsson, H. G., Larsson, A. & Graffner, C. (1996). Water solid interactions II. Effect of moisture sorption and glass transition temperature on compactability of microcrystalline cellulose alone or in binary mixtures with polyvinyl pyrrolidone. *International Journal of Pharmaceutics*, 134, 79-88.

- Sun, C. C. (2008). Mechanism of moisture induced variations in the density and compaction properties of microcrystalline cellulose. *International Journal of Pharmaceutics*, 346, 93-101.
- Sxchuh, V., Allard, K., Herrmann, K., Gibis, M., Kohlus, R. & Weiss, J. (2013). Impact of carboxymethyl cellulose (CMC) and microcrystalline cellulose (MCC) on functions characteristics of emulsified sausages. *Meat Science*, 93, 240-247.
- Thoorens, G., Krier, F., Leclercq, B., Carlin, B., & Evrard, B. (2011). Microcrystalline cellulose, a direct compression binder in a quality by design environment, *International Journal of Pharmaceutics*, 473, 64-72.
- Trache, D., Donnot, A., Khimeche, K., Benelmir, R., & Brosse, N. (2014). Physico-chemical properties and thermal stability of microcrystalline cellulose isolated from Alfa fibres. *Carbohydrate Polymers*, 104, 223-230.
- van Soest, J. J. G. & Vliegenthart, J. F. G. (1997). Crystallinity in starch plastics: consequences for material properties. *Trends in Biotechnology*, 15, 208-213.
- Vieira, M. G. A., da Silva, M. A., dos Santos, L. O. & Beppu, M. M. (2011). Natural-based plasticizers and biopolymer films: A review. *European Polymer Journal*, 47, 254-263.
- Wong, S., Shanks, R., Hodzic, A., (2002). Properties of poly(3-hydroxybutyric acid) composites with flax fibres modified by plasticiser absorption. *Macromolecular Materials and Engineering*, 287, 647-655.
- Zampaloni, M., Pourboghrat, F., Yankovich, S. A., Rodgers, B. N., Moore, J., Drzal, L. T., Mohanty, A. K., Misara, M. (2007). Kenaf natural fiber reinforced polypropylene composites: a discussion on manufacturing problems and solutions. *Composites: Part A, Applied Science and Manufacturing*, 38, 1569-1580.

## CHAPTER 7

# CONCLUSIONS AND FUTURE WORK

The purpose of this chapter is to summarise the results obtained during the current study, and make recommendations for further work.

### 7.1 CONCLUSIONS

The origin of this PhD project was based on an awareness through direct communication with the Australian food industry, *via* surveys, research collaboration, workshop attendance, and informal discussions, of the challenge of preparing foods that are affordable, readily available and possess optimum techno-functionality. One pressing issue is a detailed knowledge of value added value embodiments such as salt (mainly sodium chloride or calcium chloride) in starch based foods, where the molecular structure-function relationship amongst ingredients is not well understood (Australian Division of World Action on Salt & Health, 2015; Belz, Ryan, & Arendt, 2012; Charlton, Macgregor, Vorster, Levitt, & Steyn, 2007; Kloss, Meyer, Oraeve, & Vetter, 2015; Mccann & Day, 2013; National Heart Foundation of Australia, 2012).

The issue is particularly pronounced in snacks, a major component of the contemporary lifestyle diet, where few seem inclined to change their eating habits, and want to eating on the go! The major ingredient in snacks is potato starch (although tapioca starch is not uncommon) combined with flavouring agents, colorants, salts and sugars (Brennan, Derbyshire, Tiwari, & Brennan, 2013) (Obadiana, Oyewole, & Williams, 2013), Spinello Leonel, Mischan & do Carmo, 2014 previous research work has demonstrated that different sources and type of starch result in different physical properties of the final products, such as structure and expansion ratio during extrusion of the final products (Ah-Hen et al, 2014; Fayose, 2013; van der Sman, & Broeze, 2014). Along with starch cultivar,

increasing use of other ingredients particularly salt to achieve a variety of textures and sensory properties can have a profound effect on the physicochemical characteristics of the final products (Pitts, Favaro, Austin, & Day, 2014). However, molecular studies on the incorporation of salt in snacks, a high solids system, are scant in the literature, although the subject has important technological implications and affects the techno-functionality of products.

Based on the above, this research project started as described in Chapter 3 by considering the structural properties and textural consistency of potato starch–sodium chloride based systems, which find widespread commercial applications across the food industry in existing product concepts (van der Sman & Broeze, 2013) and in the development of new formulations (Chapter 3). The work demonstrated the potential of sodium-ion interactions with potato starch -hydroxyl and -phosphate groups to yield structures that are softer than starch–water systems at ambient temperature, which are indicative of mobile systems. In the absence of consequential starch crystallinity, a glassy state consistency is recorded, where sodium chloride addition creates hard matrices at subzero temperatures, with preparations exhibiting glassy consistency with thermal treatment. It was confirmed that increasing amounts of cation ( $\text{Na}^+$ ) lead to higher  $T_g$  thus supporting an antiplasticising effect of the salt on the condensed matrix of potato starch. Immediately, the question arose as to whether calcium chloride addition, i.e. a cation member towards the opposite end of the lyotropic series (Hofmeister, 1888; Kunz, Henle, & Ninham, 2004), would also alter the molecular dynamics of a glassy starch matrix.

The above hypothesis was examined in Chapter 4 by examining the behaviour of potato starch with calcium chloride in order to assist in the rationalisation of the functional properties of cereal based food products (Bassetti et al, 2014; Quilez & Salas-Salvado, 2012) and the formulation of biodegradable food packaging (Penhasi, & Meidan, 2014). In the process, the starch granule was gelatinised to convert it into a polymeric material, which upon subsequent cooling exhibited

classical mechanical behaviour of glassy consistency, when compared to classical master curve of viscoelasticity. As in Chapter 3, a series of physical probes was then utilised to provide good evidence for the preparation of macroscopically homogeneous mixtures where calcium chloride molecules dissociate to their ions. Dissolved calcium ions ( $\text{Ca}^{2+}$ ) then forms specific electrostatic interactions with the polar and negatively charged sequences of the potato starch molecule, which contains phosphorylated amylopectin.

The results suggest that with the thermal conditions and sample composition of this investigation, dissolved calcium ions, as opposed to crystallised solid calcium chloride molecules, have an antiplasticising effect on potato starch that stabilises the polymeric matrix in the glassy state. This outcome further emphasizes the importance of the relative strength of specific electrostatic between hydrophilic parts of the starch molecule, negatively charged phosphate groups and the positively charged counterions, with the latter belonging to opposite ends of the Hofmeister series, with the  $\text{Na}^+$  being a “salting out” cation and  $\text{Ca}^{2+}$  as a “salting in” cation (Hofmeister, 1888; Kunz, Henle, & Ninham, 2004). The stronger antiplasticising effect of calcium ions, as dense charge carriers, in comparison to that of the monovalent sodium ions, indicates that the focus of the discussion to interpret the behaviour of these systems should be on the added cations as opposed to the chloride anions.

Thus, the stronger antiplasticising effect of the calcium ion, as compared to that of the sodium ion, highlights the role of the phosphorylated amylopectin sequences in potato starch. This suggests the formation of calcium mediated bridges occur, which increase chain interactions and lead to enhance molecular stability, which is reflected in elevated estimates of the  $T_g$ . This hypothesis was further examined using tapioca starch-based films, which are non-phosphorylated and neutral in aqueous solutions as compared to the highly anionic potato-starch preparations (Muhammad, Kusnandar, Hashim, & Rahman, 1999). Introduction of sodium and calcium cations in the tapioca carbohydrate matrix results in the formation of

electrostatic interactions with the starch's hydroxyl groups inducing an antiplasticising effect on the matrices of tapioca sample, as described in Chapter 5. Although the increase in the values of the  $T_g$  with increasing salt addition at a given moisture level was observed, here, was no significant variation in the values of the  $T_g$  with either sodium or calcium chloride at equal levels of addition, an outcome which emphasizes the importance of cation/phosphate interactions in antiplasticising glassy starch matrices.

The final Results and Discussion Chapter of this Thesis (Chapter 6) opens new avenues in this research field by introducing microcrystalline cellulose (MCC) to potato starch, with the aim of assessing its effect on the structural properties of the binary composites. It was observed that MCC addition resulted in the formation of homogeneous blends, where cellulose particles formed the filler phase within the gelatinised and largely amorphous three-dimensional phase of potato starch. There are no direct, or specific interactions between the two polymeric materials, with MCC acting as an inert filler that reinforces the mechanical strength of condensed mixture. Further, under the thermal conditions of processing in this investigation, inclusion of MCC consistently lowers the  $T_g$  of the composite with increasing fibre amount. This outcome reflects the reduction of starch content to keep a constant level of solids with the addition of MCC, and argues that the observed glass transition phenomena are due solely to the starchy matrix. Therefore, MCC inclusion has a plasticising effect on the network of potato starch, an observation which contrasts strongly with the antiplasticising effect of sodium or calcium ion addition to these systems.

## 7.2 FUTURE WORK

An obvious lead from this work is, of course, the assessment of salt addition to binary blends of potato starch and MCC in order to document the effect of counterion electric charge on polysaccharide glycosidic linkage in systems more relevant to food technology applications. Other equally important extensions could include:

- (i) Altering the processing conditions in terms of temperature range, and duration of thermal treatment, in order to assess the variation in  $T_g$  of extruded starch in the presence of salt *via* the competing mechanisms of increased molecular mobility, increased moisture retention or the action of salt as a catalyst for caramelisation, which is due to the hydrolysis of starch to glucose by a large number of ions during high-temperature extrusion (Moreau, Bindzus, & Hill, 2011).
- (ii) Document the effect of salt on the physical and structural properties of high-solid samples incorporating the following soluble dietary fibre components: low methoxy pectin, high guluronate alginate, agarose, deacylated gellan, guar gum and xanthan gum (Peressini, Foschia, Tubaro, & Sensidoni, 2015). These have been selected based on fundamental considerations spanning the range of conformational type: disordered (guar gum), isolated order (xanthan gum) and aggregated order: (alginate and agarose); charge density ranging from neutral (agarose) to one charge (deacylated gellan) and two charges (pectin) per repeat sequence; and capacity for network formation ranging from non-gelling guar gum to gelation at concentrations down to about 0.1% for agarose.
- (iii) Utilise the molecular understanding achieved from the present work to follow the rubber-to-glass transition in mixtures of starch with soluble or insoluble dietary fibre on the basis of molecularly miscible or phase



separated binary gels. Such a study could be analysed using a suitable framework of thought based on the “sophisticated synthetic polymer approach” adapted for the particular research scenario. Such a study would include, the postulates of free volume theory at the microscale level and the specific contribution of local segmental motions of the polymer chain at the nanoscale level to the estimated  $T_g$  according to the molecular coupling theory (Kasapis, 2008).

## 7.3 REFERENCES

- Ah-Hen, K., Lehnebach, G., Lemus-Mondaca, R., Zura-Bravo, L., Leylen, P., Vega-Gálvez, A., Figuerola, F. (2014). Evaluation of different starch sources in extruded feed for Atlantic salmon. *Aquatic Nutrition*, 20, 183-191.
- Australian Division of World Action on Salt & Health. (2015). Salt and its detrimental effects on health. Retrieved on 21 February 2016.  
<http://www.awash.org.au/drop-the-salt-campaign/the-food-industry/>
- Bassetti, M. N., Pérez-Palacios, T., Capriano, I., Cardoso, P., Ferreira, I., M. P. L., V. O., Samman, N., & Pinho, O. (2014). Development of bread with NaCl reduction and calcium fortification: Study of its quality characteristics. *Journal of Food Quality*, 37, 107-116.
- Belz, M. C. E., Ryan, L. A. M., & Arendt, E. K., (2012). The impact of salt reduction in bread-A review. *Critical Reviews in Food Science and Nutrition*, 52, 514-524.
- Brennan, M. A., Derbyshire, E., Tiwari, B. K., & Brennan, C. S. (2013). Ready-to-eat snack products: the role of extrusion technology in developing consumer acceptable and nutrition snacks. *International Journal of Food Science and Technology*, 48, 839-902.
- Charlton, K. E., Macgregor, F., Vorster, N. H., Levitt, N. S., & Steyn, K. (2007). Partial replacement of NaCl can be achieved with potassium, magnesium and calcium salts in brown bread. *International Journal of Food Science and Nutrition*, 58, 508-521.
- Fayose, F. T. (2013). Expansion characteristics of selected starchy crops during extrusion. *The West Indian Journal of engineering*, 35, 58-64.
- Hofmeister, F. (1888), Zur Lehre von der Wirkung der Salze. *Arch. Experimental Pathology and Pharmacology*, 24, 247-260.
- Kasapis, S. (2008). Recent advances and future challenges in the explanation and exploitation of the network glass transition of high sugar/biopolymer mixtures. *Critical Review in Food Science and Nutrition*, 48, 185-203.

- Kloss, L., Meyer, J. D., Oraeve, L., & Vetter, W. (2015). Sodium intake and its reduction by food reformulation in the European Union-A review, *NFS Journal*, 1, 9-19.
- Kunz, W., Henle, J., & Ninham, B. W. (2004). 'Zur Lehre von der Wirkung der Salze' (about the science of the effect of salts): Franz Hofmeister's historical papers. *Current Opinion in Colloid and Interface Science*, 9, 19-37.
- Maccann, T. H. & Day, L. (2013). Effect of sodium chloride on gluten network formation, dough microstructure and rheology in relation to breadmaking. *Journal of Cereal Science*, 57, 444-452.
- Moreau, L., Bindzus, W., & Hill, S. (2011). Influence of salts on starch degradation: Part II- salt classification and caramelisation. *Starch/Stärke*, 63,676-682.
- Muhammad, K., Kusnandar, F., Hashim, D. M., & Rahman, R. A., (1999), Application of native and phosphorylated tapioca starches in potato starch noodle. *International Journal of Food Science and Technology*, 34, 275-280.
- National Heart Foundation of Australia (2012). Rapid review of the evidence- Effectiveness of food reformulation as a strategy to improve population health. Heart Foundation, pp. 28.
- Obadiana, A. O., Oyewole, O. B., & Williams, O. E. (2013). Improvement in the traditional processing method and nutritional quality of traditional extruded cassava-based snack (modified Ajogun). *Food Science & Nutrition*, 1, 350-356.
- Penhasi, A., & Meidan, V. M. (2014). Preparation and characterization *in situ* ionic cross-linked pectin films: Unique biodegradable polymers. *Carbohydrate Polymers*, 102, 254-260.
- Peressini, D., Foschia, M., Tubaro, F., & Sensidoni, A. (2015). Impact of soluble dietary fibre on the characteristics of extruded snacks. *Food Hydrocolloids*, 43, 73-81.

- Pitts, K. F., Favaro, J., Austin, P., & Day, L. (2014). Co-effect of salt and sugar on extrusion processing, rheology, structure and fracture mechanical properties of wheat-corn blend. *Journal of Food Engineering*, *127*, 58-66.
- Quilez, J., & Salas-Salvado, J. (2012). Salt in bread in Europe: potential benefits and reduction. *Nutrition Reviews*, *70*, 666-678.
- Shankar, S. & Rhim, J. (2016). Preparation of nanacellulose from micro-crystalline cellulose: The effect on the performance and properties of agar-based composite films. *Carbohydrate Polymers*, *135*, 18-26.
- Spinello, A. M., Leonel, M., Mischán, M. M., & do Carmo, E. L. (2014). Cassava and turmeric flour blends as new raw materials to extruded snacks. *Ciência e Agrotechnologia*, *38*, 68-75.
- van der Sman, R. G. M. & Broeze, J. (2013). Structuring of indirectly expanded snacks based on potato ingredients: A review. *Journal of Food Engineering*, *114*, 413-425.
- van der Sman, R. G. M. & Broeze, J. (2014). Effects of salts on the expansion of starchy snacks: A multiscale analysis. *Food & Function*, *12*, 3076-3082.

# APPENDIX

Food Chemistry 184 (2015) 65–71



Contents lists available at ScienceDirect

Food Chemistry

journal homepage: [www.elsevier.com/locate/foodchem](http://www.elsevier.com/locate/foodchem)



## Effect of sodium chloride on the glass transition of condensed starch systems



Lillian Chuang, Naksit Panyoyai, Robert Shanks, Stefan Kasapis\*

School of Applied Sciences, RMIT University, City Campus, Melbourne, Vic 3001, Australia

### ARTICLE INFO

#### Article history:

Received 19 December 2014

Received in revised form 16 February 2015

Accepted 11 March 2015

Available online 16 March 2015

#### Keywords:

Glass transition

Sodium chloride

Starch

High-solid systems

### ABSTRACT

The present investigation deals with the structural properties of condensed potato starch–sodium chloride systems undergoing a thermally induced glass transition. Sample preparation included hot pressing at 120 °C for 7 min to produce extensive starch gelatinisation. Materials covered a range of moisture contents from 3.6% to 18.8%, which corresponded to relative humidity values of 11% and 75%. Salt addition was up to 6.0% in formulations. Instrumental work was carried out with dynamic mechanical analysis in tension, modulated differential scanning calorimetry, Fourier transform infrared spectroscopy, scanning electron microscopy and wide angle X-ray diffraction. Experimental conditions ensured the development of amorphous matrices that exhibited thermally reversible glassy consistency. Both moisture content and addition of sodium chloride affected the mechanical strength and glass transition temperature of polymeric systems. Sodium ions interact with chemical moieties of the polysaccharide chain to alter considerably structural properties, as compared to the starch–water matrix.

© 2015 Published by Elsevier Ltd.

### 1. Introduction

Starch, from cereals, tubers and roots, is commonly used as the major food reserve to provide, at low cost, a bulk nutrient and energy source in the diet of man. In terms of techno-functionality, starch is able to impart thickening and gelling properties to processed foods where relatively small amounts of the material can bind large quantities of water bringing about a desirable change in textural consistency (Mishra & Rai, 2006). Its biocompatibility and degradability afford additional application in pharmaceuticals, thermoplastics, paper, textile, etc. (Copeland, Blazek, Salman, & Tang, 2009).

In the main, starch has two major components, i.e. amylose, which is essentially a linear polymer of variable molecular size (approximately  $10^5$ – $10^6$  Da) comprising (1 → 4)-linked  $\alpha$ -D-glucopyranosyl units, and amylopectin, the major component of starch, which is a larger molecule than amylose with molecular weight of  $10^7$ – $10^9$  Da. The latter is a highly branched fraction, with the structure being built up from chains of  $\alpha$ -D-glucopyranosyl residues linked together mainly by  $\alpha$ -(1 → 4) and 5–6%  $\alpha$ -(1 → 6) linkages (Considine et al., 2011).

Potato starch has an amylose-to-amylopectin ratio of 1:3 and contains large oval spherical granules, with their size ranging

between 5 and 100  $\mu$ m (Zobel & Stephen, 2006). It can be produced in a refined grade containing a minimal protein (0.2% max) or fat (0.1% max) content. This gives the starch powder a clear white colour and the cooked material characteristics of neutral taste, long texture and clarity with minimal tendency to solution yellowing (Alvani, Qi, & Tester, 2012). Phosphate is bound to the molecule of potato starch, as opposed to other botanical sources, giving the solution a slightly anionic character, high swelling power and a relatively low gelatinisation temperature of around 60 °C, which is accompanied by high viscosity (Singh, Singh, Kaur, Sodhi, & Gill, 2003).

Sodium chloride (NaCl) is the most widely used salt in the food industry as preservative and flavour enhancer (Albarracín, Sánchez, Grau, & Barat, 2011). Sodium cation is the counterion for the chlorine anion and *vice versa* in order to maintain electric neutrality. In the Hofmeister series, the order of cations is given as:  $\text{NH}_4^+ > \text{K}^+ > \text{Na}^+ > \text{Li}^+ > \text{Mg}^{2+} > \text{Ca}^{2+} > \text{guanidinium}$  (Hofmeister, 1888; Kunz, Henle, & Ninham, 2004). Early members (on the left) of the series increase the solvent surface tension, hence decrease the solubility of protein and polysaccharide molecules in a phenomenon known as “salting out”. In contrast, later salts in the series, e.g. guanidinium, increase the solubility of macromolecules (“salting in”), hence decrease “the order” of water molecules in solution (Zhou et al., 2014).

Besides the classification of ions according to lyotropic series, literature argues that salts have an effect on polysaccharides even

\* Corresponding author. Tel.: +61 3 992 55244; fax: +61 3 992 55241.

E-mail address: [stefan.kasapis@rmit.edu.au](mailto:stefan.kasapis@rmit.edu.au) (S. Kasapis).



## Calcium chloride effects on the glass transition of condensed systems of potato starch



Lillian Chuang, Naksit Panyoyai, Lita Katopo, Robert Shanks, Stefan Kasapis\*

School of Applied Sciences, RMIT University, City Campus, Melbourne, Vic 3001, Australia

### ARTICLE INFO

#### Article history:

Received 15 July 2015

Received in revised form 3 December 2015

Accepted 17 December 2015

Available online 18 December 2015

#### Keywords:

Glass transition

Calcium chloride

Potato starch

High-solid systems

Anti-plasticizing effect

### ABSTRACT

The effect of calcium chloride on the structural properties of condensed potato starch undergoing a thermally induced glass transition has been studied using dynamic mechanical analysis and modulated differential scanning calorimetry. Extensive starch gelatinisation was obtained by hot pressing at 120 °C for 7 min producing materials that covered a range of moisture contents from 3.7% w/w (11% relative humidity) to 18.8% w/w (75% relative humidity). FTIR, ESEM and WAXD were also performed in order to elucidate the manner by which salt addition affects the molecular interactions and morphology of condensed starch. Experimental protocol ensured the development of amorphous matrices that exhibited thermally reversible glassy consistency. Both moisture content and addition of calcium chloride affected the mechanical strength and glass transition temperature of polymeric systems. Highly reactive calcium ions form a direct interaction with starch to alter considerably its structural properties via an anti-plasticizing effect, as compared to the polymer-water matrix.

© 2016 Published by Elsevier Ltd.

### 1. Introduction

The thermally induced glass transition is an important concept to rationalise the textural consistency and stability of condensed starchy products and starch-based films (Liu, Xie, Yu, Chen, & Li, 2009; Talja, Helén, Roos, & Jopuppila, 2007). Starch granules contain an amorphous phase, which is the main component of linear amylose and some of the partially crystalline branched amylopectin. During vitrification that commonly follows starch gelatinisation, amorphous polymeric segments remain “frozen” in a random conformation resulting in slow molecular motions and effective immobilisation in the glassy state (Zeleznek & Hosney, 1987). Upon subsequent heating at a given scan rate, the glassy polymer converts into a rubbery system of high viscosity and increased configurational flexibility. This rubber-to-glass transformation is demarcated by the so-called glass transition temperature,  $T_g$ , which depends on the amylose/amylopectin content, surrounding relative humidity, molecular interactions between starch and low molecular weight co-solute, and the nature of measuring protocol (Perdomo et al., 2009).

Starch based biomaterials and processed foods experience plasticising or anti-plasticising phenomena that alter considerably glass-transition behaviour. Increase in the plasticizer content of

water and polyols depresses the glass transition temperature and reduces the mechanical strength (Hulleman, Janssen, & Feil, 1998; Lourdin, Coignard, Bizot, & Colonna, 1997; Róz, Carvalho, Gandini, & Curvelo, 2006). Glycerol and xylitol, for example, form hydrogen bonds with the hydroxyl groups of starch leading to a reduction in intermolecular polymer associations and entanglements, and retention of backbone flexibility (Chaudhary, Adhikari, & Kasapis, 2011). Conversely, linoleic and oleic acids can act as anti-plasticizers aided by the steric accommodation of the fatty acid molecule within the hydrophobic cavity of amylose helices. This leads to an upward shift of  $T_g$  values in the cassava starch matrices at a moisture content lower than 11% and in the presence of at least 2% added fatty acid (Luk, Sandoval, Cova, & Müller, 2013).

Various types of salt are regularly utilised in starch based formulations in order to enhance techno-functionality. Sodium chloride is a traditional preservative widely added in starch to act as a taste and/or flavour enhancer and a water-holding capacity or water activity modifier (Albarracin, Sánchez, Grau, & Barat, 2011). The effect of sodium chloride on the glass transition of condensed starches (more than 80% solids in preparations) was investigated. Differential scanning calorimetry was used and results were rationalised on the basis of non-dissociated (crystalline) salt molecules or dissociated (amorphous) atoms depending on moisture levels (Farahnaky, Farhat, Mitchell, & Hill, 2009).

\* Corresponding author.

E-mail address: [stefan.kasapis@rmit.edu.au](mailto:stefan.kasapis@rmit.edu.au) (S. Kasapis).